Customized Surface-Guided Total Knee Replacement for Natural Kinematics and Deep Flexion

by

Shabnam Pejhan

A Thesis submitted to the Faculty of Graduate Studies of

The University of Manitoba

in partial fulfillment of the requirements of the degree of

Doctor of Philosophy

Department of Mechanical Engineering

University of Manitoba

Winnipeg

Dedicated to my parents, Mehri and Ali, my sister, Shervin, and my brother, Khashayar,

for their endless love and encouragement.

Abstract

Total knee replacements (TKRs) are developed and used to improve the quality of the life of patients by relieving pain and restoring normal knee function. The motivation of this dissertation was to develop and evaluate a TKR that provides close to normal movement pattern for all flexion ranges including deep flexion. The objective was to determine the design features of a customized surface-guided knee implant so that no intercondylar motion guiding cam and post is required. In this design concept, specially shaped asymmetric articulating surfaces aim to guide the motion through a predefined target pattern of motion. The novel design features of the tibiofemoral articulation surfaces were generated based on patient-specific anatomic measurements of the reference landmarks and axes. The customized surface-guided TKR has a congruent partial ball and socket configuration on the medial condyle. On the lateral side, the multi-radii curvature with an incremental change of the inner and outer contacting arcs provides the expected guiding of the motion between the artificial joint compartments. Principal component analysis along with parametric analytical optimization was used to define the combination of design variables that can reach a high range of flexion, with the least deviation from the desired pattern of motion. This analysis showed that the location and orientation of the flexion-extension axis, and the tibial sagittal slope were the most influential parameters on the kinematic performance of the TKR all through deep flexion angles up to 140 degrees.

Abstract

The design target for this new knee implant was to restore close to normal kinematic behavior, while reaching a high range of flexion. Virtual simulations and experimental testing were used to verify the capability of the customized surface-guided TKR in reproducing the desired tibiofemoral motion pattern, as the joint bent to high flexion angles. The load-controlled tests using a knee wear simulator made it possible to examine the kinematic behavior, considering the geometric design variables alone. The new surface-guided TKR can achieve a high range of flexion, while following the design target pattern of motion. In the improved TKR design from the parametric analytical optimization process, the tibial insert rotated about 23° internally around a medial condyle, as the joint bent up to 140 degrees of flexion. Such rotation occurred as a result of larger posterior translation of the lateral condyle in comparison to that of the medial side.

This dissertation introduced the improved combination of design variables for a custom designed surface-guided TKR. The findings of this study prove that a customized surface-guided TKR with a lateral motion guiding articulation and a medial pivot center restores close to normal kinematics. This research is another step in the ongoing process of developing artificial knee joints that allow normal functionality and higher range of motion, and thereby improve the patient's satisfaction.

Acknowledgments

First, I would like to express my special appreciation and thanks to my advisor, Dr. Urs Wyss, for his continuous support, guidance, brilliant ideas, and patience. Urs, your kind and encouraging attitude, and the passion that you have for the research was motivational during tough times in this study. Thank you for being a tremendous mentor for me.

I would also like to thank my committee members, Dr. Jan-Mels Brandt, Dr. Yunhua Luo, and Dr. Zahra Moussavi for their great comments and suggestions. I appreciate all your contributions of time and ideas to improve the quality of my research. My sincere thanks also go to Dr. Eric Bohm at the Orthopaedic Innovation Center, who gave me advice on medical and orthopaedic aspects of this research. Dr. Bohm, I am grateful for sharing your knowledge with me, for giving me the chance to observe a total knee replacement surgery, and for your kindness and commitment in providing feedback on my study.

The experimental testing of this study would not have been possible without the technical support from Orthopaedic Innovation Center members. Martin Petrak, your enthusiasm about this project and your great ideas for further development of the proposed knee design has been a precious support. Trevor Gascoyne, thank you so much for helping me with printing prototypes and conducting the experiments. I appreciate your patience, hard work, and valuable comments in all stages of fighting the challenges of the tests. Leah Guenther, Meaghan

Coates, and Lawrence Cruz, thanks for your invaluable technical assistance during the experimental testing.

I am also thankful to Dr. Shahram Amiri for giving advice and sharing his knowledge and experience on the surface-guided knee replacement with me. To my collaborators, Olivia Essex and Ida Khosravipour, thank you for your tireless work and positivity during design development and evaluation processes. To Dr. Joe Ackerman and Elsie Jordaan, with whom I shared an office in the Engineering building of the University of Manitoba over years of my PhD study, thanks for the friendship and fun memories.

I would like to gratefully acknowledge the funding sources from DePuy Synthes and the University of Manitoba that made my PhD possible.

Lastly, a special thanks to my family for all their love and encouragement throughout my life. To my devoted parents, Mehri and Ali, and the best sister and brother ever, Shervin and Khashayar, words cannot express how grateful I am having a supportive family like you. Thank you and I love you all.

Table of Contents

List of Tables

List of Figures

Glossary

Acronyms	Description
ACL	Anterior cruciate ligament
AMTI	American Mechanical Technologies Inc.
AP	Anterior-Posterior direction
BCR	Bi-cruciate retaining
CAD	Computer aided design
CIHI	Canadian Institute for Health Information
CJRR	Canadian Joint Replacement Registry
CoCr	Cobalt-chrome (CoCr alloy)
CR	Cruciate-retaining
FE	Flexion-Extension
HDPE	High density polyethylene
IE	Internal-External
ISO	International Organization for Standardization
LCL	Lateral collateral ligament
MCL	Medial collateral ligament
ML	Medial-Lateral
MRI	Magnetic resonance image
OA	Osteoarthritis
PCL	Posterior cruciate ligament
RMSE	Root mean square error
ROM	Range of motion
TKA	Total knee arthroplasty
TKR	Total knee replacement
UHMWPE	Ultra high molecular weight polyethylene

Chapter 1

Introduction

General overview

Arthritis is among the first three common chronic diseases that have been reported in Canada [1]. Arthritis includes a large group of disorders with devastating effect on the performance of the musculoskeletal system. The major symptoms are joint pain, stiffness and swelling that result in physical disability in performing activities of daily living (ADL), and impair quality of everyday life [1,2]. The Canadian Community Health Survey (CCHS) in 2013 shows that a significantly higher proportion (59%) of people in Canada living with arthritis have difficulties with performing ADL in comparison to other chronic conditions such as heart diseases, diabetes, asthma, migraine, high blood pressure, and back problems [1]. Osteoarthritis (OA) is the common type of arthritis mainly occurring in the joints bearing body weight such as knees, hips, feet, and spine [3,4]. In an osteoarthritic knee, the joint space is narrowed, which results in stiffening of the bone structure (sclerosis), and forming of bony spurs or extra bone (osteophytes) around the joint (Figure 1-1). Murphy et al. [4,5] indicated that knee OA is more common than hip and foot arthritis. They reported about a 45% lifetime

risk of developing symptoms of knee OA for a sample population with an average age of 61 years (between 45 to 93 years old).

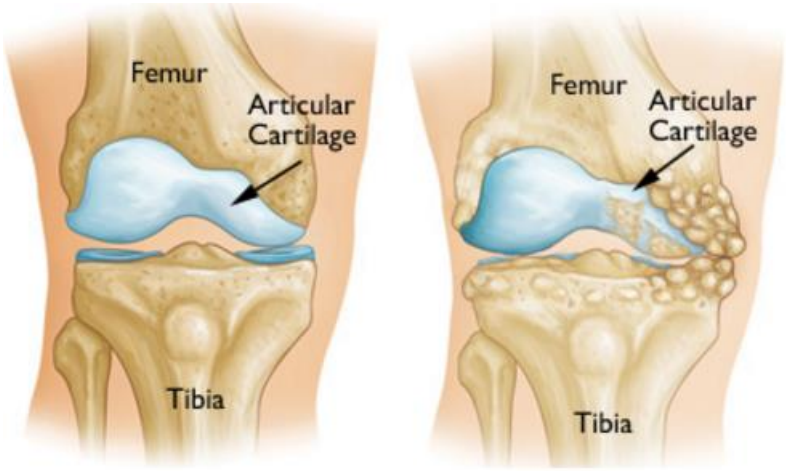

Figure 1-1 Knee joint before and after osteoarthritis (a) Normal knee joint (b) Osteoarthritic knee- Reproduced with permission from OrthoInfo. © American Academy of Orthopaedic Surgeons. http://orthoinfo.aaos.org [6]

If medical therapy fails in controlling the development of OA of the knee joint, the treatment would be a knee replacement, in which the damaged parts of the joint are substituted with artificial components. The United States Bone and Joint Initiative reported that in 2011, 56% of the total joint replacements were performed on the knee, while 95% of them were due to osteoarthritis [7]. The number of knee replacement procedures has substantially escalated, and current trends indicate that such procedures will further increase with time. The annual report from the Canadian Joint Replacement Registry (CJRR) by the Canadian Institute for Health Information (CIHI) [8] revealed that in 2015 there were 61421 knee replacements in Canada. This report indicated a 20.3% increase from the 2011 number of knee replacements. Kurtz et al. [9] reported from the Nationwide Inpatient Sample that in 2006, 41% of the Total Knee Replacements (TKRs) were performed in patients younger than 65 years, while only 25%

of TKRs were performed in patients within this age range in 1993. The projections for the number of the knee joint replacements in the United States show that the demand for total knee replacement would grow 673% by 2030 [10]. Kurtz et al. [9] anticipated that by 2030, the demand for TKR for patients younger than 65 years would be 55-62% of the knee arthroplasties, while the fastest growth would occur for patients with 45 to 54 years. CJRR also reports that in 2015, the largest annual increase in knee replacement rates was observed among males and females aged less than 45 years (21.1% and 9.6%, respectively) [8]. Therefore, the requirements and expectations of younger and more active patients must be considered in the new knee replacement designs.

Although knee replacements are known to be successful operations, the percentage of the satisfied patients is reported to be around 81–89% [11-13]. Bourne et al. [11] reported that 1 in 5 patients was not satisfied after TKR; while about 30% of them were not satisfied with the functionality of the joint during different activities of daily living. Limited range of motion, wear, loosening, instability and infection are among the major reasons reported for the dissatisfaction of the patients [8,11,14]. According to the report by CJRR [8], 6.8% of the knee replacements in 2015 have been revision surgeries, which is a procedure where the surgeon removes and replaces a problematic implant. According to this report, the most common reason for revision was loosening (21.8%), followed by instability (12.1%), infection (10.3%), and poly wear (5.0%). Therefore, the purpose of the knee replacement is not only to relieve pain, but also to restore function, and provide stability and durability.

Research on the kinematics of the knee joint shows that the pattern of motion changes after TKR. It is due to the limitations in the geometry of the components, deficiencies in the soft

tissues, and the inability of the remaining tissues in performing their function. The abnormal kinematics reduces the maximum range of motion, and results in the ineffectiveness of the muscle function, and makes the patient dissatisfied with the outcome of the TKR [15-20]. Thus, the implant that substitutes the intact knee is expected to have certain characteristics; while providing high range of motion and close to normal kinematic behavior.

Objectives

This study aimed to apply a concept of surface-guided knee replacement to generate a customized artificial knee joint. Therefore, the geometric design features that were used to implement the motion guiding concept were extracted from a patient's magnetic resonance image (MRI) of the knee joint. The guiding features were generated by special shapes of the articulating surfaces at the tibiofemoral joint, such that the function of the sacrificed soft tissues could be replicated to guide the implant in a desired pattern of motion. The novel design features to be implemented at the tibiofemoral articulation surfaces were generated based on the patient specific anatomic requirements, and the general idea of a motion guiding concept introduced by Amiri, Wyss and Cooke [21,22].

Another objective of this research was to investigate the influence of the geometric design variables on the kinematic performance of the surface-guided TKR. The main design variables were first determined, and their contributions to the kinematic measures were investigated by principal component analysis combined with a virtual simulation of deep squatting. Finally, an analytical optimization study was used to define the combination of design variables that can reach a high range of flexion, while following the target normal pattern of motion.

This TKR was designed to achieve a high range of motion with a close to normal kinematic performance. Therefore, another objective was to evaluate the kinematic behavior of the customized surface-guided TKR during load and motion conditions of activities of daily living. Simple gait, lunging, and squatting were considered as three major ADL case studies for the virtual and experimental evaluations. The experimental testing was performed using the prototypes of the components mounted on a knee wear simulator under the load-controlled condition.

Furthermore, the contact behavior at the tibiofemoral articulating interface for the designed TKR was studied for different activities, such as lunging and squatting. The contact area and mean contact stress were measured mechanically by pressure sensitive films at specific flexion angles. For this experiment, a knee wear simulator with displacement-controlled condition was used to orient the components of the TKR at specific flexion angles and apply the loads to the TKR.

Structure of dissertation

This dissertation is composed of six chapters, beginning with the introduction. In the following section of this chapter, an overview of natural knee joint anatomy is provided. Chapters 2 through 4 are written in manuscript format. Therefore, a detailed literature review is provided separately within each chapter. The required overview of the background concepts includes a description of total knee replacements, clinical outcomes of current knee implants, kinematics and range of motion in the natural knee joint and after TKR, as well as the optimization attempts and studies to improve the artificial knee joint performance.

Chapter two describes the design methodology that was performed based on the extracted geometry from a subject's MRI, and the concept of surface-guided implants [21,22]. This chapter is published in the Journal of Engineering in Medicine [23]. Chapter three investigates the influence of geometric design features on the kinematic of the proposed customized surface-guided TKR. In this chapter, a quantified criterion is determined to measure the kinematic performance of different design versions and find the combination of design variables with the optimum kinematic behavior. This chapter is accepted for publication in the Journal of Orthopaedic Surgery. Chapter four provides the process of evaluation of the kinematic performance of the proposed customized surface-guided TKR by the virtual simulations and mechanical tests with a knee wear simulator. The contents of this chapter were presented at the Orthopedics Research Society (ORS) annual meetings in 2015 and 2016, and submitted to the Journal of Medical Engineering & Physics. In Chapter 5, the experimental evaluation of the contact area and mean contact pressure at the tibiofemoral articulating surfaces of the surface-guided TKR is provided. The content of this chapter is submitted to the Journal of Clinical Biomechanics.

Chapter 6 provides a general discussion of the findings of this dissertation, and describes the limitations and shortcomings. Chapter 7 concludes the dissertation, highlighting the major achievements, in addition to the recommendations for future work.

Background

Anatomical terms and definitions

In anatomical description terminology, the "median" plane is the vertical plane passing longitudinally through the body and dividing the body into right and left halves. Based on the median plane, three major planes are used in description of different parts of the body:

- Sagittal plane: the vertical planes passing through the body parallel to the median plane (dividing the body part into right and left sections)
- Frontal or Coronal plane: the vertical planes passing through the body and perpendicular to the median plane (dividing the body part into anterior and posterior sections)
- Transverse or Horizontal Plane: the vertical planes passing through the body and normal to the median and frontal planes (dividing the body part into superior and inferior sections)

The specific anatomical terminology that is commonly used to locate the body parts and their relative position are summarized in Table 1-1 and Figure 1-2.

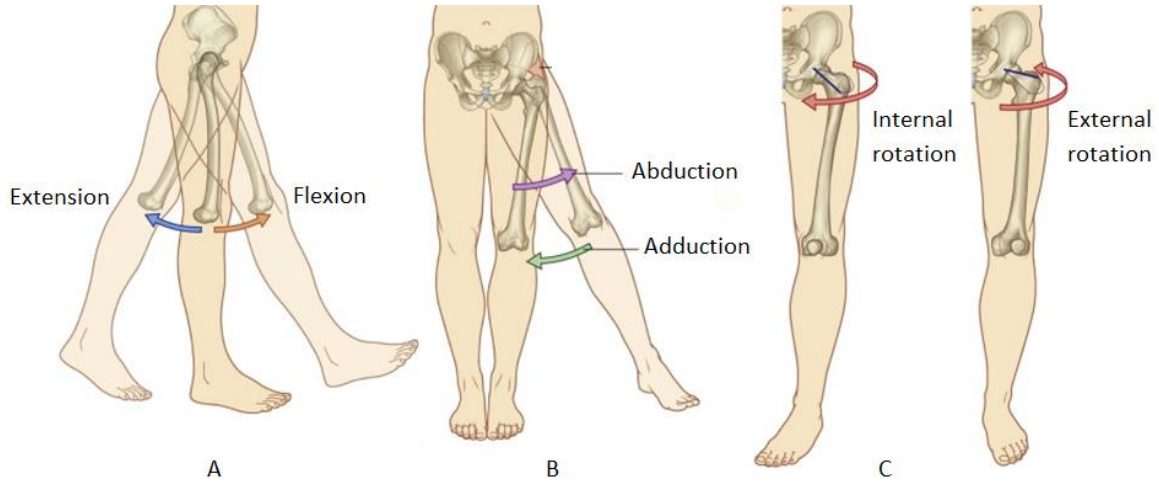

Figure 1-2 Anatomic terms of rotation and orientation (Adapted from Gray's Anatomy for Students [24], with permission from Elsevier)

Table 1-1 Anatomic terms of rotation and orientation

Term	Description
	Orientation terms
Proximal	Closer to the point of attachment of a limb to the trunk
Distal	Further to the point of attachment of a limb to the trunk
Anterior (Ventral)	Toward or at the front
Posterior (Dorsal)	Toward or at the back or behind
Medial	Toward or at the median plane of the body
Lateral	Away from the median plane of the body
	Movement terms
Flexion	Bending (decreasing angle between bones or parts of body)
Extension	Straightening (increasing angle between bones or parts of body)
Internal or medial rotation	Turning of the part of body such that the anterior face of the part becomes closer to the median plane
External or rotation	Turning of the part of body such that the anterior face of the part goes away from the median plane
Abduction	Moving away from the median plane
Adduction	Moving toward the median plane

Tibiofemoral joint anatomy

The knee joint is the largest and most complex synovial joint in the human body, in which the articulation of three major bones forms the motion: the femur (thigh bone), the tibia (shin bone), and the patella (knee cap). As it is depicted in Figure 1-3, the complex knee joint could be considered as three major separate sub-joints. The distal end of the femur has a concave curved articular surface with a 'horseshoe' shape, which is called the femoral medial and lateral condyles. These surfaces articulate with the corresponding medial and lateral tibial plateaus. These articulations make the medial and lateral tibiofemoral joints. The articulation of the

patella and the anterior surface of the femur at the trochlear groove is the third sub-joint called patellofemoral joint. The articulating areas are covered with a layer of fibrous connective tissue called articular cartilage.

Flexion and extension are the primary motions in the knee, but this joint is not a simple "hinge," and it also provides anterior-posterior (AP) movements, small amounts of abduction and adduction, and internal-external (IE) rotations around a long axis. The AP displacement during knee joint flexion is, in fact, a combination of both rolling and gliding of the femoral condyles on the tibia. Rolling is the translation of tibiofemoral contact points and the joint axis in the AP direction. In gliding, the contact points are transferred without moving the joint axis [25,26].

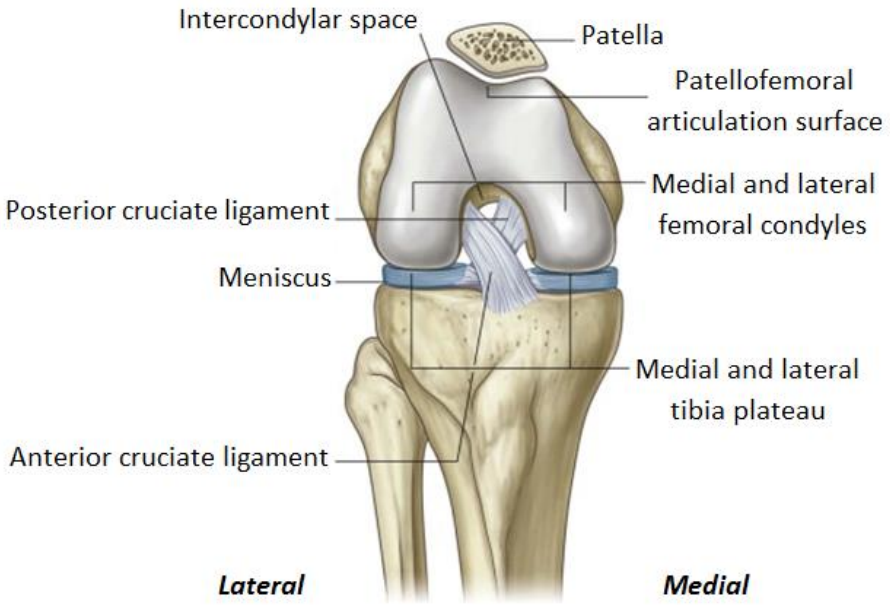

Figure 1-3 Knee joint structure (Adapted from Gray's Anatomy for Students [24], with permission from Elsevier)

The complex mechanism of motion at the knee joint requires ligaments and muscle forces to maintain stability [27,28]. The muscles load the joint based on the requirements of the

movement and provide active stability. The contraction of the quadriceps muscle that is located in the front of the thigh and connected to the patella by the quadriceps tendon (Figure 1-4) causes the extension of the knee. Hamstrings are the second main muscle group which stabilizes the knee flexion movement by their contraction. The motion of the patella on the femur increases the length of the moment arm of the quadriceps, and in turn, improves the stabilizing influence of the muscle. Furthermore, the interaction of the ligaments and menisci resist excessive displacements during articulations and control the path of motion, and provide passive stability [27-29]. Two main ligament groups stabilize the motion of the knee joint: the collateral ligaments and the cruciate ligaments (Figure 1-4).

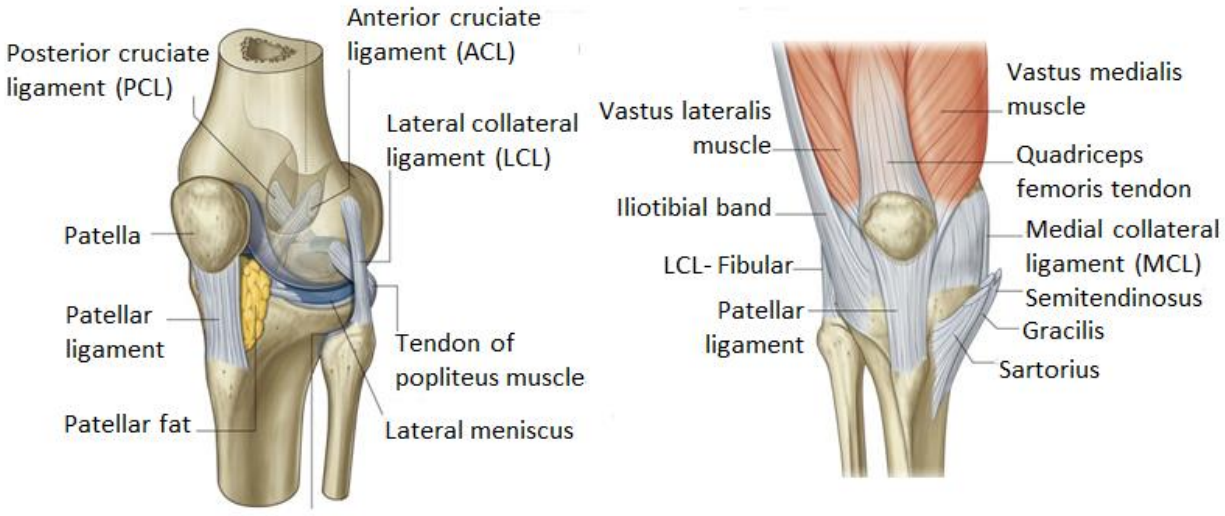

Figure 1-4 Fibrous membrane of the knee joint capsule (Adapted from Gray's Anatomy for Students [24], with permission from Elsevier)

The Anterior Cruciate Ligament (ACL) is attached to the anterior intercondylar area of the tibia and extends to the posterior part of the femoral condyle. On the other hand, the Posterior Cruciate Ligament (PCL) originates from the posterior part of the tibia, and by crossing the ACL, it extends to the anterior part of the femoral condyle at the intercondylar notch. The cruciate

ligaments control the AP translation during different activities. In fact, tightening of the ACL prevents the femur from sliding off the tibia as the tibia moves anteriorly, and the PCL restrains the sliding of the tibia to the rear. On the sides of the knee joint are the Medial and Lateral Collateral Ligaments (MCL and LCL), which provide stability in the medial-lateral direction. It has been reported by Amiri et al. [28] that the LCL plays a critical role in controlling the passive motion of the knee joint by constraining the posterior displacement of the tibia while restraining its external rotation.

As it is shown in Figure 1-3, two wedge-shaped disks separate the femur and tibia which are called menisci. The medial meniscus is almost a semicircle in shape, while the lateral one is about four-fifth of the circle and covers a larger area than the medial one. The menisci distribute the load by deforming under the imposed weight, and by increasing the contact area at the articulation. They also cushion the extremes of flexion and extension [24].

Total knee replacement

When tibiofemoral articulating surfaces of the knee joint get damaged, knee implants replace the resected cartilage and bone parts. In the current designs of total knee replacements a metallic femoral part articulates with a polyethylene tibial insert (Chapter 2). Long term satisfaction of the patients and survival of the TKR depends on better restoration of normal joint feel, stability, range of motion, and function. Biomechanical factors including kinematics, contact stresses, and wear at the polyethylene tibial plateau have been used to verify and validate the performance of the knee implants [30].

The Freeman–Swanson knee implant [31] is known as the first condylar knee replacement [32], which has been the inspiring concept for a large variety of condylar knee replacement designs with the goal of providing close to normal knee laxity and stability. In order to provide a mechanism to control the posterior displacement of the femoral component through high flexion and to avoid anterior paradoxical motion, the condylar and intercondylar guiding features were added to the design of the knee implants [33]. The studies of the kinematics behavior of the total knee replacements show that the normal relative motion of the tibiofemoral joint alters, which results into a reduced range of motion, insufficient control over the femoral rollback, abnormal rotation of the tibia, and finally a knee that does not feel normal [16,34-36]. Peter Walker [32,37], Amiri et al. [21], and the current study in this dissertation develop the concept of guided-motion knees with the goal of achieving motion characteristics similar to the normal anatomic patterns of movement. In this concept, the normal kinematics are considered as the goal for the optimal design, and they are achieved by the interaction of the condylar articulating surfaces of the tibiofemoral components [21,23,37].

Another factor affecting the longevity of a knee implant is the wear of the polyethylene tibial insert bearings, since the accumulation of wear debris in the surrounding tissues can lead to an infection, osteolysis, long-term aseptic loosening, and eventual failure of the implant [38-40]. There are different mechanisms of polyethylene wear including delamination, abrasion, pitting, scratching, burnishing, deformation, and embedded debris. The factors influencing the wear mechanism and amount of wear generation include:

- kinematics after TKR [39-43]
- design of the implant, including geometric features of the contacting surfaces [38-40,44]

- material properties of the bearings components [39,45,46]
- micro-motion between tibial insert and the backing metal tray [47,48]
- alignment of the TKR components [49,50]

The tibiofemoral contact area depends on the articulating geometry of the femoral and tibial components. Bearing surface designs with more conformity allows distribution of the joint load over a larger contact area, which results into a decrease of contact stresses and better wear resistance characteristics. In addition, lower conformity of the bearing surfaces is discussed to be correlated with more AP sliding and an increase in wear volume [51]. Blunn et al. [38] reported that in the TKR designs with high conformity, rotational restrictions and sudden changes in the radii of curvature result into delamination of the PE surface. Abrasive wear due to the entrapped cement particles was also among the wear mechanisms that Blunn et al. [38] reported for high conformity designs.

A combination of rolling, sliding (in anterior-posterior and medial-lateral directions), and flexion-extension, as well as internal-external rotation induces shear stress and tractive forces leading to different mechanisms of wear in the knee [39,40,42,52]. Increased range of translational and rotational motions have shown to raise the PE wear [39,39,41,53,54]. Kawanabe et al. [53] reported that the wear track would extend posteriorly with considering a combination of rolling and sliding motions as the femoral component translates backward on the tibial plateau. Willing et al. [55] quantified the conflict that exists in the relationship between the volumetric wear and kinematic performance based on the maximum flexion angle and stability in comparison to a normal knee. In general, preclinical testing of wear and kinematic behavior of a TKR is necessary to evaluate its success and functionality.

References

[1] The Arthritis Society. 2013. *Arthritis in Canada: Arthritis Community Research and Evaluation Unit (ACREU)*.

[2] Public Health Agency of Canada. 2010. *Life with Arthritis in Canada: A Personal and Public Health Challenge*.

[3] Bombardier, Claire, G. Hawker, and D. Mosher. 2011. "The Impact of Arthritis in Canada: Today and Over the Next 30 Years." *Toronto, CA: Arthritis Alliance of Canada*.

[4] Murphy, Louise B., T. A. Schwartz, C. G. Helmick, J. B. Renner, G. Tudor, G. Koch, A. Dragomir, W. D. Kalsbeek, G. Luta, and J. M. Jordan. 2008. "Lifetime Risk of Symptomatic Knee Osteoarthritis." *Arthritis Care & Research* 59 (9): 1207-1213.

[5] Murphy, Louise B., S. Moss, B. T. Do, C. G. Helmick, T. A. Schwartz, K. E. Barbour, J. Renner, W. Kalsbeek, and J. M. Jordan. 2016. "Annual Incidence of Knee Symptoms and Four Knee Osteoarthritis Outcomes in the Johnston County Osteoarthritis Project." *Arthritis Care & Research* 68 (1): 55-65.

[6] "American Academy of Orthopaedic Surgeons.", http://orthoinfo.aaos.org/topic.cfm?topic=A00591.

[7] United States Bone and Joint Initiative. 2014. *The Burden of Musculoskeletal Diseases in the United States (BMUS)*.

[8] Hip and Knee Replacements in Canada: Canadian Joint Replacement Registry 2016. Ottawa, ON: Canadian Institute for Health Information (CIHI).

[9] Kurtz, Steven M., E. Lau, K. Ong, K. Zhao, M. Kelly, and K. J. Bozic. 2009. "Future Young Patient Demand for Primary and Revision Joint Replacement: National Projections from 2010 to 2030." *Clinical Orthopaedics and Related Research®* 467 (10): 2606-2612.

[10] Kurtz, Steven M., K. Ong, E. Lau, F. Mowat, and M. Halpern. 2007. "Projections of Primary and Revision Hip and Knee Arthroplasty in the United States from 2005 to 2030." *The Journal of Bone and Joint Surgery. American* Volume 89 (4): 780-785.

[11] Bourne, Robert B., B. M. Chesworth, A. M. Davis, N. N. Mahomed, and K. D. J. Charron. 2010. "Patient Satisfaction after Total Knee Arthroplasty: Who is Satisfied and Who is Not?" *Clinical Orthopaedics and Related Research®* 468 (1): 57-63.

[12] Baker, Paul N., J. H. van der Meulen, J. Lewsey, P. J. Gregg, and National Joint Registry for England and Wales. 2007. "The Role of Pain and Function in Determining Patient Satisfaction After Total Knee Replacement. Data from the National Joint Registry for England and Wales." *The Journal of Bone and Joint Surgery. British* Volume 89 (7): 893-900.

[13] Robertsson, Otto, M. Dunbar, T. Pehrsson, K. Knutson, and L. Lidgren. 2000. "Patient Satisfaction After Knee Arthroplasty: A Report on 27,372 Knees Operated on between 1981 and 1995 in Sweden." *Acta Orthopaedica Scandinavica* 71 (3): 262-267.

[14] Rand, James A., R. T. Trousdale, D. M. Ilstrup, and W. S. Harmsen. 2003. "Factors Affecting the Durability of Primary Total Knee Prostheses." *The Journal of Bone and Joint Surgery. American* Volume 85-A (2): 259-265.

[15] Dennis, Douglas A., R. D. Komistek, and M. R. Mahfouz. 2003. "In Vivo Fluoroscopic Analysis of Fixed-Bearing Total Knee Replacements." *Clinical Orthopaedics and Related Research* 410 (410): 114-130.

[16] Dennis, Douglas A., R. D. Komistek, S. A. Walker, E. J. Cheal, and J. B. Stiehl. 2001. "Femoral Condylar Lift-Off in Vivo in Total Knee Arthroplasty." *The Journal of Bone and Joint Surgery. British* Volume 83 (1): 33-39.

[17] Victor, Jan, S. A. Banks, and J. Bellemans. 2005. "Kinematics of Posterior Cruciate Ligament-Retaining and -Substituting Total Knee Arthroplasty: A Prospective Randomized Outcome Study." *The Journal of Bone and Joint Surgery. British* Volume 87 (5): 646-655.

[18] Horiuchi, Hiroshi, S. Akizuki, T. Tomita, K. Sugamoto, T. Yamazaki, and N. Shimizu. 2012. "In Vivo Kinematic Analysis of Cruciate-Retaining Total Knee Arthroplasty during Weight-Bearing and non–weight-Bearing Deep Knee Bending." *The Journal of Arthroplasty* 27 (6): 1196-1202.

[19] Kuroyanagi, Yuji, S. Mu, S. Hamai, W. J. Robb, and S. A. Banks. 2012. "In Vivo Knee Kinematics during Stair and Deep Flexion Activities in Patients with Bicruciate Substituting Total Knee Arthroplasty." *The Journal of Arthroplasty* 27 (1): 122-128.

[20] Victor, Jan, J. K. P. Mueller, R. D. Komistek, A. Sharma, M. C. Nadaud, and J. Bellemans. 2010. "In Vivo Kinematics after a Cruciate-Substituting TKA." *Clinical Orthopaedics and Related Research®* 468 (3): 807-814.

[21] Amiri, Shahram, T. D. V. Cooke, and U. P. Wyss. 2011. "Conceptual Design for Condylar Guiding Features of a Total Knee Replacement." *Journal of Medical Devices* 5 (2): 025001-1.

[22] Wyss, Urs, S. Amiri, and T. D. V. Cooke. 2010. *Knee Prosthesi*s.Patent: US20120179265.

[23] Pejhan, Shabnam, E. Bohm, J. M. Brandt, and U. Wyss. 2016. "Design and Virtual Evaluation of a Customized Surface-Guided Knee Implant." *Proc IMechE Part H: J Engineering in Medicine* 230 (10): 949-961.

[24] Drake, Richard, A. W. Vogl, and A. W. M. Mitchell. 2014. *Gray's Anatomy for Students,* Elsevier Health Sciences.

[25] Pinskerova, Vera, P. Johal, S. Nakagawa, A. Sosna, A. Williams, W. Gedroyc, and M. A. Freeman. 2004. "Does the Femur Roll-Back with Flexion?" *The Journal of Bone and Joint Surgery. British* Volume 86 (6): 925-931.

[26] Iwaki, H., V. Pinskerova, and M. A. R. Freeman. 2000. "Tibiofemoral Movement 1: The Shapes and Relative Movements of the Femur and Tibia in the Unloaded Cadaver Knee." *Journal of Bone & Joint Surgery, British* Volume 82 (8): 1189-1195.

[27] Masouros, Spyros D., A. M. J. Bull, and A. A. Amis. 2010. "(i) Biomechanics of the Knee Joint." *Orthopaedics and Trauma* 24 (2): 84-91.

[28] Amiri, Shahram, D. Cooke, I. Y. Kim, and U. Wyss. 2007. "Mechanics of the Passive Knee Joint. Part 2: Interaction between the Ligaments and the Articular Surfaces in Guiding the Joint Motion." *Proceedings of the Institution of Mechanical Engineers. Part H, Journal of Engineering in Medicine* 221 (8): 821-832.

[29] Blankevoort, Leendert, R. Huiskes, and A. De Lange. 1991. "Recruitment of Knee Joint Ligaments." *Journal of Biomechanical Engineering* 113 (1): 94-103.

[30] Carr, Brandi C. and T. Goswami. 2009. "Knee implants–Review of Models and Biomechanics." *Materials & Design* 30 (2): 398-413.

[31] Freeman, Michael A. R., S. A. V. Swanson, and R. C. Todd. 1973. "Total Replacement of the Knee using the Freeman-Swanson Knee Prosthesis." *Clinical Orthopaedics and Related Research* 94: 153-170.

[32] Walker, Peter S. 2014. "Application of a Novel Design Method for Knee Replacements to Achieve Normal Mechanics." *The Knee* 21 (2): 353-358.

[33] Walker, Peter S. and S. Sathasivam. 2000. "Controlling the Motion of Total Knee Replacements using Intercondylar Guide Surfaces." *Journal of Orthopaedic Research* 18 (1): 48-55.

[34] Walker, Peter S. 2015. "The Design and Pre-Clinical Evaluation of Knee Replacements for Osteoarthritis." *Journal of Biomechanics* 48 (5): 742-749.

[35] Pritchett, James W. 2004. "Patient Preferences in Knee Prostheses." *The Journal of Bone and Joint Surgery. British* Volume 86 (7): 979-982.

[36] Dennis, Douglas A., R. D. Komistek, M. R. Mahfouz, B. D. Haas, and J. B. Stiehl. 2003. "Multicenter Determination of in Vivo Kinematics after Total Knee Arthroplasty." *Clinical Orthopaedics and Related Research* (416) (416): 37-57.

[37] Walker, Peter S. 2001. "A New Concept in Guided Motion Total Knee Arthroplasty." *The Journal of Arthroplasty* 16 (8): 157-163.

[38] Blunn, Gordon W., A. B. Joshi, R. J. Minns, L. Lidgren, P. Lilley, L. Ryd, E. Engelbrecht, and P. S. Walker. 1997. "Wear in Retrieved Condylar Knee Arthroplasties: A Comparison of Wear in Different Designs of 280 Retrieved Condylar Knee Prostheses." *The Journal of Arthroplasty* 12 (3): 281-290.

[39] McEwen, HMJ, PI Barnett, CJ Bell, R. Farrar, DD Auger, MH Stone, and J. Fisher. 2005. "The Influence of Design, Materials and Kinematics on the in Vitro Wear of Total Knee Replacements." *Journal of Biomechanics* 38 (2): 357-365.

[40] Naudie, Douglas D. R., D. J. Ammeen, G. A. Engh, and C. H. Rorabeck. 2007. "Wear and Osteolysis around Total Knee Arthroplasty." *Journal of the American Academy of Orthopaedic Surgeons* 15 (1): 53-64.

[41] Kretzer, Philippe J., E. Jakubowitz, R. Sonntag, K. Hofmann, C. Heisel, and M. Thomsen. 2010. "Effect of Joint Laxity on Polyethylene Wear in Total Knee Replacement." *Journal of Biomechanics* 43 (6): 1092-1096.

[42] Patten, Eli W., D. Van Citters, M. D. Ries, and L. A. Pruitt. 2013. "Wear of UHMWPE from Sliding, Rolling, and Rotation in a Multidirectional Tribo-System." *Wear* 304 (1): 60-66.

[43] Barnett, Petra I., J. Fisher, D. D. Auger, M. H. Stone, and E. Ingham. 2001. "Comparison of Wear in a Total Knee Replacement under Different Kinematic Conditions." *Journal of Materials Science: Materials in Medicine* 12 (10-12): 1039-1042.

[44] Willing, Ryan and I. Y. Kim. 2009. "Three Dimensional Shape Optimization of Total Knee Replacements for Reduced Wear." *Structural and Multidisciplinary Optimization* 38 (4): 405-414.

[45] Tanner, Michael G., L. A. Whiteside, and S. E. White. 1995. "Effect of Polyethylene Quality on Wear in Total Knee Arthroplasty." *Clinical Orthopaedics and Related Research* 317: 83-88.

[46] Muratoglu, Orhun K., A. Mark, D. A. Vittetoe, W. H. Harris, and H. E. Rubash. 2003. "Polyethylene Damage in Total Knees and use of Highly Crosslinked Polyethylene." *The Journal of Bone and Joint Surgery. American* Volume 85-A Suppl 1: S7-S13.

[47] Conditt, Michael A., M. T. Thompson, M. M. Usrey, S. K. Ismaily, and P. C. Noble. 2005. "Backside Wear of Polyethylene Tibial Inserts: Mechanism and Magnitude of Material Loss." *The Journal of Bone and Joint Surgery. American* Volume 87 (2): 326-331.

[48] O'Brien, Sean, Y. Luo, C. Wu, M. Petrak, E. Bohm, and J. M. Brandt. 2013. "Computational Development of a Polyethylene Wear Model for the Articular and Backside Surfaces in Modular Total Knee Replacements." *Tribology International* 59: 284-291.

[49] Hernigou, P., A. Poignard, P. Filippini, and S. Zilber. 2008. "Retrieved Unicompartmental Implants with Full PE Tibial Components: The Effects of Knee Alignment and Polyethylene Thickness on Creep and Wear." *The Open Orthopaedics Journal* 2: 51-56.

[50] Laz, Peter J., S. Pal, A. Fields, A. J. Petrella, and P. J. Rullkoetter. 2006. "Effects of Knee Simulator Loading and Alignment Variability on Predicted Implant Mechanics: A Probabilistic Study." *Journal of Orthopaedic Research* 24 (12): 2212-2221.

[51] Benjamin, James, J. Szivek, G. Dersam, S. Persselin, and R. Johnson. 2001. "Linear and Volumetric Wear of Tibial Inserts in Posterior Cruciate-Retaining Knee Arthroplasties." *Clinical Orthopaedics and Related Research* 392: 131-138.

[52] Wimmer, Markus A. and T. P. Andriacchi. 1997. "Tractive Forces during Rolling Motion of the Knee: Implications for Wear in Total Knee Replacement." *Journal of Biomechanics* 30 (2): 131-137.

[53] Kawanabe, Keiichi, I. C. Clarke, J. Tamura, M. Akagi, V. D. Good, P. A. Williams, and K. Yamamoto. 2001. "Effects of A–P Translation and Rotation on the Wear of UHMWPE in a Total Knee Joint Simulator." *Journal of Biomedical Materials Research* 54 (3): 400-406.

[54] Cornwall, Bryan G., J. T. Bryant, and C. M. Hansson. 2001. "The Effect of Kinematic Conditions on the Wear of Ultrahigh Molecular Weight Polyethylene (UHMWPE) in Orthopaedic Bearing Applications." *Proc IMechE Part H: J Engineering in Medicine* 215 (1): 95-106.

[55] Willing, Ryan and I. Y. Kim. 2012. "Quantifying the Competing Relationship between Durability and Kinematics of Total Knee Replacements using Multiobjective Design Optimization and Validated Computational Models." *Journal of Biomechanics* 45 (1): 141-147.

Chapter 2

Design of a Customized Surface-Guided Total Knee Replacement

Abstract

Total knee replacement (TKR) is generally a successful operation aiming to provide patients with close to normal knee function, as well as relieving pain. However, many studies have shown that a TKR can result in significant changes in the kinematics of the joint, causing limitations in the flexion range, and performing activities of daily living [1-3]. The design of the tibiofemoral articulating surfaces contributes to kinematic characteristics and patterns of motion after knee arthroplasty. This chapter defines the design features for a customized surface-guided total knee replacement with the goal of achieving a target normal motion pattern. MRI data of the knee joint was used to generate the design features, as they relate to the functionality of the implant. This design aims to guide the motion by a partial ball and socket configuration on the medial side, and varying radii of the curvature on the lateral articulating surfaces. Therefore, any guiding feature at the intercondylar space is avoided. Major design features included location and orientation of the flexion-extension and pivoting

axes, the trace of the contact points on the tibia, and the radii of the guiding arcs on the lateral condyle.

Introduction

One of the initial designs of the knee implants is the Themistocles Gluck [5] hinge joint knee made of ivory, that was only able to provide the flexion and extension rotations. Nevertheless, that joint failed very soon within a few months due to chronic infection caused by the lack of antibiotics [5]. Evolutions of the knee replacement implants with the concept of mimicking normal knee motion is based on the first non-hinged implant designed by Frank Gunston in 1968 [5,6]. Frank Gunston considered separate artificial components to replace the medial and lateral condyles, while the collateral and cruciate ligaments were retained [6]. Since then, numerous types of designs for the knee implants have been developed and used by surgeons throughout the world.

Reviewing the development of different knee implants, Carr and Goswami [7] report that at least 150 different designs have been developed and used in the market. Knee implants are different in geometric shape, stability and motion control mechanism, materials, fixation and surgical methods. However, a typical knee implant includes a tibial component usually made from ultra-high molecular weight polyethylene (UHMWPE) with titanium (Ti) or cobalt-chrome (CoCr) alloy backing, and a femoral compartment that is usually made of cobalt-chrome (CoCr) alloy. If the patella needs to be replaced, a dome-shaped polymer patellar component with or without metal backing will also substitute the articulating surface of the worn patella. (Figure 2-1)

Based on the design of the tibial insert, the implant would be categorized as fixed or mobile bearing. In the fixed insert design, the tibial insert is clipped to the tibial tray, or a unit of the tibial component is fixed to the bone. On the other hand, in mobile designs, the tibial insert slides or rotates to some extent on a tray. It is reported that the second approach requires more support from soft tissues to avoid the dislocation of the implant [8].

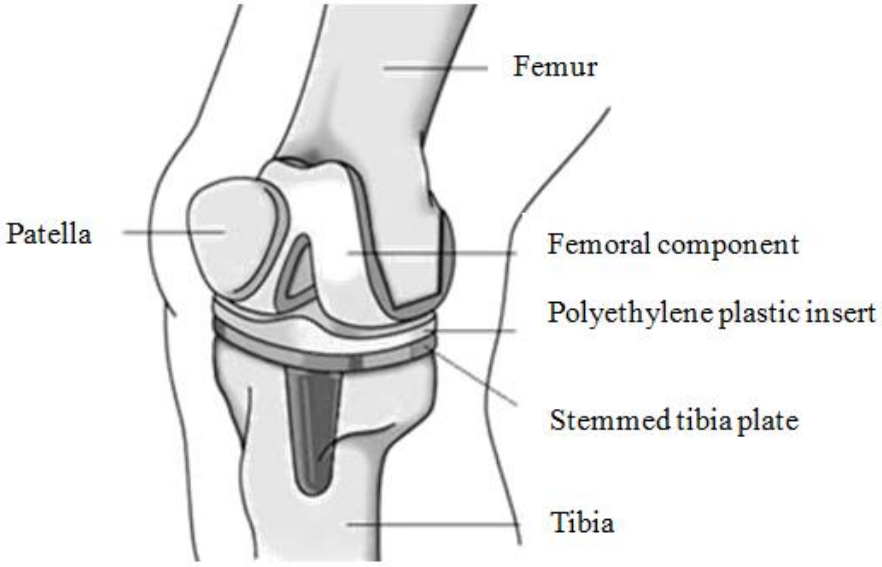

Figure 2-1 Typical components of a TKR- Reproduced with permission from OrthoInfo. © American Academy of Orthopaedic Surgeons. http://orthoinfo.aaos.org [8]

During normal healthy knee joint flexion, two major motions occur at the same time, an unequal posterior roll-back of the femur on the tibia and internal rotation of the tibia [9-14]. The surface geometry guides the motion, and the cruciate ligaments mainly provide the stability and control the movement [11,15,16]. Another criterion for categorizing the design of the implants is the type of the cruciate ligaments that could be retained during TKR. In the "cruciate retaining (CR)" designs (Figure 2-2), the PCL is the ligament that is usually retained. Nevertheless, the paradoxical tibiofemoral motion of the femur, forward sliding during flexion,

is a major problem reported about the knee implants, especially for the CR designs, and mostly on the medial side [2,17,18]. If the PCL has to be removed, the implant should be able to stabilize the knee movement and substitute the posterior cruciate ligament function. One group of such implant designs are the "Posterior Stabilized (PS)" knees (Figure 2-2).

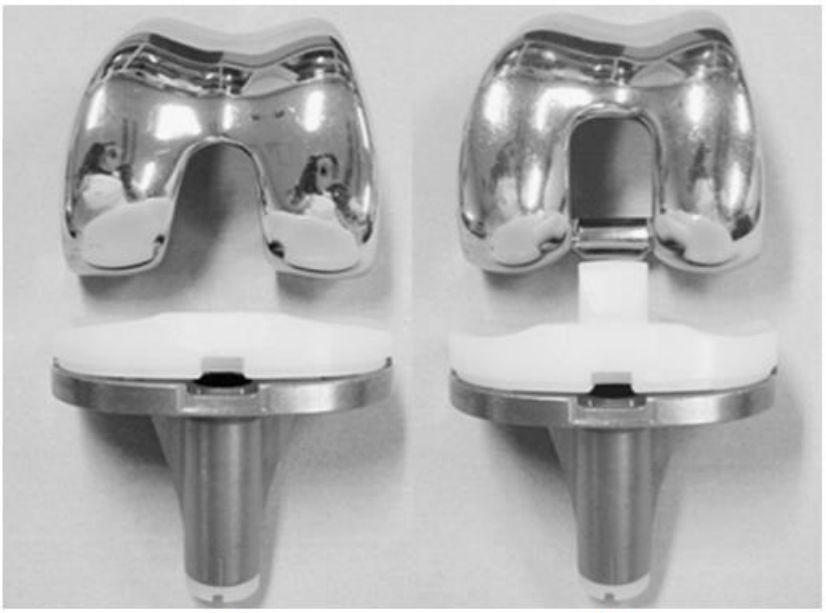

Figure 2-2 (a) Cruciate retaining design (NexGen CR-Flex Knee by Zimmer) (b) Posterior Stabilizing design (NexGen Legacy PS Knee by Zimmer) - adapted with permission from "High-flex posterior cruciate-retaining vs posterior cruciate-substituting designs in simultaneous bilateral total knee arthroplasty: a prospective, randomized study", by K. Yagishita et al., The Journal Of Arthroplasty, 27(3), p.368:374 [19], with permission from Elsevier

In a PS design, the tibial component has a raised surface with an internal post fitting into a bar called the "cam" on the femoral component. The cam-post mechanism in posterior stabilizing knees aims to prevent paradoxical motion; however, this would only happen when the cam-post mechanism becomes active, usually in higher degrees of flexion. Also, the absence of the ACL still lets the tibia slide forward and puts the femur more posteriorly in the initial

position (Figure 2-3). Therefore, as the knee bends, the femoral condyles move forward to compensate such a posterior initial location [3,20]. Numerous studies compare the CR and PS designs considering the functionality, range of motion, and wear of the polyethylene inserts. However, there is still a continuing debate on the superiority of any of these two design concepts [19,21-28].

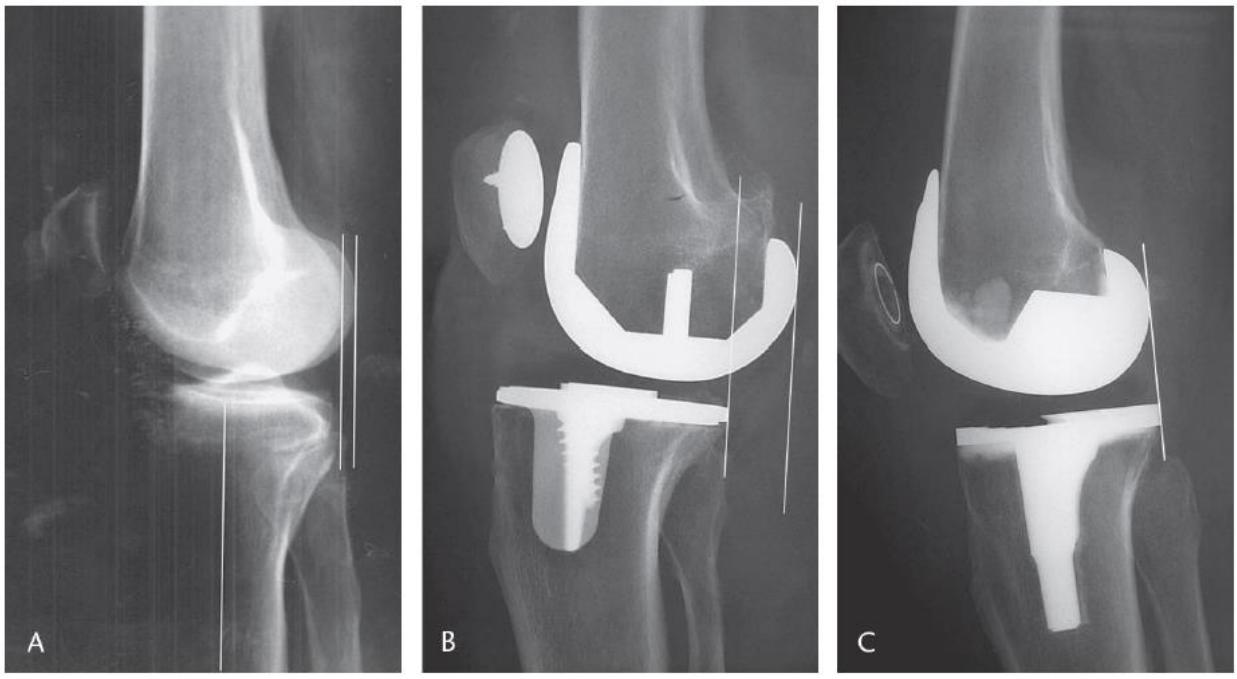

Figure 2-3 Sagittal view of the tibiofemoral joint near full extension (a) normal knee with posterior condyle lined up with the posterior border of the tibia (b) posteriorly located lateral femoral condyle after TKR which causes an anterior slide as knee flexes (c) close to normal orientation after TKR with an implant having physiological sagittal geometry - adapted with permission from "Physiologic kinematics as a concept for better flexion in TKA", by J. Victor and Johan Bellemans, Clinical Orthopaedics and Related Research, 452, p.53:58 [20]

Limitations in the design of the surface geometries, anterior cruciate ligament deficiency after TKA, and the inability of the posterior cruciate ligament (PCL) in performing its function in the absence of the anterior cruciate ligament (ACL), cause abnormal kinematics of the artificial

tibiofemoral joint. Major indications that are reported for such an altered kinematics include different direction of rotation in comparison with the normal knee, anterior sliding of the femur on the tibia, and the abnormal adduction and abduction center, which causes the lateral femoral condyle "lift-off". The altered kinematics result in decreased range of motion and cause limitations on performing activities of daily living. [2,17,18,29-31]

Another design concept for mimicking the constraining performance of the cruciate ligaments is the surface guiding design, in which the required guidance of the tibiofemoral motion is achieved by creating specially shaped articulating surfaces on the femoral condyles and the corresponding tibial plateau [32-35]. In recent years, a few conceptual designs of the surface-guided TKR have emerged by Peter Walker [33,34,36], and Amiri and colleagues [32,37]. In the surface-guided knees, the shape of the tibiofemoral articulating surfaces guides the motion with little or no dependence on the cruciate ligaments, or the intercondylar post and cam. It is theorized that such a design concept can provide the required guidance for normal kinematics, which in turn could improve clinical results and increase the level of satisfaction of patients.

Peter Walker [34] described a variety of the surface-guided knee designs from the "Condylar Guided Motion" to the "Intercondylar Guided Motion" designs. In the "Condylar Guided Motion" concept suggested by Walker et al. [33], the lateral femoral compartment is created by continuous variation of the frontal radius along with a reduction in the bearing space at each increment of flexion, while the medial condyle has a constant radius. The bearing distance is described as the distance between the medial and lateral contact points at each increment of motion [32,33]. In the concept introduced by Amiri et al. [32], a constant bearing distance is

considered throughout the motion, and the variation of the internal and external radii of the contact profiles, named as the "guiding curves," produces enforced gliding and rolling movement at the tibiofemoral joint. In both of these conceptual designs, the interaction between the tibiofemoral articulating surfaces defines the location and orientation of the femur on the tibia.

One of the main features in the proposed surface-guided knee designs is the medial constraint [32,33]. The concept of medial pivoting in the design of the implants is based on the idea that a combination of medial pivoting and lateral roll-back of the femoral condyle occurs during a significant range of flexion of a normal healthy knee joint [2,9,38]. Some roll back of the medial condyle at deep flexion (beyond 120°) is reported in the literature [10,38]. However, a major assumption in a medial pivoting design concept is no anterior-posterior (AP) displacement of the center at the medial femoral condyle. Studies about the performance of the medial pivot knee designs report the success of this concept in providing the required functionality [39,40]. Based on a 2-year follow-up study, Bae et al. [39] reported an increase of the Knee Society knee score, the function score, as well as the range of motion of the joint up to 122.8° ± 12.8° for patients with medial pivot TKRs. The result of Pritchett's evaluation of 344 patients having TKR on both knees shows that patients prefer designs with ACL and PCL retained or a substituting mechanism with the medial or lateral pivoting [41]. The major reported reasons for such preference included [41]:

- an implant that felt more like a normal knee
- implanted knee strength on stairs
- stability
- experiencing fewer clicks

Another promising approach which has been more widely used in recent years is the patient-specific TKRs. Conventional knee implants are based on an average joint anatomy, but it has been shown that patient's specific anatomical features can positively influence the outcomes, including bone coverage, movement patterns, and the stress distribution within the components [38,42-45]. The initial step of the custom-design method is creating a three-dimensional model of the patient's knee joint from a CT scan or MRI. Then, the outer contour of the implant is generated from the surface data of the patient's bone or cartilage. Therefore, the following factors have a large influence on the accuracy of the reconstructed surface geometries:

- Resolution of the CT/ MRI images
- Distance between image slices
- Process of adjusting the contrast and choosing the appropriate threshold value for segmenting the bone or cartilage area

There are two approaches for the customized TKR design. In the first one, a smooth articulating surface of the femur is created over a set of spline curves along the interface surface of the femur in a radial pattern [42,44]. The second approach is to generate simplified geometries with design parameters extracted from patient's anatomy [46]. Heever [44] introduced a self-organizing map algorithm to predict the unhealthy knee geometries by using a database of healthy knee geometric measurements, as well as some specific reference measurements from the patient. In that algorithm, the healthy knee geometries in a mathematical format (Spline coefficients) were the input. The relationships between the reference measurements from the patient and those input coefficients were identified and

used to predict the articulating geometries in spline format for an unhealthy knee joint [44]. The reference measurements in Heever's study included anterior and posterior length of the joint, mediolateral length, and the distance between the most anterior points on the medial and lateral condyles [44, 46].

The process of custom designing implants for each patient based on CT or MRI data has the following advantages compared with conventional implant designs:

- If the bone-implant interface is also customized, less bone will be resected; however, the technique to provide such an ideal interface on the bone is limited. Harryson et al. [42] reported that up to 40% less bone removal could be achieved for the custom-designed femoral components. [42,43,47]
- Customizing the design of the bone-implant interface would also make the stress at the bone interface more evenly distributed. As a result, bone remodeling would be more uniform, and the risk of loosening would decline. [42]
- A patient-derived constant coronal curvature on the femoral compartment and a matching curved tibial insert provides homogenous contact pressure at different flexion angles. [43]
- Since the positioning and alignment of these implants are based on patient knee anatomy, they would allow for a better fit. [42]

However, customized TKR designs are limited to customization of the anatomic geometry, while other parameters, such as the motion guiding capability, the stability of the TKR,

conformity between the articulating surfaces, and the specific needs of the patients would also affect the kinematics and long-term performance of the implants.

Based on the ultimate goal of restoring a normal range and pattern of motion after TKR, in this study, the design requirements for a customized surface-guided knee implant, based on the concept introduced by Amiri, Wyss and Cooke [37] were investigated. The main objective was to develop the guiding features of the tibiofemoral articulating surfaces, based on the patient's joint geometry with no additional intercondylar feature. Therefore, the shape of the articulating surfaces of the implant was created by extracting the geometrical parameters, including flexion-extension (FE) and pivoting axes and range of radii of guiding arcs, from a patient's MRI.

Methodology

Customized surface-guided TKR design

The 3D models of the bone and cartilage geometry of the knee were created by segmentation of MRI data set from the studies by Guess et al. [48-50]. The features of the MRI scans, as shown in Table 2-1, were almost in agreement with the quality of the images used in the studies on patient-specific knee designs. However, improvement in the quality of the images enhances the accuracy of the extracted parameters.

The image was imported in Mimics 16.00 (Materialise Mimics®, Leuven, Belgium) to reconstruct the 3D surfaces of the joint. As the first step, the contrast was adjusted and the threshold value for generating the regions of bone/cartilage was defined. Segmentation by setting the thresholds means that the pixels with a gray value within the defined range are

separated from the rest of the image. As Harrysson et al. [42] reported, if the threshold value is selected too low, the resulting model would be smaller than the actual knee joint, and vice versa. Since the thresholding function was not sufficient for isolating the bones and cartilage from rest of the image, the "Live Wire" tool was used to define the boundary of the bone and cartilage geometry more precisely.

Table 2-1 Comparison of the MRI specifications with other patient-specific knee designs

	Resolution (Pixels)	Slice distance (mm)	# of slices
MRI from studies by Guess et al. [48-50]	512×512	0.352	192
Heever et al. [44]	512×512	0.412	-
Harrysson et al. [42]	512×512	0.391	217
Mootanah et al. [51]	512×512	0.6	-

The 3D models were then exported into 3-matic v.8.0 (Materialise 3-matic®, Leuven, Belgium) to define the required geometric parameters for the design process. Visible landmarks on the femur and the tibia were used. In addition, the findings of previous studies on the knee functional axes [52,53] were considered to define the required geometric features including the axes of rotation. Two reference axes were used for this design, including mechanical and anatomic axes of the femur and the tibia. By definition, the femoral mechanical axis is the line from the center of the femoral head to the center of the knee joint, and the anatomic axis is the axis of the femoral shaft. For the tibia, the mechanical and anatomic axes are considered to coincide and to be the line from the center of the knee to the center of the ankle joint.

However, the available MRI for this study included only a short distal section of the femur and a short proximal section of the tibia (about 8 cm and 6 cm, respectively). Therefore, a good approximation of the angles between the joint line and the axes of the tibia and the femur was used [52,53] to estimate the orientation of the reference axes. The joint line was defined as the line passing through the distal ends of the medial and lateral femoral condyles (Figure 2-4). Then, the reference axes including the FE axis, mechanical and anatomic axes of the femur, and the tibia longitudinal axis were determined.

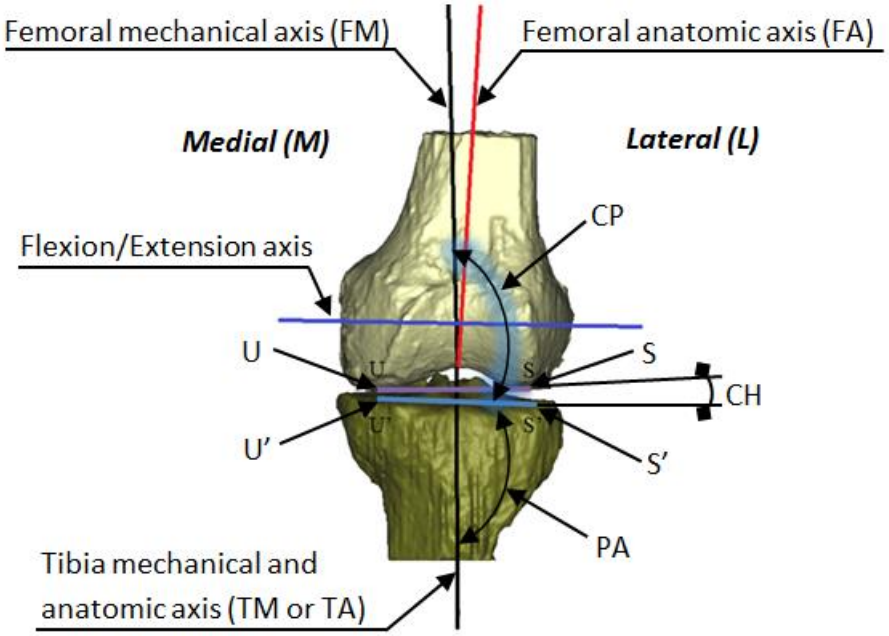

Figure 2-4 Functional axes extracted from a 3D model of the patient's joint MRI [35]

U and S: medial and lateral ends of the femoral distal tangent line; U' and S': medial and lateral ends of the tibial proximal tangent; CP: the angle between the femoral distal tangent and the femoral mechanical axis (1.85°±1.61° [53]); PA: the angle between the tibial proximal tangent and the tibial anatomic axis (3.08°±2.33° [53]); CH: the angle between the femoral distal tangent line and the tibial plateau tangent (3.96°±2.33° [53]).

In the present study, the surface guiding concept introduced by Amiri, Wyss and Cooke [32,37] was implemented as the basis for the design. This TKR aims to achieve a predefined

pattern of motion that included the posterior translation of the femoral condyle and simultaneous external rotation or pivoting of the femoral component around a center of the medial condyle. Therefore, the location and the dimension of the medial partial ball and socket configuration were first determined. As Figure 2-5 illustrates, a sphere was fitted to the posterior part of the tibiofemoral articulating surface on the 3D model of the medial femoral condyle of the patient's joint in 3-matic v.8 (Materialise®, Leuven, Belgium). To set the motion of the knee, the flexion-extension and medial pivoting axes were required. The axis of flexion was considered as a line connecting the centers of the best-fitted spheres to the medial and lateral posterior femoral condyles. The pivoting axis was oriented in the direction of the anatomic axis of the tibia, and it passed the center of the sphere on the medial condyle (Figure 2-5 (a)). The trace of the posterior translation of the femoral condyle over the tibial plateau was determined based on a target pattern of internal-external (IE) rotation or pivoting around the center of the medial condyle.

Two sets of target pivoting angle versus the flexion angle were investigated. In the initial design of the implant, the recommended curve of IE rotation angle by Wyss et al. [37] was considered, in which 12° of pivoting was expected for flexion of 120° of the joint. In the next revision of the design, the target pattern of IE rotation was set as described by Amiri et al. [32] for an unloaded knee pattern of motion, which provided larger range of IE rotation. (Figure 2-5 (b)).The direction of the flexion-extension axes for each increment of motion was defined based on the design target curve.

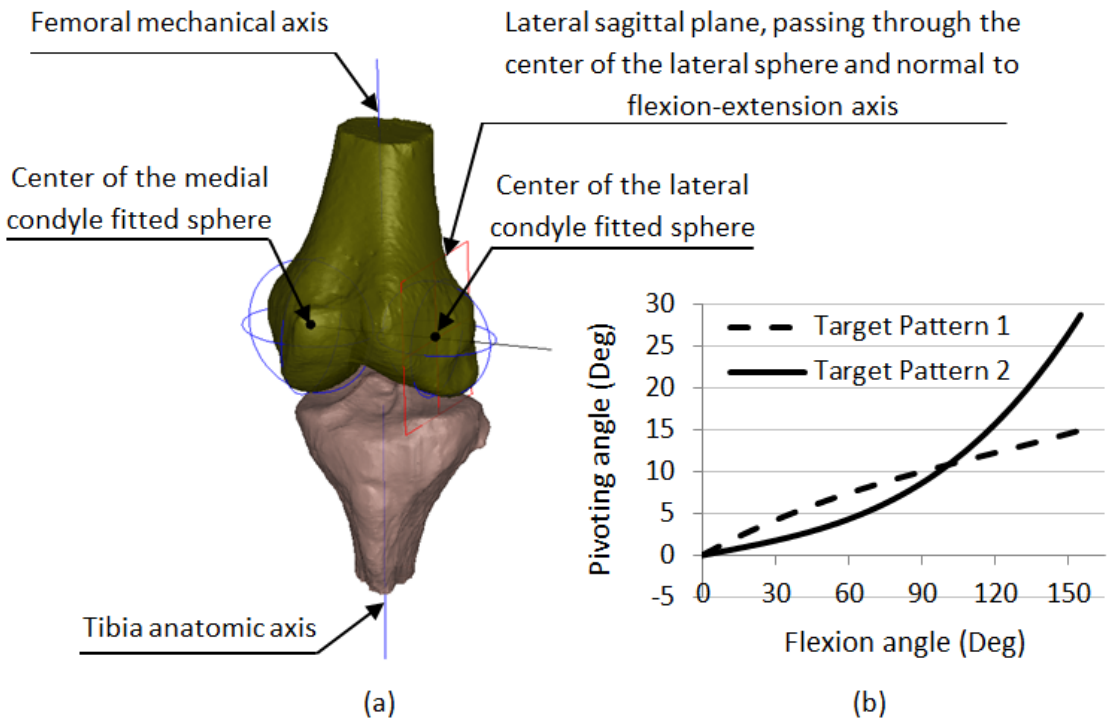

Figure 2-5 a) Reference parameters extracted from MRI data (b) Cubic polynomial curve showing the function between flexion angles and pivoting angle [35]

The articulating surfaces of the joint were generated on reference planes on the tibia and the femur. For each increment of flexion between 0 and 155°, a reference plane on the tibia was defined as a plane including both the flexion and pivoting axes. The lateral sagittal contact points on the tibia were generated by intersecting each reference plane with an arc fitted to the dome shape of the lateral sagittal intersection of the tibia (Figure 2-6). Then, a sphere was created with the center at the same location as the center of the partial medial sphere, and a larger radius equal to 60±25% of the width of the tibial plateau. This sphere was named as "lateral sphere" in Figure 2-6.

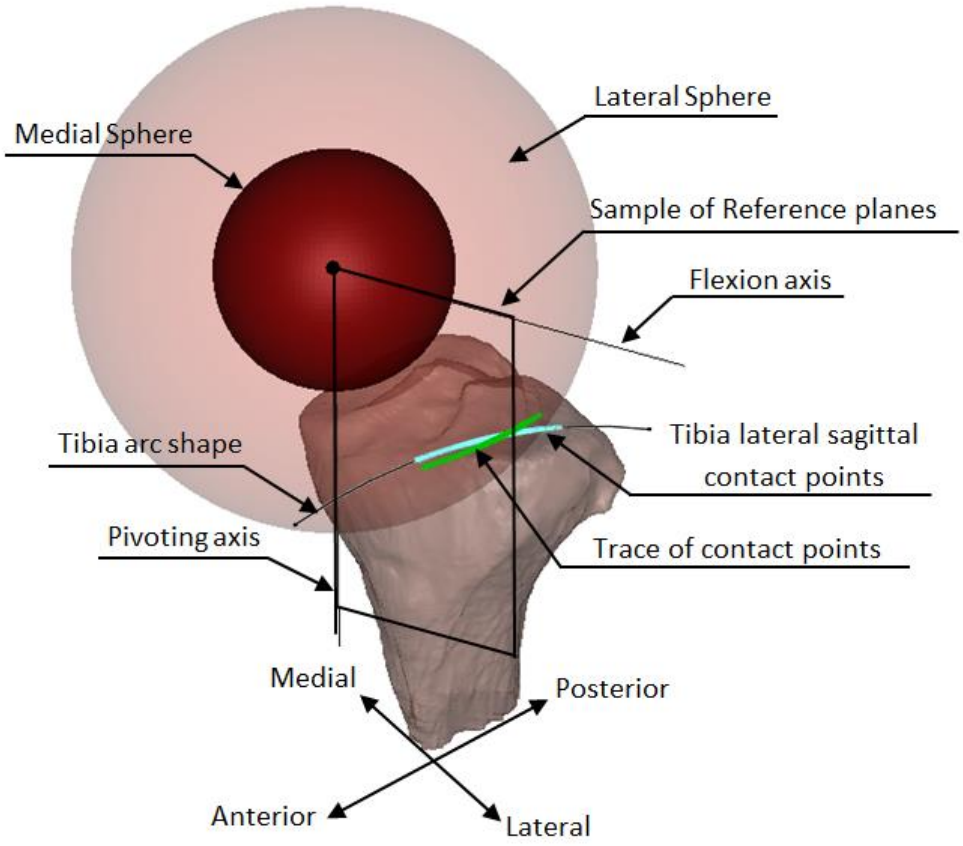

Figure 2-6 Schematic description of trace of contact points defined during design process [35]

By projection of the generated lateral sagittal contact points on the "lateral sphere", the trace of the location of the lateral contact points on the tibial plateau was estimated. In order to evaluate the results, the anterior-posterior distance of each contact point to a line representing the tangent to the posterior cortex of the tibia was measured and compared to the available data in the literature reported for the healthy knees.

Considering the incremental motion of the femur around two axes of flexion-extension and medial pivoting, the orientation of the corresponding common contact point on the femur for each degree of flexion was determined. Then, the femoral reference planes were generated (Figure 2-7 (a)), which passed through the femoral contact points and the pivoting axis. On each

femoral reference plane, two circular inner and outer arcs were drawn, that are named as the "guiding arcs" of the articulating surface on the lateral side. These arcs were tangent to each other at the contact point, and their radius was defined such that the articulating surface followed the geometric shape of the 3D model of the patient's lateral femoral condyle. Also, the radius of the inner and outer guiding arcs gradually changed in opposite directions with increasing or decreasing of the flexion angles. Since the trace of the common contact points on the lateral femoral condyle was generated on a spherical surface with the same center as the partial medial sphere, the distance between medial and lateral contact point remained constant throughout the motion (Figure 2-7 (a)). Therefore, the difference between the radii of the inner and outer arcs makes the femur roll and glide over the tibia as knee flexes or extends. Then, the surface of the femoral lateral side was created by using the trace of the contact points and the guiding arcs on each reference plane. On the medial side, the generated partial sphere was trimmed to fit the width of the extracted 3D model of the patient's joint. The anterior and patellofemoral surfaces of the femoral component were created by following the geometric shape of the anterior and proximal sections of the patient's femoral 3D model.

In the process of generating the tibial insert, the matching inner and outer guiding arcs were first created on the tibial reference planes. Similar to the femoral guiding arcs, the tibial arcs passed through the common contact points on the tibial plateau, and they were tangent to each other. Then, the surface of the tibial lateral side was created by using the trace of the contact points and the guiding arcs on each reference plane of the tibia. This surface was then subtracted from a box-shaped part, which represented the tibia profile at the cut intersection.

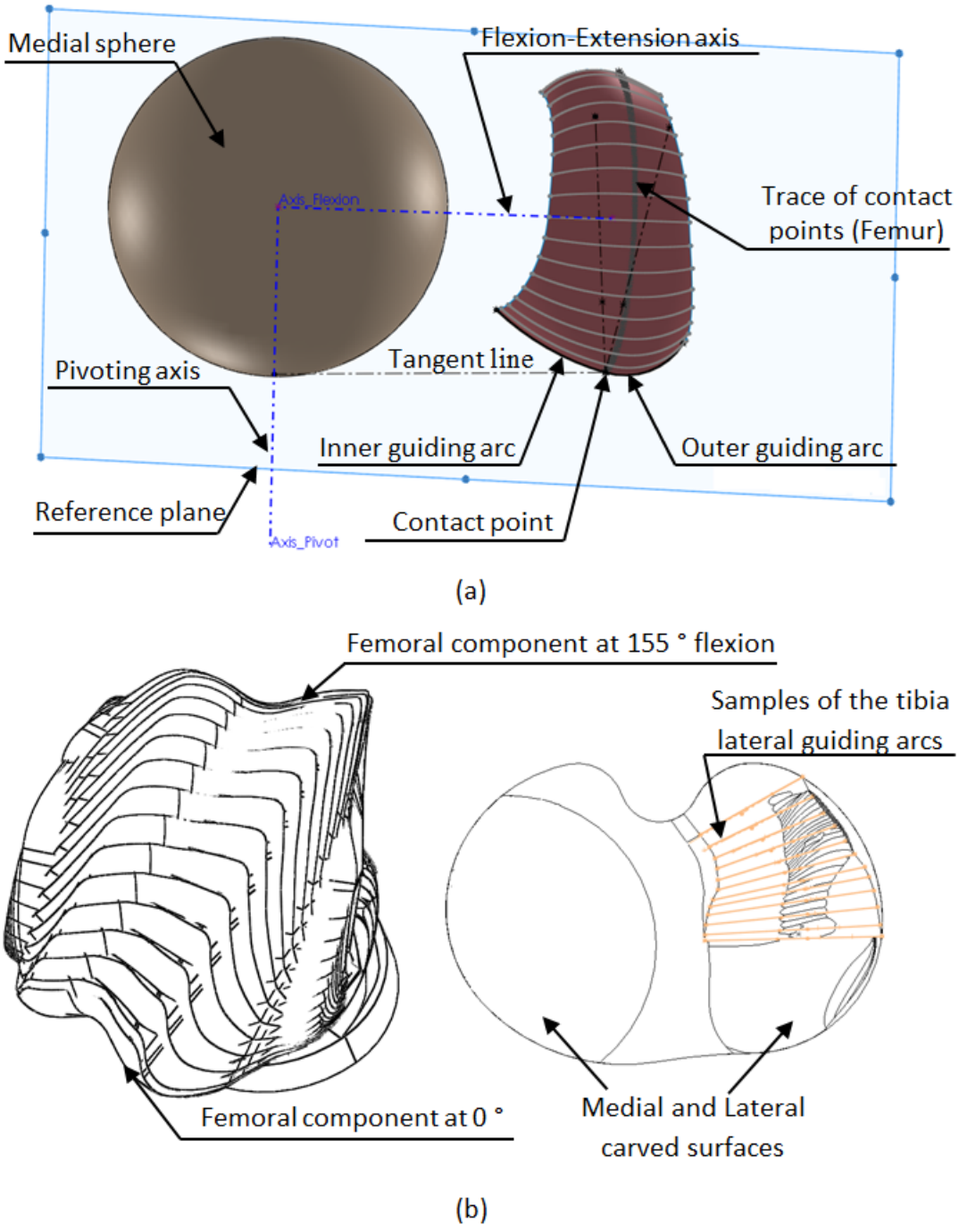

Figure 2-7 (a) Design features of the medial and lateral femoral condyles (b) Schematic of the process for generation of the tibial insert by orientating the femur at each increment of motion [35]

Finally, the tibia was carved by incrementally moving the designed femoral part around the FE and the pivoting axes, and subtracting the overlapping sections between the femoral part

and the solid tibial part at each degree of flexion. (Figure 2-7 (b)). The solid models of the femoral and tibial components were made in the SolidWorks (©Dassault Systemes), and the final surfaces before printing the prototypes were generated in 3-matic v.8 (©Materialise NV, Leuven, Belgium).

Results

Design of the surface-guided TKR

Dimensions of the critical design parameters of the customized surface-guided implant are summarized in Table 2-2. This table describes the initial design that is based on the desired target pattern number 1. The distance between the medial and the lateral contact points at each increment of motion was fixed and equal to 50.1 mm for this implant. Moreover, in the proposed surface-guided implant, the radius of the inner arc of the lateral articulating condyle increased up to 3.62 times, while the radius of outer arc decreased by almost the same amount (3.51 times). (Figure 2-8)

Table 2-2 Dimensions of the implant

TKR component	Dimensions in mm	
Tibia	Medial-lateral width	71.5
	Anterior-posterior length[a]	41.2
Femur	Medial-lateral width	83.2
	Radius of the partial medial sphere	26.1

a. AP length describes the average of the measurements on medial plateau, central section, and lateral plateau

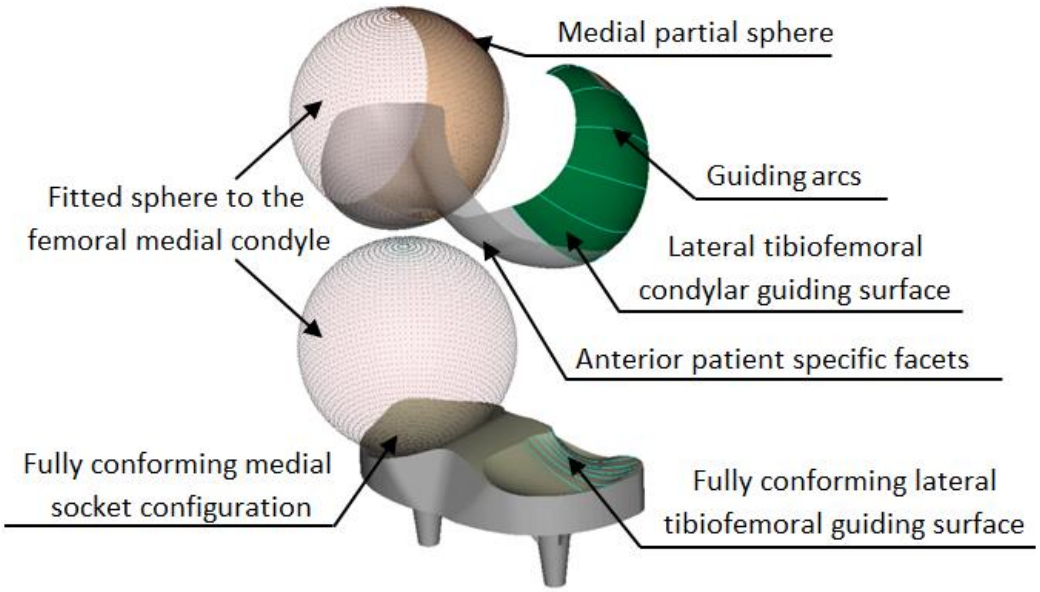

Flexion angle (Deg.)	Radius of inner guiding arc (mm)	Radius of outer guiding arc (mm)
0	40	11
30	28.55	13.98
60	19.93	18.22
90	16.63	23.39
120	12.45	30.22
150	11.03	38.51

Figure 2-8 CAD model of the customized surface-guided implant [35]

The trace of contact points on the tibia at the lateral sagittal plane was one of the critical inputs in this design concept. The distance of the defined contact points to the posterior cortex line (a line passing through the most posterior point of the tibia on the lateral sagittal plane) showed agreement with the similarly measured distance reported by previous studies of the normal knee kinematics [38]. As a comparison, the distance between the predicted contact points for the surface-guided implant to the posterior cortex line is plotted for each flexion angle in Figure 2-9. This figure shows that the predicted contact points are in almost the same distance as what Pinskerova et al. [38] measured for the unloaded and loaded knee in normal

subjects. The distance of the medial center point to the posterior cortex line was considered constant and equal to 19.2 mm, which was in agreement with the 20 to 23 mm distance that was reported for 120 degrees of flexion of the healthy knee joint by Pinskerova et al.[38].

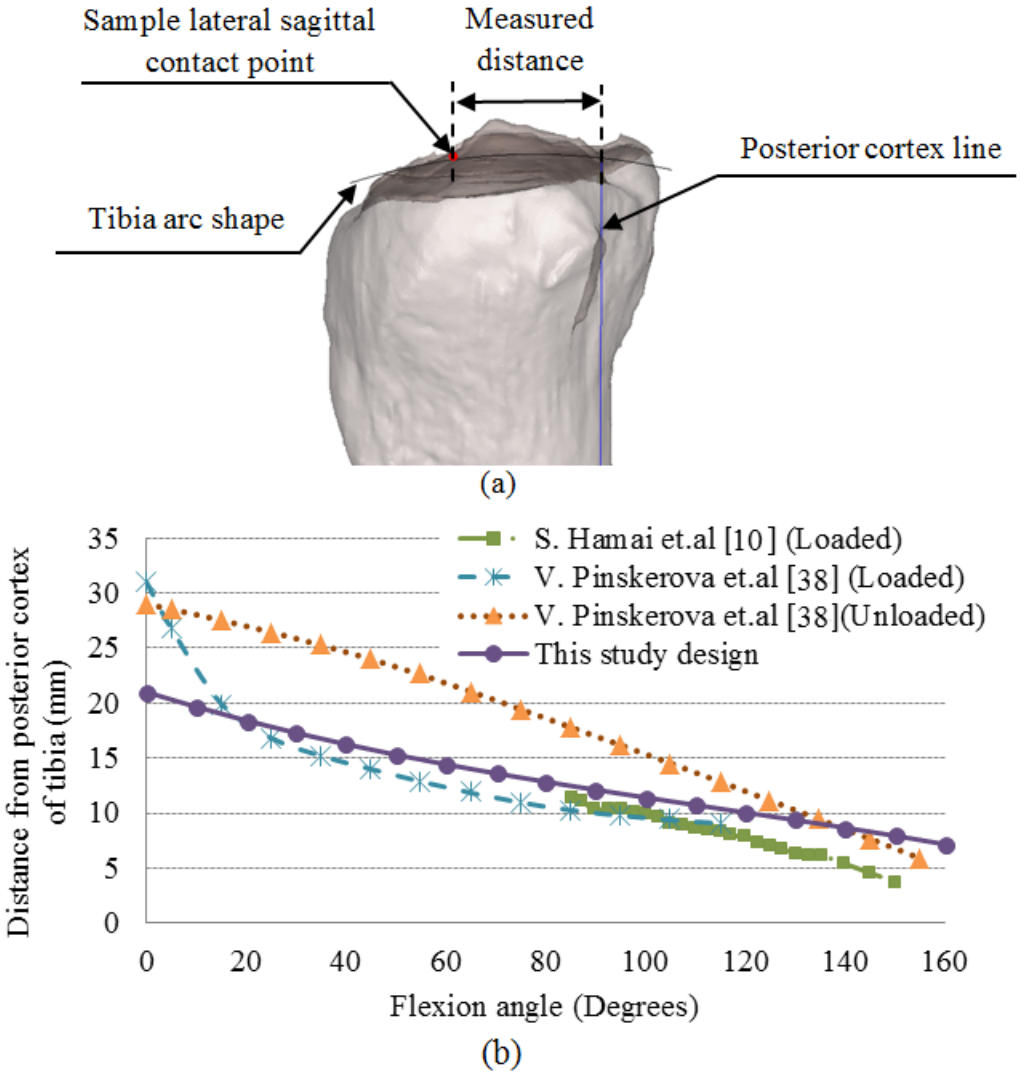

Figure 2-9 (a) Distance of the lateral sagittal contact points to the posterior cortex line (b) Distance of the contact points to the posterior cortex line in this study compared with data from literature [35]

Discussion

In this study, the development of a customized surface-guided knee implant is presented. The patient-specific geometric features and parameters were extracted from pre-operative MRI

data, to which the surface guiding concept was implemented. Results of the design process showed that the radii and positioning of the guiding arcs on the lateral condyle were influenced by the orientation of the reference planes. The location and direction of these planes, in turn, were affected by the trace of the contact points on the tibia and the direction of the FE and pivoting axes. Therefore, the axis of flexion-extension has a crucial role in this design concept. This axis was defined as the line connecting the center of the spheres fitted to the posterior condyles in a region between the posterior ends of the condyles and the intercondylar notch. The trans-epicondylar axis (TEA), the line joining the medial and the lateral epicondyles, has also been introduced as the flexion-extension axis in the literature [32,37,56]. However, the TEA was not an appropriate choice in this design due to a low reliability of the detection of the required landmarks on the epicondyles. Also, the flexion-extension axis used in this design is in agreement with recent studies showing that flexion-extension occurs about an axis passing through the posterior part of the femoral condyles, while the posterior condyles have a circular shape in the sagittal plane [11,12,56,57].

Another important design feature in this study was the design target trace of contact points on the tibial insert. The distance between the calculated trace of target contact points on the lateral side and the posterior cortex of the tibia was found to be in harmony with the characteristics of the trace of contact points in motions expected from normal knees described in the literature (Figure 2-9).

The medial tibiofemoral articulating surface of this design was approximated with a partial sphere fitted to the posterior section of the 3D model of the femoral condyle. In a normal healthy knee joint, the femoral condyle has a multi-radii circular profile. Freeman and

colleagues [9,11] describe the geometry of the medial femoral condyles on the sagittal plane with two circular arcs, while the arc fitted to the anterior section had a larger radius. A medial partial ball and socket configuration is in agreement with the findings in the literature, which report medial pivoting for the tibiofemoral motion in normal healthy knee joints [13,58]. There are studies in the literature that describe laxity in AP direction on the medial side at high flexion angles (often above 130° of flexion) for certain activities [10,59]. However, it is believed that such laxity can be provided by considering a larger radius on the tibia in comparison to the corresponding femoral condyle, while the conformity is retained. As Omori et al. [40] has discussed, reproducing both medial pivot motion and femoral roll-back after TKR needs a new design concept. The presented study proposes such a design by considering surface-guiding curves on the lateral side, and a congruent ball and socket configuration for the medial condyle.

The customized surface-guided TKR of this study was designed to provide medial pivoting along with the guided pattern of motion over the predefined lateral trace of contact points. The design target was set based on the static knee passive kinematics. However, as Mu et al.[14] reports, there is no significant difference between kinematic patterns measured statically or dynamically. Another limitation of this study is that perfect alignment of the femur and the tibia on the bone was assumed. In addition, the segmentation of the MRI and reconstruction of the joint compartments were affected by the quality of the image, and the accuracy of the segmentation approach. Broeck et al. [61] used a similar technique for segmentation of the tibia and reported a dimensional root means square error of less than two times the voxel size of the image. Therefore, it is estimated that the error of the extracted dimensions for the design purpose of this study was less than 1 mm.

This study resulted in a new customized surface-guided knee implant with particularly shaped asymmetric tibiofemoral articulation surfaces. The guiding features were incorporated in the geometry of the bearing surfaces; therefore there is no need for an intercondylar feature. Since the intercondylar space was not affected by this design, it provides the opportunity for one or both cruciate ligaments to be retained.

References

[1] Bourne, Robert B., B. M. Chesworth, A. M. Davis, N. N. Mahomed, and K. D. J. Charron. 2010. "Patient Satisfaction after Total Knee Arthroplasty: Who is Satisfied and Who is Not?" *Clinical Orthopaedics and Related Research®* 468 (1): 57-63.

[2] Dennis, Douglas A., R. D. Komistek, and M. R. Mahfouz. 2003. "In Vivo Fluoroscopic Analysis of Fixed-Bearing Total Knee Replacements." *Clinical Orthopaedics and Related Research* 410 (410): 114-130.

[3] Victor, Jan. 2009. "A Comparative Study on the Biomechanics of the Native Human Knee Joint and Total Knee Arthroplasty." *Doctoral thesis in Medical Sciences*, Universiteit Leuven.

[4] International Standard Organization. 2002. *Implants for Surgery -- Wear of Total Knee-Joint Prostheses -- Part 1: Loading and Displacement Parameters for Wear-Testing Machines with Load Control and Corresponding Environmental Conditions for Test*.

[5] Riley Jr, lee H. 1976. "The Evolution of Total Knee Arthroplasty." *Clinical Orthopaedics and Related Research* 120: 7-10.

[6] Robinson, Raymond P. 2005. "The Early Innovators of Today's Resurfacing Condylar Knees." *The Journal of Arthroplasty* 20: 2-26.

[7] Carr, Brandi C. and T. Goswami. 2009. "Knee Implants–Review of Models and Biomechanics." *Materials & Design* 30 (2): 398-413.

[8] "American Academy of Orthopaedic Surgeons." http://orthoinfo.aaos.org/icm/PrintModule.cfm?screen=icm005_s08_p1&module=icm005

[9] Freeman, Michael A. R. and V. Pinskerova. 2005. "The Movement of the Normal Tibiofemoral Joint." *Journal of Biomechanic*s 38 (2): 197-208.

[10] Hamai, Satoshi, T. Moro-Oka, N. J. Dunbar, H. Miura, Y. Iwamoto, and S. A. Banks. 2012. "In Vivo Healthy Knee Kinematics during Dynamic Full Flexion." *BioMed Research Internationa*l 2013.

[11] Iwaki, H., V. Pinskerova, and MAR Freeman. 2000. "Tibiofemoral Movement 1: The Shapes and Relative Movements of the Femur and Tibia in the Unloaded Cadaver Knee." *Journal of Bone & Joint Surgery, British Volum*e 82 (8): 1189-1195.

[12] Kozanek, Michal, A. Hosseini, F. Liu, S. K. Van de Velde, T. J. Gill, H. E. Rubash, and G. Li. 2009. "Tibiofemoral Kinematics and Condylar Motion during the Stance Phase of Gait." *Journal of Biomechanic*s 42 (12): 1877-1884.

[13] Moro-oka, Taka-aki, S. Hamai, H. Miura, T. Shimoto, H. Higaki, B. J. Fregly, Y. Iwamoto, and S. A. Banks. 2008. "Dynamic Activity Dependence of in Vivo Normal Knee Kinematics." *Journal of Orthopaedic Researc*h 26 (4): 428-434.

[14] Mu, Shang, T. Moro-Oka, P. Johal, S. Hamai, M. A. R. Freeman, and S. A. Banks. 2011. "Comparison of Static and Dynamic Knee Kinematics during Squatting." *Clinical Biomechanic*s 26 (1): 106-108.

[15] Dennis, Douglas A., M. R. Mahfouz, R. D. Komistek, and W. Hoff. 2005. "In Vivo Determination of Normal and Anterior Cruciate Ligament-Deficient Knee Kinematics." *Journal of Biomechanic*s 38 (2): 241-253.

[16] Amiri, Shahram, D. Cooke, I. Y. Kim, and U. Wyss. 2007. "Mechanics of the Passive Knee Joint. Part 2: Interaction between the Ligaments and the Articular Surfaces in Guiding the Joint Motion." *Proceedings of the Institution of Mechanical Engineers. Part H, Journal of Engineering in Medicin*e 221 (8): 821-832.

[17] Victor, Jan, S. Banks, and J. Bellemans. 2005. "Kinematics of Posterior Cruciate Ligament-Retaining and -Substituting Total Knee Arthroplasty: A Prospective Randomised Outcome Study." *The Journal of Bone and Joint Surgery. British Volum*e 87 (5): 646-655.

[18] Kuroyanagi, Yuji, S. Mu, S. Hamai, W. J. Robb, and S. A. Banks. 2012. "In Vivo Knee Kinematics during Stair and Deep Flexion Activities in Patients with Bicruciate Substituting Total Knee Arthroplasty." *The Journal of Arthroplast*y 27 (1): 122-128.

[19] Yagishita, Kazuyoshi, T. Muneta, Y. Ju, T. Morito, J. Yamazaki, and I. Sekiya. 2012. "High-Flex Posterior Cruciate-Retaining vs Posterior Cruciate-Substituting Designs in Simultaneous Bilateral Total Knee Arthroplasty: A Prospective, Randomized Study." *The Journal of Arthroplast*y 27 (3): 368-374.

[20] Victor, Jan and J. Bellemans. 2006. "Physiologic Kinematics as a Concept for Better Flexion in TKA." *Clinical Orthopaedics and Related Researc*h 452: 53-58.

[21] Dennis, Douglas A., R. D. Komistek, J. B. Stiehl, S. A. Walker, and K. N. Dennis. 1998. "Range of Motion after Total Knee Arthroplasty the Effect of Implant Design and Weight-Bearing Conditions." *The Journal of Arthroplast*y 13 (7): 748-752.

[22] Clark, Charles R., C. H. Rorabeck, S. MacDonald, D. MacDonald, J. Swafford, and D. Cleland. 2001. "Posterior-Stabilized and Cruciate-Retaining Total Knee Replacement: A Randomized Study." *Clinical Orthopaedics and Related Researc*h 392: 208-212.

[23] Tanzer, Michael, K. Smith, and S. Burnett. 2002. "Posterior-Stabilized versus Cruciate-Retaining Total Knee Arthroplasty: Balancing the Gap." *The Journal of Arthroplast*y 17 (7): 813-819.

[24] Maruyama, Shigeki, S. Yoshiya, N. Matsui, R. Kuroda, and M. Kurosaka. 2004. "Functional Comparison of Posterior Cruciate-Retaining versus Posterior Stabilized Total Knee Arthroplasty." *The Journal of Arthroplast*y 19 (3): 349-353.

[25] Yoshiya, Shinichi, N. Matsui, R. D. Komistek, D. A. Dennis, M. Mahfouz, and M. Kurosaka. 2005. "In Vivo Kinematic Comparison of Posterior Cruciate-Retaining and Posterior Stabilized Total Knee Arthroplasties under Passive and Weight-Bearing Conditions." *The Journal of Arthroplast*y 20 (6): 777-783.

[26] Harato, Kengo, R. B. Bourne, J. Victor, M. Snyder, J. Hart, and M. D. Ries. 2008. "Midterm Comparison of Posterior Cruciate-Retaining versus-Substituting Total Knee Arthroplasty using the Genesis II Prosthesis: A Multicenter Prospective Randomized Clinical Trial." *The Knee* 15 (3): 217-221.

[27] Walker, Peter S., G. Yildirim, S. Arno, and Y. Heller. 2010. "Future Directions in Knee Replacement." *Proceedings of the Institution of Mechanical Engineers. Part H, Journal of Engineering in Medicin*e 224 (3): 393-414.

[28] Lozano-Calderón, Santiago A., J. Shen, D. F. Doumato, D. A. Greene, and S. B. Zelicof. 2013. "Cruciate-Retaining Vs Posterior-Substituting Inserts in Total Knee Arthroplasty: Functional Outcome Comparison." *The Journal of Arthroplast*y 28 (2): 234-242. e1.

[29] Dennis, Douglas A., R. D. Komistek, S. A. Walker, E. J. Cheal, and J. B. Stiehl. 2001. "Femoral Condylar Lift-Off in Vivo in Total Knee Arthroplasty." *The Journal of Bone and Joint Surgery. British Volum*e 83 (1): 33-39.

[30] Horiuchi, Hiroshi, S. Akizuki, T. Tomita, K. Sugamoto, T. Yamazaki, and N. Shimizu. 2012. "In Vivo Kinematic Analysis of Cruciate-Retaining Total Knee Arthroplasty during Weight-Bearing and non–weight-Bearing Deep Knee Bending." *The Journal of Arthroplast*y 27 (6): 1196-1202.

[31] Victor, Jan, J. K. P. Mueller, R. D. Komistek, A. Sharma, M. C. Nadaud, and J. Bellemans. 2010. "In Vivo Kinematics after a Cruciate-Substituting TKA." *Clinical Orthopaedics and Related Research*® 468 (3): 807-814.

[32] Amiri, S., T. D. V. Cooke, and U. P. Wyss. 2011. "Conceptual Design for Condylar Guiding Features of a Total Knee Replacement." *Journal of Medical Device*s 5 (2): 025001.

[33] Walker, Peter S. 2001. "A New Concept in Guided Motion Total Knee Arthroplasty." *The Journal of Arthroplast*y 16 (8): 157-163.

[34] Walker, Peter S. 2014. "Application of a Novel Design Method for Knee Replacements to Achieve Normal Mechanics." *The Kne*e 21 (2): 353-358.

[35] Pejhan, Shabnam, E. Bohm, J. M. Brandt, and U. Wyss. 2016. "Design and Virtual Evaluation of a Customized Surface-Guided Knee Implant." Proc IMechE Part H: J Engineering in Medicine, 230, 10, 949-961.

[36].Walker, Peter S. 2015. "The Design and Pre-Clinical Evaluation of Knee Replacements for Osteoarthritis." *Journal of Biomechanic*s 48 (5): 742-749.

[37] Wyss, Urs, S. Amiri, and T. D. V. Cooke. 2010. *Knee Prosthesi*s; Patent: US20120179265.

[38] Pinskerova, Vera, P. Johal, S. Nakagawa, A. Sosna, A. Williams, W. Gedroyc, and M. A. Freeman. 2004. "Does the Femur Roll-Back with Flexion?" *The Journal of Bone and Joint Surgery. British Volum*e 86 (6): 925-931.

[39] Bae, Dae Kyung, S. J. Song, and S. D. Cho. 2011. "Clinical Outcome of Total Knee Arthroplasty with Medial Pivot Prosthesis: A Comparative Study between the Cruciate Retaining and Sacrificing." *The Journal of Arthroplast*y 26 (5): 693-698.

[40] Omori, Go, N. Onda, M. Shimura, T. Hayashi, T. Sato, and Y. Koga. 2009. "The Effect of Geometry of the Tibial Polyethylene Insert on the Tibiofemoral Contact Kinematics in Advance Medial Pivot Total Knee Arthroplasty." *Journal of Orthopaedic Scienc*e 14 (6): 754-760.

[41] Pritchett, James. W. 2004. "Patient Preferences in Knee Prostheses." *The Journal of Bone and Joint Surgery. British Volum*e 86 (7): 979-982.

[42] Harrysson, Ola L., Y. A. Hosni, and J. F. Nayfeh. 2007. "Custom-Designed Orthopedic Implants Evaluated using Finite Element Analysis of Patient-Specific Computed Tomography Data: Femoral-Component Case Study." *BMC Musculoskeletal Disorder*s 8: 91.

[43] Steklov, Nick, J. Slamin, S. Srivastav, and D. D'Lima. 2010. "Unicompartmental Knee Resurfacing: Enlarged Tibiofemoral Contact Area and Reduced Contact Stress using Novel Patient-Derived Geometries." *The Open Biomedical Engineering Journa*l 4: 85-92.

[44] Van den Heever, D. Jacobus. 2011. “Development of Patient-Specific Knee Joint Prostheses for Unicompartmental Knee Replacement (UKR).” *PhD dissertation*, Stellenbosch University.

[45] Liu, Yu-Liang, K. Lin, C. Huang, W. Chen, C. Chen, T. Chang, Y. Lai, and C. Cheng. 2011. "Anatomic-Like Polyethylene Insert could Improve Knee Kinematics after Total Knee arthroplasty—a Computational Assessment." *Clinical Biomechanic*s 26 (6): 612-619.

[46] Jun, Yongtae. 2011. "Morphological Analysis of the Human Knee Joint for Creating Custom-made Implant Models." *The International Journal of Advanced Manufacturing Technolog*y 52 (9-12): 841-853.

[47] Van den Heever, Dawie J, C. Scheffer, P. Erasmus, and E. Dillon. 2011. "Contact Stresses in a Patient-Specific Unicompartmental Knee Replacement." *Clinical Biomechanics* 26 (2): 159-166.

[48] Guess, Trent M., G. Thiagarajan, M. Kia, and M. Mishra. 2010. "A Subject Specific Multibody Model of the Knee with Menisci." *Medical Engineering & Physics* 32 (5): 505-515.

[49] Bloemker, Katherine H., T. M. Guess, L. Maletsky, and K. Dodd. 2012. "Computational Knee Ligament Modeling using Experimentally Determined Zero-Load Lengths." *The Open Biomedical Engineering Journal* 6: 33-41.

[50] Guess, Trent M., H. Liu, S. Bhashyam, and G. Thiagarajan. 2013. "A Multibody Knee Model with Discrete Cartilage Prediction of Tibiofemoral Contact Mechanics." *Computer Methods in Biomechanics and Biomedical Engineering* 16 (3): 256-270.

[51] Mootanah, Rajshree, C. Imhauser, F. Reisse, D. Carpanen, R. W. Walker, M. Koff, M. Lenhoff, R. Rozbruch, A. Fragomen, and Y. Kirane. 2014. "Development and Verification of a Computational Model of the Knee Joint for the Evaluation of Surgical Treatments for Osteoarthritis." *Computer Methods in Biomechanics and Biomedical Engineering* 17: 1502-1517.

[52] Yoshioka, Yuki, D. Siu, and T. D. Cooke. 1987. "The Anatomy and Functional Axes of the Femur." *The Journal of Bone and Joint Surgery. American Volume* 69 (6): 873-880.

[53] Cooke, Derek, A. Scudamore, J. Li, U. Wyss, T. Bryant, and P. Costigan. 1997. "Axial Lower-Limb Alignment: Comparison of Knee Geometry in Normal Volunteers and Osteoarthritis Patients." *Osteoarthritis and Cartilage* 5 (1): 39-47.

[54] MSC Software Corporation. 2013. *MSC. ADAMS User Manual* MSC.

[55] Godest, A. C., M. Beaugonin, E. Haug, M. Taylor, and PJ Gregson. 2002. "Simulation of a Knee Joint Replacement during a Gait Cycle using Explicit Finite Element Analysis." *Journal of Biomechanics* 35 (2): 267-275.

[56] Victor, Jan, D. Van Doninck, L. Labey, F. Van Glabbeek, P. Parizel, and J. Bellemans. 2009. "A Common Reference Frame for Describing Rotation of the Distal Femur: A CT-Based Kinematic Study using Cadavers." *The Journal of Bone and Joint Surgery. British Volume* 91 (5): 683-690.

[57] Eckhoff, Donald G., J. M. Bach, V. M. Spitzer, K. D. Reinig, M. M. Bagur, T. H. Baldini, and N. M. Flannery. 2005. "Three-Dimensional Mechanics, Kinematics, and Morphology of the Knee Viewed in Virtual Reality." *The Journal of Bone and Joint Surgery. American Volume* 87 Suppl 2: 71-80.

[58] Asano, Taiyo, M. Akagi, K. Tanaka, J. Tamura, and T. Nakamura. 2001. "In Vivo Three-Dimensional Knee Kinematics using a Biplanar Image-Matching Technique." *Clinical Orthopaedics and Related Research* 388: 157-166.

[59] Johal, Parm, A. Williams, P. Wragg, D. Hunt, and W. Gedroyc. 2005. "Tibiofemoral Movement in the Living Knee. A Study of Weight Bearing and Non-Weight Bearing Knee Kinematics using 'interventional' MRI." *Journal of Biomechanics* 38 (2): 269-276.

[60] Komistek, Richard D., D. A. Dennis, and M. Mahfouz. 2003. "In Vivo Fluoroscopic Analysis of the Normal Human Knee." *Clinical Orthopaedics and Related Research* 410: 69-81.

[61] Van den Broeck, Joyce, E. Vereecke, R. Wirix-Speetjens, J. Vander Sloten. 2014. "Segmentation Accuracy of Long Bones." *Medical engineering & physics* 36 (7): 949-953.

Chapter 3

Parametric Analysis of the Influence of Geometric Design Variables on the Kinematic Performance of a Customized Surface-guided Total Knee Replacement

Abstract

Variability in the design of the total knee replacements (TKRs) and limitations in alignment and motion of the joint are among the critical factors contributing to the performance of the implant. The purpose of this study was to investigate the influence of the geometric design parameters on the kinematic behavior of a customized surface-guided TKR. In this design, the specially shaped articulating tibiofemoral surfaces are expected to guide a predefined pattern of motion. In addition, a kinematic related objective function was used to quantify the kinematic behavior of the designed TKR, and to implement a parametric analysis, in order to define the design with the best kinematic performance.

Based on Latin Hypercube Sampling method, different combinations of six design variables were generated to create design candidates. A cycle of deep squatting was simulated in a

multibody contact model to estimate the kinematic behavior of each design candidate. The internal-external (IE) rotation of the tibia, and the anterior-posterior (AP) translation of the medial and lateral centers of the femoral condyles were recorded from the simulation of each design candidate. The contribution of the design parameters was determined and analyzed by principal component analysis. This analysis was performed using the results of the kinematic performance outcomes and the input design variable combinations. The objective function for the parametric analysis considered the sum of errors between the desired pattern of motion, and the kinematic outcomes from the virtual simulation.

This study revealed that the location and orientation of the flexion-extension (FE) axis, and the tibial medial sagittal slope were the most influential parameters on the kinematics throughout flexion up to 140 degrees. On the other hand, the conformity between the guiding arcs on the lateral condyle had the least contribution on the modes of variation in the kinematic performance. Finally, the parametric analysis defined the combination of sagittal tibial slope, radii of the medial and lateral spheres, AP locations of the centers of the femoral condyles, and tibiofemoral conformity ratio, which resulted in the maximum agreement with the target pattern of motion. Simulations show that the customized surface-guided TKR with improved design variables reached deep flexion angles (140°) under high squat loads, while the tibia pivoted internally about 23 degrees around the medial center. Such rotation of the tibia is within the expected range of IE rotation from healthy knee joints.

Introduction

Due to an increasing number of younger and more active patients who require knee arthroplasty [1], the need for implant designs with a high range of motion has also increased. It is reported that the maximum limit of knee flexion in a TKR is affected by the AP location of the femur on the tibial plateau, which in turn is related to the geometric design of the tibiofemoral components [2]. Also, the design of the tibiofemoral articulating surfaces contributes to the pattern of motion after TKR [3-6]. Achieving close to normal kinematics relates to better restoration of the joint feel and function.

A surface-guided TKR is intended to guide the motion of the femur on the tibia based on the desired target path of tibiofemoral contact points [7,8]. The specific geometric design features of the articulating surfaces provide the rollback motion of the femur as knee flexes, with no need for an intercondylar mechanism [8-10]. The novelty of this design is that it avoids an intercondylar feature like post and cam mechanism by the patient-specific guiding features that are incorporated into the lateral tiobiofemoral articulating surfaces. For the TKR of this study, the geometric design could be summarized by the following major points [9,10]:

- incrementally changing radii of the tangent inner and outer guiding arcs on the lateral side
- constant distance between the medial and lateral contact points
- partial medial ball and socket configuration, which provides a medial pivot center
- target pattern of pivoting versus flexion angle.

For a typical total knee replacement, different geometric design variables, the alignment and positioning of the components after surgery, and also patient-specific variables such as the

hip load, the quadriceps force, and ligaments attachments influence the kinematic outcome behavior [11-13]. Previous studies used different computational methods to analyze the influence of design factors either on the pattern of motion, or the contact characteristics and articulation wear for the conventional implants [11-15]. Different design variables have been the subject of these studies, including radii of the femoral component in the sagittal and frontal planes, the slope of the tibial insert, and the conformity between the articulating surfaces.

Sathasivam and Walker [14] analyzed the influence of four design parameters for a conventional TKR on delamination wear and the kinematic behavior during the stance phase of walking. These parameters included the femoral frontal radius, the transition angle between the posterior and distal segments of the sagittal femoral radius, tibial sagittal radius, and the clearance between the femoral and the tibial frontal radius. They conducted a rigid body analysis along with a finite element model of sixteen different design combinations to find the AP and rotational motions and the strain energy density for the stance phase of level walking. They reported that the tibial sagittal radius and the femoral radii transition angle were the two parameters that contributed to changes in AP and IE laxity. Also, designs with a larger femoral frontal radius and less clearance experienced lower contact stresses. Sathasivam and Walker finally introduced a combination of design variables that provided closer to normal kinematics, as well as less delamination wear [14]. One major limitation of their study was that only the stance phase of a gait cycle was analyzed, while for high flexion activities higher contact forces and different kinematics were expected.

Willing and Kim [15] implemented an optimization method to determine the shape of the tibiofemoral articular surfaces in a TKR using a three-dimensional finite element model, and a

wear model based on sliding distance, contact area, and contact pressure. The objective function of that study was to minimize the volumetric wear considering constrains on the maximum von-Mises stress and the maximum wear depth. Their parametric models of the femoral component and polyethylene insert of a TKR included ten design variables: the distal, posterior and frontal radii of the femoral condyles, the frontal and sagittal tibiofemoral conformity ratio, and the distance in the medial-lateral direction from the implant mid-line to the lowest point of the femoral condyles. They found that a reduction in the sagittal radii of the femoral condyles, a decrease of the conformity between the tibiofemoral components, and an increase of the femoral frontal radii of curvature, would minimize the wear volume [15]. In another optimization study, Willing and Kim [11] used kinematic simulations of basic laxity and unconstrained flexion on a conventional TKR to calculate a kinematic objective function based on the maximum flexion range and overall laxity in comparison to the natural knee joint. They showed that the optimization based on kinematics during a laxity test resulted in small frontal and sagittal radii of the femoral curvature, while the lateral side had larger radii with less conformity than that of the medial side. In another study, Willing and Kim [16] combined their optimization investigations in a multi-objective process. They used a rigid body TKR kinematic simulation model, in addition to a 3D finite element analysis and a wear model to implement the optimization algorithm. The objective function of that study was the weighted sum of the volumetric wear and the kinematics criteria, including the range of flexion of the joint and the AP, as well as the IE constraints. The results of the multi-objective optimization revealed that the kinematic and wear objectives were conflicting. They reported a rise in the volumetric wear with an increasing maximum range of flexion or an increase in the IE rotational laxity [16].

Fitzpatrick et al. [12,13] reported that design factors such as the distal and posterior radii of the femoral condyles and the tibial insert slope are critical parameters affecting the performance of a TKR at deep flexion angles. In their analysis, the design variables were limited to a posterior stabilized TKR design, and a finite element probabilistic model was used for analyzing high flexion activities such as squatting, stepping down, and the standing phase of the gait. They reported that the design variables of the implant had a significant influence on the tibiofemoral contact mechanics, and the kinematics of the joint at high flexion angles. Though, surgical alignment parameters mostly affected the tension of the ligaments, and thus the guiding and control of the motion. The patient specific variables like the joint forces or ligament attachment positions contributed mainly to the amount of joint load and tension in muscles, and consequently to the kinematics of the joint [12,13].

A combination of the finite element analysis and probabilistic and Principal Component Analysis (PCA) methods have been previously used to investigate the effect of different factors on the kinematic and wear performance of conventional TKR designs [17,18]. PCA reduces the dimensionality of a set of interrelated data, and defines a set of new variables (modes or principal components) showing the changes in the original data [17,19]. In other words, PCA finds the relation between all parameters, including input variables and outcome measures together. Fitzpatrick et al. [17] implemented PCA combined with a probabilistic analysis using a finite element model to analyze the influence of alignment and loading conditions on the patellofemoral kinematics after TKR. They reported that the analysis of the modes of variation based on PCA provides a complete understanding of the interrelation between parameters (inputs and outputs), which was not possible by traditional sensitivity analysis [17].

The first goal of our study was to quantify the influence of six major design parameters (input variables) of the customized surface-guided TKR on the kinematic performance. Principal component analysis was conducted based on the outcome kinematic variables, incremental IE rotation of the tibia, and the AP translation of the center of the medial and lateral femoral condyles. The kinematic outcomes were measured from a virtual simulation of deep squatting. The second goal was to determine the combination of geometric design variables with optimum kinematic performance. For this parametric optimization study, a kinematic objective function was considered, which quantified the kinematic behavior of each candidate TKR in comparison to the desired target pattern of motion.

Methodology

Principal Component Analysis

Based on the motion guiding concept described in Chapter 2, a series of design candidates were generated considering six major geometric design variables. For the reference design, the design variables were determined from the anatomic tibial and femoral geometries, which were extracted from a magnetic resonance image (MRI) data provided in the studies by Guess et al. [20-22]. As it is illustrated in Figure 3-1, the input design variables for this analysis were:

- Sagittal slope of the medial tibial plateau (X_1)
- Radius of the lateral sphere (X_2)
- AP location of the medial and lateral centers of the femoral condyles (X_3 and X_4)
- Radius of the partial medial sphere (X_5),
- Conformity between the tibial and femoral lateral guiding arcs (X_6)

The tibial insert of this study was designed with a slope on the medial compartment in the sagittal plane. The lower and higher bounds of this design variable (X_1) were determined based on the pooled variance and standard deviation extracted from previous studies on the slope of the medial tibial plateau in healthy knee joints [23-27].

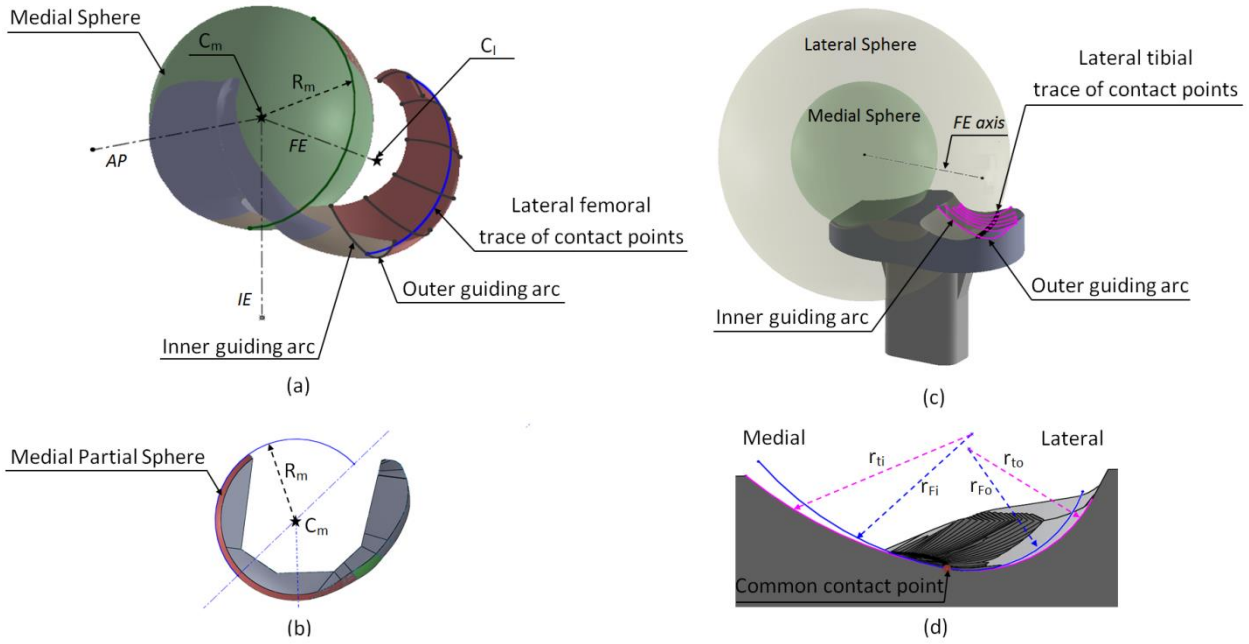

Figure 3-1 Geometric design parameters of the surface-guided TKR

(a) R_m is the radius of the medial sphere (X_5), and C_m and C_l show the locations of the centers at the medial and lateral femoral condyles (X_3 and X_4). (b) Medial sagittal view. (c) R_l is the radius of the lateral sphere (X_2), the trace of the lateral contact points are resulted from projection of the sagittal plane contact points on the lateral sphere. The tibial insert has a sagittal slope on the medial compartment (X_1). (d) r_{fi} and r_{fo} are radii of the inner and outer femoral guiding arcs and r_{ti} and r_{to} are the radii of the corresponding tibial guiding arcs. The difference between the radii of the lateral guiding arcs on the femoral and tibial parts is another design variable (X_6)

Based on the surface-guided concept of this TKR [9,10], the location of the lateral sagittal contact points were estimated on the sagittal plane that passed through the center of the lateral tibial plateau. The desired trace of the contact points on the lateral tibial plateau was

generated by projection of the estimated sagittal plane contact points onto a sphere named as "lateral sphere" [9]. This sphere had the same center as the center of the medial partial ball and socket configuration and a radius of 0.75 to 0.85 of the medial-lateral width of the tibia. A fraction of the width of the tibia was considered, because the second design variable (X_2) changes the medial-lateral location of the curve of the desired path of the contact points on the lateral tibial plateau. The lower and higher bounds for this variable were set based on the recommended limits for the radius of the lateral sphere by Wyss et al. [10].

In this TKR, the line connecting the centers of the medial and lateral condyles represents the Flexion-Extension (FE) axis. Originally, spheres were fitted to the posterior section of the femoral condyles to determine the locations of the medial and lateral centers [9]. Changing the AP location of these centers (third and fourth design variables) alter the orientation of the FE axis. The lower bound was set at zero, which means no shift of location of the centers. The higher bound for a shift in the AP direction was set considering the limitation in the geometry of the joint extracted from the MRI.

Another design feature for this TKR is the medial partial ball and socket configuration, which guarantees no AP translation of the medial center during flexion or extension of the joint [9,10]. The maximum and minimum radius of the medial sphere (X_5) was set based on the largest and smallest sphere that was practically possible to fit to the medial femoral condyle.

The role of the tibiofemoral conformity on the kinematic behavior has been studied previously for traditional TKR designs [11,14]. The conformity between the lateral guiding arcs on the femoral and tibial components was considered as another design input variable (X_6). No

difference between the radii of the tibiofemoral guiding arcs or full conformity was considered as the lower limit. The higher bound of this variable was set based on the geometry of the joint from MRI data and previous design iterations.

Based on a uniform distribution of the described input design variables (Table 3-1), Latin Hypercube Sampling (LHS) method was used to generate 30 randomized design variables of the femoral and tibial components of the surface guided TKR. In LHS, the range of each variable is divided into non-overlapping intervals with equal probability. Therefore, for every point P_i in the sample space, each value P_{ij} would be unique.

Table 3-1 Design variables for the customized surface-guided TKR

Design Variable	Range for sampling	Final design
X_1- Sagittal slope of the medial tibial plateau	3-10°	6.82°
X_2- Radius of the lateral sphere[a]	0.75-0.85	0.78
X_3- AP location of the medial femoral center[b]	0-5 mm	3.62 mm
X_4- AP location of the lateral femoral center[b]	0-2 mm	1.8 mm
X_5- Radius of the partial medial sphere	26-33 mm	28.2 mm
X_6- Conformity between the tibial and femoral lateral guiding arcs[c]	0-5 mm	1.32 mm

a. The radius of the lateral sphere = coefficient × width of the tibia.
b. The AP location was defined as the distance to the initial location of the centers.
c. The conformity shows the difference between the radii of the tibiofemoral arcs.

LHS is reported as a successful sampling method that uniformly covers the sample space, with a smaller sample size that would be sufficient, than that required by the traditional Mont Carlo approach [17,19]. The relatively small sample size results in ease of implication and less

costly computations. A confidence coefficient of 0.9 [28] was used to determine the sample size, which was used along with the upper and lower bounds for each variable (Table 3-1) in the LHS methodology to generate different combinations of geometric design variables.

The practically acceptable surface-guided TKR design candidates were chosen based on the requirements of the motion guiding concept [9,10], and the limitations of the joint geometry extracted from the MRI. For each design option, a cycle of deep squatting with heels down (reaching up to 140° of flexion) was virtually simulated in MSC.ADAMS (Chapter 4). The deep squatting was chosen since for activities like kneeling, gardening and sitting cross-legged, such range of flexion of the knee joint is required [29,30]. Also, it is reported that patients with traditional knee replacements experience limitation in performing high flexion activities such as squatting and kneeling [31].

The simulation model consisted of the CoCr femoral component in contact with an ultra-high molecular weight polyethylene (UHMWPE) tibial insert. The boundary condition was such that the femur was only free to rotate around the FE axis, while the tibial insert was free to move in the transverse plane [9]. The tibial axial load and FE angle profiles during a cycle of deep squat were implemented from the study of Smith et al. [32]. The “impact” contact function in MSC.ADAMS with a coefficient of friction of 0.04 between the tibiofemoral articulating surfaces was applied. Such a friction coefficient is in agreement with the reported magnitude of the friction between CoCr and PE in the literature [33]. In these simulations it was assumed that cruciate ligaments were resected, but the influence of the collateral ligaments was modeled by nonlinear springs paralleled with a damper, with the same damping coefficient for all ligament bundles. Details of the multibody model for the simulation are described in

Chapter 4. The IE rotation of the tibial insert and the AP translation of the medial and lateral centers were measured and recorded at 100 intervals throughout a deep squatting cycle. This simulation resulted in a total of 300 outcome variables that were recorded for each design candidate.

A matrix of the variables (inputs and outputs for all design candidates) was generated and called as the original date set ($T_{original}$). In this matrix (equation (3-1)), each row consisted of the input design variables in the first six elements, and the incremental outcome data from virtual simulation of one design candidate in the remaining 300 elements. The PCA algorithm as described by Fitzpatrick et al. [17] was then implemented to determine the modes of variation. The first step was to calculate the correlation coefficient matrix for the original date set ($T_{original}$). This matrix showed the correlation between all input and output variables. In this study, eigenvalue-based PCA was used to determine the modes of variation. The eigenvalues and a matrix of eigenvectors were calculated for the correlation coefficient matrix. The matrix of eigenvectors (E), which is also called the "loading" matrix [34], or the matrix of the principal components, shows the orthogonal directions sorted based on the amount of variance in each direction. For example, the first principal component is the direction where there is most of the variance. The eigenvalues indicate the amount of the variance in each direction or for each principal component [17].

$$T_{original} = \begin{bmatrix} (x_1 \cdots x_5 \; y_1 \cdots y_{100})_1 \\ \vdots \\ (x_1 \cdots x_5 \; y_1 \cdots y_{100})_N \end{bmatrix}_{N \times n} \qquad (3\text{-}1)$$

N=number of the trials or design candidates

n= total number of input and output variables (306)

The principal component score (F) is the linear combination of variables (inputs and outputs) weighted by the principal components (elements of the eigenvectors of the correlation coefficient matrix) [17,19]. Therefore, a new set of output variables were generated that were mapped from the original variables including all input and output parameters. Abdi and Williams [34] described these scores as the projection of the original variables for each observation on to the direction defined by the principal components.

$$F = T'_{original} \cdot E \qquad (3\text{-}2)$$

E= Matrix of the eigenvectors of the correlation matrix for the $T_{original}$

A traditional correlation analysis was performed to find the correlation coefficient (r) between the input design variables and the principal component scores. Another criterion for interpreting PCA results was the squared coefficient (r^2), which determines the proportion of the change of the variables at each mode of variation. Also, the input principal component score (equation (3-3)) and the percent of the contribution of each design variable in the input loading matrix was calculated and discussed.

$$F_{input} = T'_{inputs} \cdot E_{inputs} \qquad (3\text{-}3)$$

F_{input}= Principal component based on the contribution of the input variables

The influence of changing the principal component values on the output was also studied by adding two times the standard deviation of the principal component values for all trials to the computed values of the principal component score (F). Based on the new set of scores, the input and output variables were calculated and then the new outcome variables were compared with the original ones.

Analytical optimization

The objective was to find a combination of design variables that provide the most natural kinematic behavior. For this analysis, an objective function was derived based on the overall agreement between kinematic measures from virtual simulation and design target. The kinematic measures were the estimated tibial IE rotation angles and femoral AP displacement of the medial and the lateral centers of the TKR candidates generated previously for PCA. The kinematic outcomes were recorded for 100 intervals during a cycle of deep squatting with heels down. The kinematic performance objective function was defined as sum of the following factors, and the goal was to minimize the overall error:

- normalized root mean square error (NRMSE) between the measured IE angles and the design target ($NRMSE_{IE}$), which was computed as the root mean square error relative to the range of the measured IE angles (the maximum value minus the minimum value)
- NRMSE between the lateral and the medial AP displacements of the femoral condyles and the design target ($NRMSE_{lAP}$ and $NRMSE_{mAP}$), that was similar to $NRMSE_{IE}$ were calculated relative to the range of the measured AP displacements
- normalized error in the range of IE rotation angles (NE_{IE}), that was the difference between the expected range of IE rotation and the outcome of the simulation normalized with respected to the target range of IE rotation

$$error_{overall} = NRMSE_{IE} + NRMSE_{mAP} + NRMSE_{lAP} + NE_{IE} \quad (3\text{-}5)$$

Results

Principal Component Analysis

Latin Hypercube Sampling resulted in 23 TKR design candidates that were practically acceptable for further analysis based on the requirements of the surface-guided tibiofemoral design concept [9,10]. Figure 3-2 shows the outcomes of the virtual simulation (IE rotation of the tibial insert and AP displacements of the medial and lateral femoral condyles) for four different candidate TKRs.

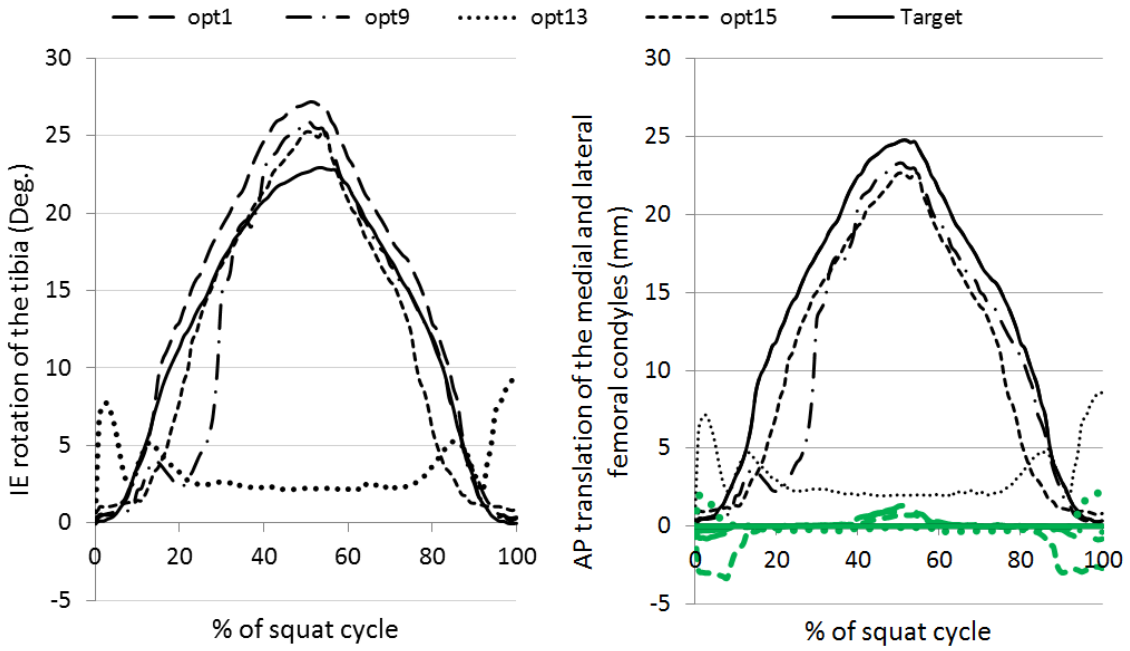

Figure 3-2 Kinematic outcomes from virtual simulation of 4 candidate TKRs.
Positive IE value means internal rotation of the tibial insert, and positive AP translation means movement in the posterior direction. In the graph for the AP translation of the femoral condyles, the green curves show the results of the medial condyle.

PCA results show that the first three principal components accounted for 87% of the total variation with the first three Eigen values having 58%, 22%, and 7% contribution in the cumulative variability, respectively (Figure 3-3). Therefore, the first three modes of variation

were considered for further analysis of the influence of the input design variables on the variations in the kinematic measures.

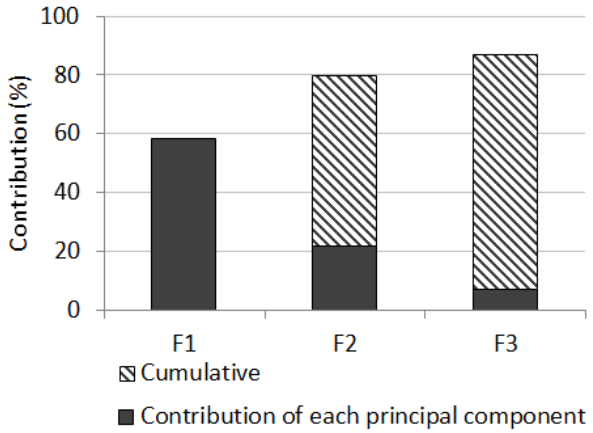

Figure 3-3 Contribution of the first three principal components in total variations

The input loadings or the input part of the eigenvector components (columns of the matrix E in equation (3-2)) indicate the contribution of each design variable in the input principal component (F_{input}). Based on Figure 3-4, the AP location of the lateral center (X_4) had the largest weight.

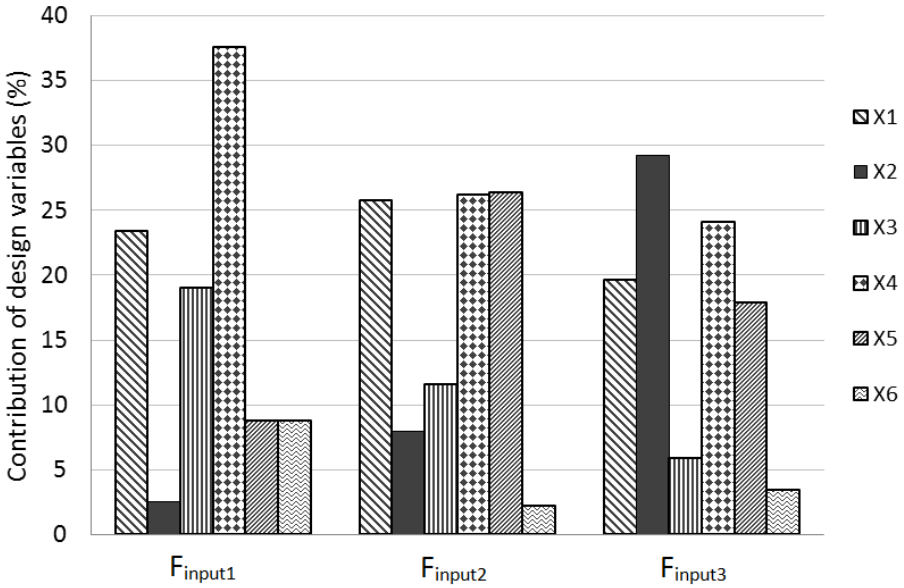

Figure 3-4 Contribution of design variables in input principal component

Three input variables almost evenly contributed to the second mode of variation: radius of the partial medial sphere (X_5), AP location of the lateral center (X_4), and the sagittal slope of the tibia medial plateau (X_1). For the third input principal component, the radius of the lateral sphere (X_2) had the largest contribution, and the AP location of the lateral center (X_4) was the second contributing factor.

Further study on the correlation between the input design variables and the principal component scores also highlighted the significance of the AP location of center of the lateral femoral condyle. This design variable is correlated with the first three modes of variation (Table 3-2 and Figure 3-5).

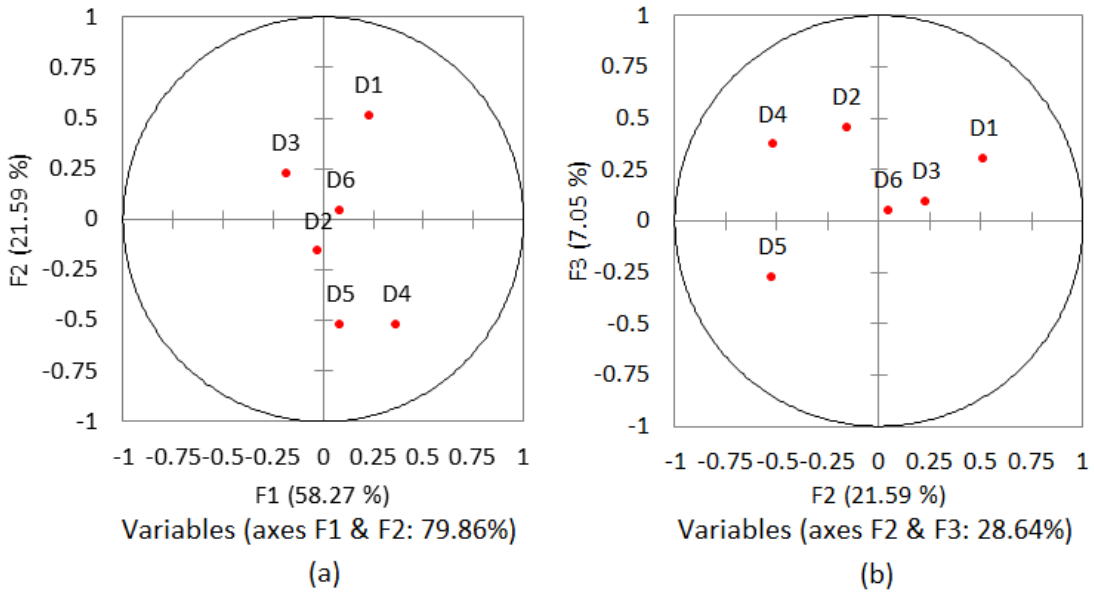

Figure 3-5 Correlations of the geometric design variables with (a) first and second principal components; (b) second and third principal components

As the circle of correlation (Figure 3-5) demonstrates, the first mode of variation was mostly correlated with the changes in AP location of the center of the lateral femoral condyle (X_4) and the sagittal slope of the medial tibial plateau (X_1).The correlation between the first mode of

variation and the radius of the lateral sphere (X_2) and AP location of the center of the medial femoral condyle (X_3) were in contrast with the correlation between the first principal component and the rest of the design variables.

For the second mode of variation, a similar correlation was found with the sagittal slope of the medial tibial plateau (X_1), the AP location of the lateral femoral center (X_4), and the radius of the medial sphere (X_5). However, there was an inverse correlation with the radius of the medial sphere and AP location of the lateral femoral center. The circle of correlation for the third principal component demonstrates that the radius of the partial medial sphere (X_5) was in contrast with all other variables, while the radius of the lateral sphere (X_2) was the most correlated parameter. The conformity between the tibial and femoral lateral guiding arcs (X_6) was in fact the design variable with a small correlation coefficient ($r<0.1$) for all first three modes of variation.

Table 3-2 Correlation of variables with the first three principal components

	Factor loadings (r)			Squared Factor Loadings (r^2)		
	F_1	F_2	F_3	F_1	F_2	F_3
X_1	0.23	0.51	0.30	0.05	0.26	0.09
X_2	-0.02	-0.16	0.45	0.00	0.03	0.20
X_3	-0.19	0.23	0.09	0.03	0.05	0.01
X_4	0.37	-0.52	0.37	0.13	0.27	0.14
X_5	0.09	-0.52	-0.28	0.01	0.27	0.08
X_6	0.09	0.04	0.05	0.01	0.00	0.00

Analysis of the kinematic outcomes shows that perturbation in the first principal component resulted in a decreased range of tibial IE rotation, along with posterior displacement (maximum

of 5 mm) of the medial femoral condyle during early flexion of the knee. The second mode of variation mostly associated with an increase in the range of IE rotation of the tibia, and a maximum of 8 mm anterior translation of the medial center on the tibia. (Figure 3-6)

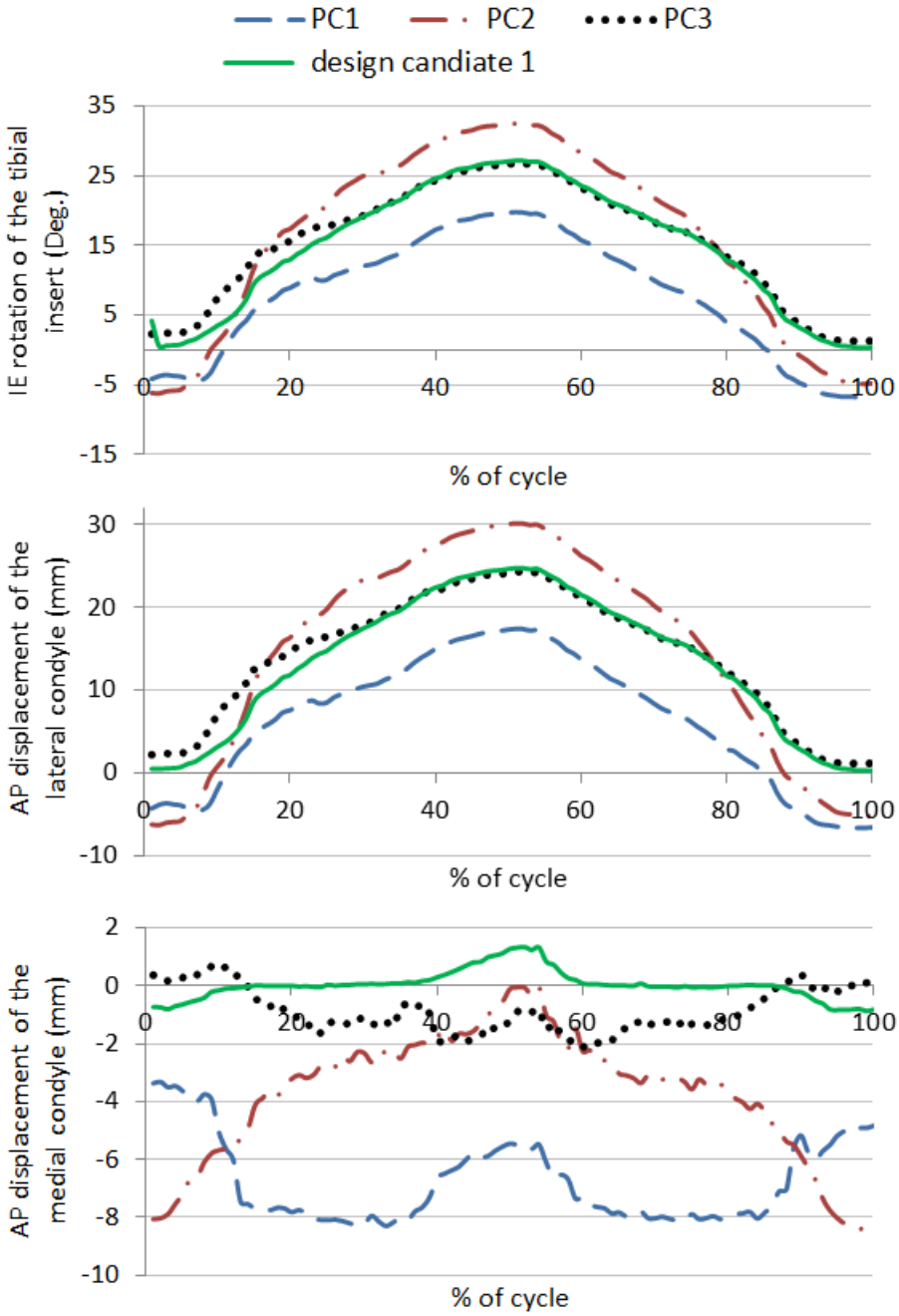

Figure 3-6 The influence of changes in modes of variations of parameters on kinematic performance (+2 times of the standard deviation of the PC scores of different design candidates for each of the first three modes of variation was considered)

Analytical optimization

The analysis of the overall error (equation (3-5)) for the 23 candidates of the TKR designs resulted in the combination of the geometric design variables that provided the best kinematic performance with the minimum overall error (Table 3-1 and Figure 3-7).

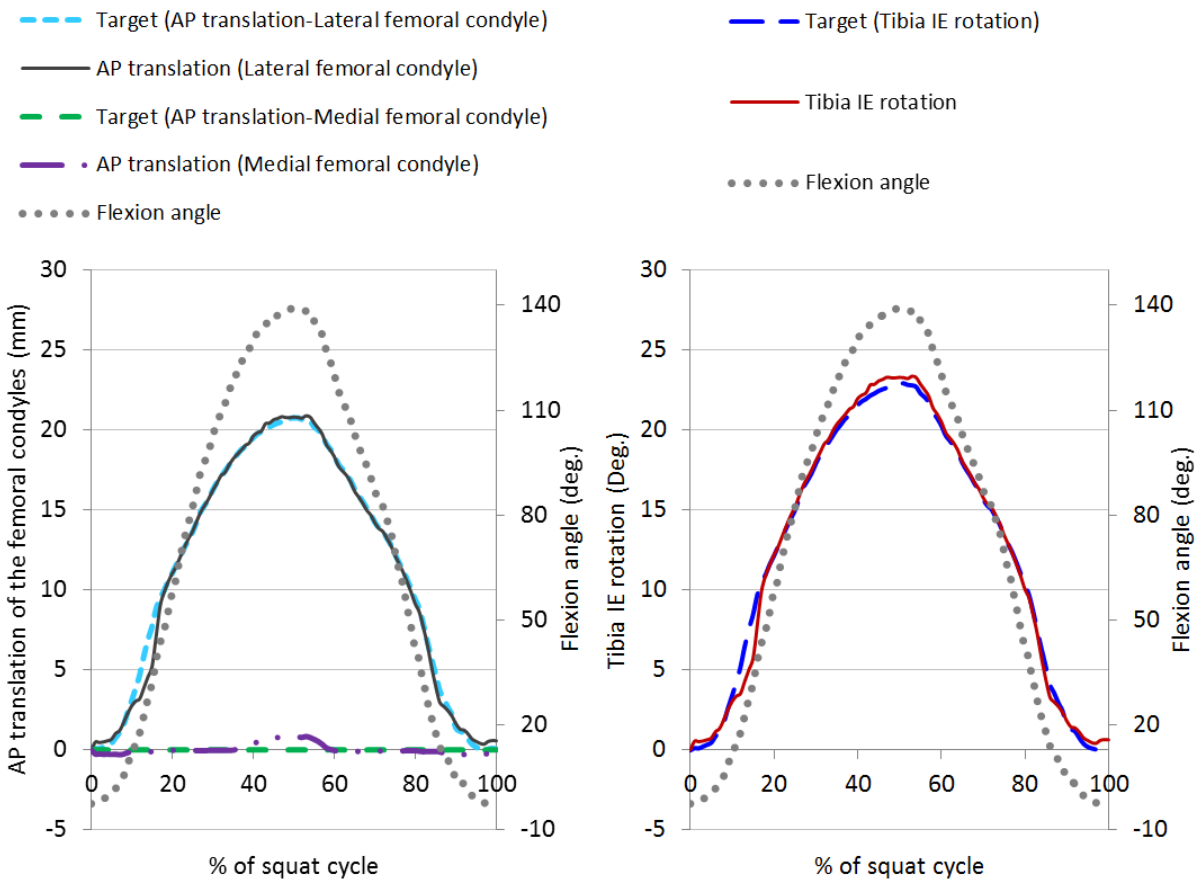

Figure 3-7 Kinematic outcomes of the surface-guided TKR with the least overall kinematic error in comparison to the design target

This design followed the target pattern of motion as the knee bent to a deep flexion angle of 140 degrees, with a 23° of IE rotation angle and an overall error of 33%. The normalized root mean square error between the IE rotation angle of the TKR with the best performance and the design target was 2.7%, while the maximum deviation of 2.75° occurred during mid-flexion

angles (Figure 3-7). There was only 1.2 mm AP displacement of the medial center through a cycle of squatting with normalized RMSE of 28%.

Discussion

The influence of the geometric design variables on the kinematic performance of TKR has been a subject of studies of the optimization of the traditional TKR designs [11,14]. This study first investigated the influence of major design variables of a surface-guided TKR on kinematic outcomes by principal component analysis combined with virtual simulation of deep squatting. The kinematic performance was quantified by IE rotation angle of the tibial insert and AP displacement of the medial and lateral centers of the femoral condyles that were recorded for 100 increments throughout one cycle of a squatting. Finally, a combination of design variables with the best kinematic performance was achieved through the analytical optimization process. This approach was based on an objective function of the overall error between measured kinematic results and the design target for the kinematics.

The traditional sensitivity analysis based on the linear correlation between input and output variables does not consider the influence of input and incremental output parameters altogether [12]. In the current study, the average of the correlation coefficient between each input geometric design variable and all increments of the output measures were determined to run a traditional sensitivity analysis. The results showed that the IE rotation of the tibial insert of the surface-guided TKR was sensitive to the initial AP location of the lateral femoral center (X_4) with $r>0.4$. The second critical parameter was the radius of the partial medial sphere ($r>0.3$). On the other hand, the AP displacement of the medial center was mostly sensitive to

the sagittal slope of the medial tibial plateau (r>0.39). The PCA over the total input and output variables also determined the AP location of the lateral center of the femoral condyle as the most contributing factor in the first mode of variation, and as the second correlating variable with the second and third principal components. According to the traditional sensitivity analysis, the radius of the lateral sagittal sphere (X_2) was amongst the variables with less correlation with the kinematic outcome measures (r<0.2). The PCA, in contrast, showed that it is the variable with the highest correlation with the third mode of variation.

The PCA was repeated to evaluate the relationship between input design variables and each of the outcome measures individually. Similar to the overall PCA, the analysis based only on the IE rotation of the tibial insert emphasized the influence of the AP location of the lateral center (X_4) on the first mode of variability in IE rotation (r=0.54). The second principal component based on IE rotation as the only performance measure was inversely correlated with the radius of the medial sphere (X_5). It is in agreement with the overall PCA; however, for the third mode of variation in the IE rotation, the results were different from analysis based on combined kinematic measures. The third principal component attributed to a combination of the sagittal slope of the medial tibial plateau (X_1) and the AP location of the lateral center (X_4) with r=0.4. PCA over the matrix of the input variables and incremental measure of the AP displacement of the medial center resulted in quite different loadings for the first principal component in comparison to the overall PCA. It showed that the first mode of variation in the AP translation of the medial center was influenced by the sagittal slope of the medial tibial plateau (X_1) and the radius of the lateral sagittal sphere (X_2). It is, however, in agreement with the traditional sensitivity analysis. These results show how the assessment of the combined outcome

measures identifies the interrelation between measures and specifies the overall influence of the input variables.

Based on the combination of all input design variables and outcome performance measures, the AP location of the lateral femoral center was determined as the critical parameter. This variable is correlated with the posterior translation of the medial side during early flexion, and causes a limitation on the range of the IE rotation of the tibial insert. Furthermore, as the surface-guided TKR bends to deep flexion angles, a combination of the slope of the tibial insert, the radius of the partial medial sphere, and the AP location of the lateral femoral center contribute to the paradoxical anterior translation of the femoral condyles. Fitzpatrick et al. [12] also reported a strong correlation between design parameters (radius of the posterior section of the femoral condyle and the slope of the tibial insert) with the tibiofemoral IE rotation and AP displacement during a cycle of squatting. Ardestani et al. [18] used a sensitivity index based on input principal component and the overall scores for the kinematic performance of a cruciate retaining TKR. They concluded that range of IE rotation of the tibial insert was sensitive first to the femoral posterior radius, and to a lesser degree to the tibial posterior and anterior radii.

The final design with the best kinematic performance can reach deep flexion angles (around 140°) following a close to deisgn target pattern of motion. The range of flexion of the TKR gained by the initially designed surface-guided TKR [9] was 120°; therefore there was about a 17% increase in the range of motion achieved through the parametric optimization process. During the flexion phase, the designed TKR experienced less than 1mm anterior displacement of the medial femoral center on the tibial component, while the lateral condyle moved 21 mm

in the posterior direction and the tibia rotated 23° internally. Studies on normal healthy knee kinematics reported a similar range of IE rotation for deep flexion of the joint [29,35-37]. Moro-oka et al. [29] showed that the internal rotation of the tibial component for flexion angles above 80° is caused by posterior translation of the lateral compartment pivoting around a medial center. They reported 30±2° of internal rotation of the tibia for the squatting activity with flexion up to 130° [29]. Hamai et al. [37] similarly showed a medial center of IE rotation during deep flexion, while the femur reached 30° of external rotation with 150° flexion. Leszko et al. [35] also described the motion of the femoral condyles during deep knee bending as posteriorly rolling and spinning of the lateral condyle throughout flexion of the joint up to 120 degrees. However, they reported rolling of both condyles for flexion beyond 120° [35]. The surface-guided TKR of the current study is based on pivoting of the lateral condyle around a medial center, which is in fact reported as a successful design concept for TKRs in the literature [38,39].

The Latin Hypercube sampling method that was used for this study is reported to be successful in generating a dense uniform arrangement of variables with a relatively small sample size [12]. However, one limitation of the current study is the limited number of design candidates due to the cost of the design process and computation. The chance to achieve an optimum design increases with more design candidates. The combination of the current sampling approach and a systematic optimization method could also give the globally optimized design. Also, the limitation in the virtual simulation could have affected the outcome variables used for principal component analysis. Those limitations included simplifications in contact modeling, the errors in detection of the insertion sites of the collateral ligaments, the reference

bundle length and wrapping of the ligaments. Furthermore, considering other variables for the PCA such as the alignment of the components, balancing of the ligament forces, or the loads due to different activities could improve the interpretations about the effective parameters on the performance of the designed TKR.

In conclusion, this study showed that in the design of the surface-guided TKR, the location of the femoral lateral center, which affects the orientation of the flexion-extension axis, is of great importance. To a lesser extent, the sagittal slope of the medial tibial plateau and the radius of the medial partial ball and socket configuration affect the kinematic performance. The analytical approach was successful in defining the combination of design variables, which creates the surface-guided TKR with the best kinematic performance in comparison to the design target. The virtual simulation of the optimized surface-guided TKR provides a close to the target pattern of motion during deep squatting activity. The design target is in fact consistent with the reported normal knee joint kinematics.

References

[1] Hip and Knee Replacements in Canada: Canadian Joint Replacement Registry 2016, Ottawa, ON: Canadian Institute for Health Information (CIHI).

[2] Banks, Scott, J. Bellemans, H. Nozaki, L. A. Whiteside, M. Harman, and W. A. Hodge. 2003. "Knee Motions during Maximum Flexion in Fixed and Mobile-Bearing Arthroplasties." Clinical Orthopaedics and Related Research (410): 131-138.

[3] Kuroyanagi, Yuji, S. Mu, S. Hamai, W. J. Robb, and S. A. Banks. 2012. "In Vivo Knee Kinematics during Stair and Deep Flexion Activities in Patients with Bicruciate Substituting Total Knee Arthroplasty." The Journal of Arthroplasty 27 (1): 122-128.

[4] Komistek, Richard D., D. A. Dennis, and M. Mahfouz. 2003. "In Vivo Fluoroscopic Analysis of the Normal Human Knee." Clinical Orthopaedics and Related Research (410) (410): 69-81.

[5] Victor, Jan, S. A. Banks, and J. Bellemans. 2005. "Kinematics of Posterior Cruciate Ligament-Retaining and -Substituting Total Knee Arthroplasty: A Prospective Randomised Outcome Study." The Journal of Bone and Joint Surgery. British Volume 87 (5): 646-655.

[6] Victor, Jan, J. K. P. Mueller, R. D. Komistek, A. Sharma, M. C. Nadaud, and J. Bellemans. 2010. "In Vivo Kinematics after a Cruciate-Substituting TKA." Clinical Orthopaedics and Related Research® 468 (3): 807-814.

[7] Walker, Peter S. 2014. "Application of a Novel Design Method for Knee Replacements to Achieve Normal Mechanics." The Knee 21 (2): 353-358.

[8] Amiri, Shahram, T. D. V. Cooke, and U. P. Wyss. 2011. "Conceptual Design for Condylar Guiding Features of a Total Knee Replacement." Journal of Medical Devices 5 (2): 025001-1.

[9] Pejhan, Shabnam, E. Bohm, J. M. Brandt, and U. Wyss. 2016. "Design and Virtual Evaluation of a Customized Surface-Guided Knee Implant." Proc IMechE Part H: J Engineering in Medicine, 230, 10, 949-961.

[10] Wyss, Urs, S. Amiri, and T. D. V. Cooke. 2010. *Knee Prosthesi*s. Patent: US20120179265.

[11] Willing, Ryan and I. Y. Kim. 2011. "Design Optimization of a Total Knee Replacement for Improved Constraint and Flexion Kinematics." Journal of Biomechanics 44 (6): 1014-1020.

[12] Fitzpatrick, Clare K., C. W. Clary, P. J. Laz, and P. J. Rullkoetter. 2012. "Relative Contributions of Design, Alignment, and Loading Variability in Knee Replacement Mechanics." Journal of Orthopaedic Research 30 (12): 2015-2024.

[13] Fitzpatrick, Clare K., C. W. Clary, and P. J. Rullkoetter. 2012. "The Role of Patient, Surgical, and Implant Design Variation in Total Knee Replacement Performance." Journal of Biomechanics 45 (12): 2092-2102.

[14] Sathasivam, Shivani and P. S. Walker. 1999. "The Conflicting Requirements of Laxity and Conformity in Total Knee Replacement." Journal of Biomechanics 32 (3): 239-247.

[15] Willing, Ryan and I. Y. Kim. 2009. "Three Dimensional Shape Optimization of Total Knee Replacements for Reduced Wear." Structural and Multidisciplinary Optimization 38 (4): 405-414.

[16] Willing, Ryan and I. Y. Kim. 2012. "Quantifying the Competing Relationship between Durability and Kinematics of Total Knee Replacements using Multiobjective Design Optimization and Validated Computational Models." Journal of Biomechanics 45 (1): 141-147.

[17] Fitzpatrick, Clare K., M. A. Baldwin, P. J. Rullkoetter, and P. J. Laz. 2011. "Combined Probabilistic and Principal Component Analysis Approach for Multivariate Sensitivity

Evaluation and Application to Implanted Patellofemoral Mechanics." Journal of Biomechanics 44 (1): 13-21.

[18] Ardestani, Marzieh M., M. Moazen, and Z. Jin. 2015. "Contribution of Geometric Design Parameters to Knee Implant Performance: Conflicting Impact of Conformity on Kinematics and Contact Mechanics." The Knee 22 (3): 217-224.

[19] Laz, Peter J. and M. Browne. 2010. "A Review of Probabilistic Analysis in Orthopaedic Biomechanics." Proceedings of the Institution of Mechanical Engineers. Part H, Journal of Engineering in Medicine 224 (8): 927-943.

[20] Guess, Trent M., G. Thiagarajan, M. Kia, and M. Mishra. 2010. "A Subject Specific Multibody Model of the Knee with Menisci." Medical Engineering & Physics 32 (5): 505-515.

[21] Bloemker, Katherine H., T. M. Guess, L. Maletsky, and K. Dodd. 2012. "Computational Knee Ligament Modeling using Experimentally Determined Zero-Load Lengths." The Open Biomedical Engineering Journal 6: 33-41.

[22] Guess, Trent M., H. Liu, S. Bhashyam, and G. Thiagarajan. 2013. "A Multibody Knee Model with Discrete Cartilage Prediction of Tibio-Femoral Contact Mechanics." Computer Methods in Biomechanics and Biomedical Engineering 16 (3): 256-270.

[23] Yoshioka, Yuki, D. W. Siu, R. A. Scudamore, and T. D. V. Cooke. 1989. "Tibial Anatomy and Functional Axes." Journal of Orthopaedic Research 7 (1): 132-137.

[24] Matsuda, Shuichi, H. Miura, R. Nagamine, K. Urabe, T. Ikenoue, K. Okazaki, and Y. Iwamoto. 1999. "Posterior Tibial Slope in the Normal and Varus Knee." The American Journal of Knee Surgery 12 (3): 165-168.

[25] Hashemi, Javad, N. Chandrashekar, B. Gill, B. D. Beynnon, J. R. Slauterbeck, R. C. Schutt Jr, H. Mansouri, and E. Dabezies. 2008. "The Geometry of the Tibial Plateau and its Influence on the Biomechanics of the Tibiofemoral Joint." The Journal of Bone and Joint Surgery. American Volume 90 (12): 2724-2734.

[26] Hudek, Robert, S. Schmutz, F. Regenfelder, B. Fuchs, and P. P. Koch. 2009. "Novel Measurement Technique of the Tibial Slope on Conventional MRI." Clinical Orthopaedics and Related Research® 467 (8): 2066-2072.

[27] Cinotti, Gianluca, P. Sessa, FR Ripani, R. Postacchini, R. Masciangelo, and G. Giannicola. 2012. "Correlation between Posterior Offset of Femoral Condyles and Sagittal Slope of the Tibial Plateau." Journal of Anatomy 221 (5): 452-458.

[28] Conover, William Jay and W. J. Conover. 1980. "Practical Nonparametric Statistics."

[29] Moro-oka, Taka-aki, S. Hamai, H. Miura, T. Shimoto, H. Higaki, B. J. Fregly, Y. Iwamoto, and S. A. Banks. 2008. "Dynamic Activity Dependence of in Vivo Normal Knee Kinematics." Journal of Orthopaedic Research 26 (4): 428-434.

[30] Acker, Stacey M., R. A. Cockburn, J. Krevolin, R. M. Li, S. Tarabichi, and U. P. Wyss. 2011. "Knee Kinematics of High-Flexion Activities of Daily Living Performed by Male Muslims in the Middle East." The Journal of Arthroplasty 26 (2): 319-327.

[31] Noble, Philip C., M. J. Gordon, J. M. Weiss, R. N. Reddix, M. A. Conditt, and K. B. Mathis. 2005. "Does Total Knee Replacement Restore Normal Knee Function?" Clinical Orthopaedics and Related Research 431: 157-165.

[32] Smith, Stacey M., R. A. Cockburn, A. Hemmerich, R. M. Li, and U. P. Wyss. 2008. "Tibiofemoral Joint Contact Forces and Knee Kinematics during Squatting." Gait & Posture 27 (3): 376-386.

[33] Godest, A. C., M. Beaugonin, E. Haug, M. Taylor, and PJ Gregson. 2002. "Simulation of a Knee Joint Replacement during a Gait Cycle using Explicit Finite Element Analysis." Journal of Biomechanics 35 (2): 267-275.

[34] Abdi, Hervé and L. J. Williams. 2010. "Principal Component Analysis." Wiley Interdisciplinary Reviews: Computational Statistics 2 (4): 433-459.

[35] Leszko, Filip, K. R. Hovinga, A. L. Lerner, R. D. Komistek, and M. R. Mahfouz. 2011. "In Vivo Normal Knee Kinematics: Is Ethnicity Or Gender an Influencing Factor?" Clinical Orthopaedics and Related Research® 469 (1): 95-106.

[36] Johal, Parm, A. Williams, P. Wragg, D. Hunt, and W. Gedroyc. 2005. "Tibio-Femoral Movement in the Living Knee. A Study of Weight Bearing and Non-Weight Bearing Knee Kinematics using 'interventional' MRI." Journal of Biomechanics 38 (2): 269-276.

[37] Hamai, Satoshi, T. Moro-Oka, N. J. Dunbar, H. Miura, Y. Iwamoto, and S. A. Banks. 2012. "In Vivo Healthy Knee Kinematics during Dynamic Full Flexion." BioMed Research International 2013.

[38] Bae, Dae Kyung, S. J. Song, and S. D. Cho. 2011. "Clinical Outcome of Total Knee Arthroplasty with Medial Pivot Prosthesis: A Comparative Study between the Cruciate Retaining and Sacrificing." The Journal of Arthroplasty 26 (5): 693-698.

[39] Omori, Go, N. Onda, M. Shimura, T. Hayashi, T. Sato, and Y. Koga. 2009. "The Effect of Geometry of the Tibial Polyethylene Insert on the Tibiofemoral Contact Kinematics in Advance Medial Pivot Total Knee Arthroplasty." Journal of Orthopaedic Science 14 (6): 754-760.

Chapter 4

Kinematic Behavior of a Customized Surface-Guided Total Knee Replacement during Simulated Knee Bending

Abstract

Patient satisfaction after total knee arthroplasty (TKA) is reported to be lower than that reported after total hip arthroplasty (THA) [1,2]. Therefore, a variety of designs for knee implants have been developed to improve the level of satisfaction of patients by providing close to the normal pattern of motion for activities of daily living. The surface-guided total knee replacements (TKRs) aim to achieve a normal range and pattern of motion through specially shaped articulating geometries [3-6].

This study uses virtual simulation along with experimental testing by a load-controlled knee wear simulator to evaluate the kinematic performance of a customized surface-guided TKR under different weight-bearing conditions. The behavior of the TKR was simulated virtually during a cycle of gait, lunging and squatting. Then, prototypes of the femoral component and

tibial insert were installed on a knee wear simulator, and lunging and squatting conditions were examined through load-controlled experiments.

The surface-guided TKR motion in the knee wear simulator was the same as the predefined design target. The tibial insert rotated internally for the experimentally simulated lunging and squatting cycles. This rotation occurred around a medial center, along with the posterior translation of the lateral condyle. The contact forces between specially shaped bearing surfaces provided the guidance of the tibiofemoral motion. The normalized root mean square error between the prediction of the virtual simulation of the tibial internal-external rotation and the test outcomes was less than 8%. These measures confirm the validity of the virtual simulation to be used for the evaluations of the customized surface-guided TKR.

Introduction

The goal of recent developments in total knee replacement is to provide patients with improved functionality and meet their expectations in performing activities of daily living. It is reported that patients with traditional knee replacements experience limitation in knee function, especially for high flexion activities such as kneeling, squatting and gardening [7]. With an increasing number of younger and more active patients, who require knee arthroplasty [8], the demand for implants capable of achieving a high range of motion with normal kinematics has increased. The amount of maximum knee flexion in a TKR with less risk of impingement between the posterior femoral condyle and tibial insert at deep flexion angles appears to be affected by the AP translation of the femur, which is related to the design of the tibiofemoral components [9].

Understanding the kinematics of the articulating surfaces is not only important in the diagnosis of joint disorders and injuries, but also when designing implants to restore the natural pattern of motion. Therefore, it is critical to evaluate the kinematic performance through preclinical in vitro tests, considering the design of the implant as the main attributing variable. A popular experimental tool for testing the kinematic behavior of TKRs is the Oxford knee rig [10,11], or simulators designed based on this rig [11-17]. In such experiments six degrees of freedom are provided for the knee, while a fixed load is applied to the hip [11,18]. Typically the load at the hip is balanced by the quadriceps attachments in order to simulate the flexion-extension of the knee. Varadarajan et al. [11] reported that a limitation of the Oxford knee rig is that the constraints at the hip and ankle joints are not physiologic. They also argued the limitations due to a fixed line of action for the balancing quadriceps force, the lower amount of the muscle forces used for the in vitro tests, and the ignorance of the effect of the co-contraction of the hamstring in a typical Oxford rig set-up [11]. DesJardins et al. [19] reported two main shortcomings for the in vitro cadaveric tests; the impact of the differences in the surgical techniques and the limitation in applying loads close enough to the physiologic conditions.

The load-controlled dynamic knee wear simulators are common for wear testing of the implant components. However, they have also been used to determine the kinematic behavior of the TKR by controlling the input flexion-extension angle of the femoral component, and the forces at the joint for different activities of daily living [5,18-21]. The input forces and torque in knee wear simulators, the axial force, AP shear and IE rotational torque, consist of the resultants of the external ground reaction forces, and the internal muscle forces on the knee

joint. Therefore, the knee wear simulator provides the set up to simulate different activities of daily living under realistic force levels. DesJardins et al. [19] described this method as a great experimental approach to isolate the influence of the TKR design from other variables such as the surgical and patient related factors on the TKR kinematic measures. In the knee wear testing simulators, the restraint from the soft tissues are mimicked by mechanical springs or a software modeling a knee's constraining tissues, combined with adaptive control as provided by the AMTI ADL knee wear simulator (Advanced Mechanical Technology Inc., Watertown, MA) [19,20]. Such adaptive control technology decreases the required tuning time with a high level of accuracy, which is a general shortcoming of the traditional load-controlled simulators [22].

Literature review of kinematics of the healthy knee joint

Advancements in imaging technologies provide researchers with a variety of tools for studying the in vivo motion of the knee joint, including magnetic resonance imaging (MRI), fluoroscopy images, roentgen Stereophotogrammetric Analysis (RSA), and motion analysis using skin-mounted or bone-mounted markers. There are pros and cons to each of these methods. For instance, fluoroscopy provides a real-time study of the kinematics of the joint; however, there is some inaccuracy due to difficulties in identifying bones in addition to the risks of radiation of the subjects [23-25]. In an analysis using makers, the motion between markers and the bones would be a source of error [24,26]. RSA also results in radiation of subjects, and similar to the motion analysis by markers there is a risk of cross-talk for this method. Alternatively, MRI has no radiation, and it provides imaging in different planes with high accuracy. However, the limited spaces inside the MRI system and availability of open-access

scanners where the subjects can perform the desired activities are major problems for the use of MRI systems for kinematic analysis [24,27].

In this study, the pattern of motion of a normal healthy joint during flexion is considered as a combination of roll-back of the femur on the tibial plateau and internal rotation of the tibia around a medial axis. The guidance of motion in a healthy knee is provided by the contact forces due to the particular shape of the femoral and tibial articulating surfaces, and the ligaments forces [28-30]. Pinskerova et al. [29] reported that the first radiological study of the kinematics of the knee was done by Zuppinger in 1904. He showed that as the knee bent, the femur rolled back on the tibia due to the influence of the cruciate ligaments. Since then, there has been a long history of discussion over the role of the femoral roll-back on the tibia (Table 4-1).

Iwaki et al. [31] examined the relative motion of the femur on the tibia at certain flexion angles for non-weight bearing cadaver knees using MRI in the sagittal view. They fitted circular arcs over the posterior and anterior sections of the femoral articular surfaces, and called them the flexion facet and the extension facet, respectively. They measured the distance from the center of the flexion facet (FFC) and the center of the extension facet (EFC) to the posterior cortex of the tibia to define the anterior-posterior (AP) displacement of the femur on the tibia. Their results show that the medial femoral condyle is composed of two arcs in the sagittal view. During flexion of the knee to about 30°, on the medial side, the center of rotation shifted from the EFC to the FFC, while from 30° to 120°, the motion of the medial condyle is described as pure sliding. From 110° to 120° of flexion, a 2 mm posterior translation of the medial FFC is reported [31]. Therefore, there is simple sliding of the femoral medial condyle on the tibia with

little displacement in the AP direction. In contrast, the lateral femoral condyle which was composed almost of one circular surface rolled backward with flexion. Such lateral rolling and sliding translated the FFC about 19 mm posteriorly from -5° to 120° of flexion. [31]

Martelli and Pinskerova [32] reported the shapes of the femoral condyles and the tibial plateau as the major contributing parameters to the tibiofemoral movement. They showed that a sphere could be fitted to the posterior part of the medial condyle, which articulates on the socket shape of the tibial plateau with an upward slope of the anterior segment. Therefore, they concluded that the medial femoral condyle rotated on the tibia around three axes passing through the center of the fitted sphere, while there was limited AP translation. On the lateral side, they described a flattening on the femoral distal end. It means that the femur could move freely in the AP direction, as the flexion occurs around an axis passing through the circular posterior sections of the medial and lateral condyles. [32]

Komistek et al. [25] used fluoroscopic images of the normal human knee to analyze the kinematics of the tibiofemoral joint for five different weight-bearing activities, deep knee bend, normal gait, rising from a chair, sitting in a chair, and stair descending. Their analysis of the medial and lateral contact positions confirmed the results of previous studies, less AP translation on the medial side than on the lateral one. For the deep flexion activities, they reported an average of 12.7 mm backward translation for the lateral femoral condyle, while the medial condyle only translated 2.9 mm. In comparison to MRI studies [24,33], they reported more posterior movement of the lateral condyle during deep knee bending activities. Hamai and colleagues [34] used the X-ray technique to investigate the kinematics during full flexion (from 85° to 150°). Their results showed that the medial and lateral contact points on the tibia

moved 2 mm and 8 mm, respectively toward the posterior edge of the tibial plateau at 150° flexion, which was equal to 15° internal rotation of the tibia [34].

Table 4-1 Summary of studies about tibiofemoral kinematics of the normal healthy knee joint

Study	ROM	Activity	Medial condyle backward movement (mm)	Lateral condyle backward movement (mm)
Iwaki et al. [31]	0 to 120°	Unloaded- Cadaver	1.5	19
Hill et al. [36]	-5 to 110°	Unloaded- Cadaver	2	17
		Squatting	4	12
Nakagawa et al. [33]	133 to162°	Unloaded- In vivo	4.5	15
Komistek et al. [25]	0° to 90°	Chair sitting	2.9	12.8
		Chair rising	-2.2[b]	-16.9
		Stair descent	-2	3.9
		Deep knee bend	1.5	14.1
		Gait	0.9	4.3
Pinskerova et al. [29]	-5 to120°	Unloaded- In vivo	0	14
		Squatting	1	20
		Unloaded- Cadaver	2	21
Johal et al. [37]	-5 to120°	Squatting	1.4	21.1
	120 to 140°		8.4	9.8
DeFrate et al. [35]	0 to 90°	Lunge	1.4	13.26
Dennis et al. [23]	0° to 120°	Deep knee bend	1.94	21.07
Hamai et al. [34]	85° to150°	Lunge full flexion	2	8

Other studies in the literature also confirm these findings. As it is summarized in Table 4-1, when the knee bends from -5° to about 110-120° under loaded condition, the lateral condyle moves significantly greater than the medial one in the posterior direction [23-25,29,31,33-35]. During deep flexion beyond 130°, both the medial and lateral condyles move backward in the weight-bearing and unloaded conditions [24,25,33,34]. The combination of little AP movement

on the medial side, and the lateral roll-back of the femur on the tibia results in internal rotation of the tibia around a medial axis.

Literature review of the kinematics after TKR

After knee arthroplasty, the simplified and different geometric design of the articulating surfaces, the lack of cruciate ligaments, or insufficient control of stability by the remaining ligaments, result in abnormal kinematics. The paradoxical motion in the AP direction, anterior sliding of the femur during knee flexion, is reported as one of the major problems after TKR. Dennis et al. [38,39] performed an in vivo fluoroscopic analysis of the kinematic performance of different designs of the traditional total knee replacements. They reported that during deep knee bending, 72% of the patients having a PCL-retaining fixed-bearing TKR experienced the paradoxical femoral movement of more than 3 mm. They found that there was more posterior condylar motion with the posterior stabilized (PS) knees; however, it was less than the magnitude of the femoral condylar roll-back expected for the normal knee. Also, they reported that patients with PS knees experienced paradoxical femoral motion on the medial side at flexion angles higher than 60 degrees. It means that an opposite axial rotation could have happened or less axial rotation around the long axis of the tibia was experienced than what occures in a normal healthy joint.

Victor et al. [40] also investigated the kinematic performance of the CR and PS types of a specific TKR. They confirmed that forward sliding of the medial condyle during knee flexion occurred in subjects with the cruciate retaining implants. They reported that the total amount of axial rotation was similar for CR and PS knee replacements, while in the CR knees, the

anterior movement of the medial condyle led to the internal rotation of the tibia. In the PS knees, such rotation was produced by a backward translation of the lateral condyle [40]. Anterior sliding of the femur on the tibia results in decreased range of motion, and consequently limiting the capability of the patients in doing activities of daily living. Horiuchi et al. [41] studied the posterior cruciate retaining TKR during weight-bearing and non-weight bearing deep knee bending. The results of this study showed that loading condition contributed to the kinematics for various activities. They also reported that in the weight-bearing condition, co-contraction of the muscles, the balance of the ligaments, and correct alignment of the components prevented anterior femoral condyle translation during early flexion angles.

In the bicruciate substituting (BSC) TKR, the anterior and posterior cruciate ligaments are replaced with two femoral cams articulating on the anterior and posterior portions of the intercondylar post of the tibia. The anterior post-cam mechanism is expected to be in articulation during early flexion, and the posterior cam-post mechanism becomes engaged when the knee bends beyond 60 degrees [42]. Kuroyanagi et al. [42] studied 20 patients having a BCS total knee replacement, while they performed kneeling and lunge. The results indicated that the condyles moved posteriorly from 0° to 70°, while a medial pivot pattern of rotation was observed due to the greater amount of backward translation on the lateral side. They reported that flexion of the knee beyond 70° led to the almost symmetric posterior translation of both medial and lateral condyles. Victor et al. [43] also investigated the patterns of motion in subjects with both cruciate substituting implants during deep knee bending using fluoroscopy. They reported an average amount of 14 mm and 23 mm posterior femoral rollback on the medial and lateral sides, respectively, mostly occurring between 0 to 30 degrees of flexion [43].

Such a pattern of motion is quite different from normal kinematics, as a small amount of medial translation would take place in a normal knee within such range of flexion [25,29,34,42]. The greater posterior translation on medial side increases the risk of getting overload on the medial section [43].

Achievement of closer to normal kinematic behavior would improve the functional performance, and provide the patients with a knee that "feels more normal". In the design of the customized surface-guided TKR of this dissertation, asymmetric tibiofemoral bearing surfaces with the partial ball and socket configuration on the medial side, and the lateral articulation surfaces with incrementally changing radii was implemented. It was assumed that such articulation surface geometries could guide the motion following a predefined design target. This study answers the question if such specially shaped tibiofemoral articulating surfaces are capable of reproducing close to normal kinematics, as described by the target pattern of motion. This study aims to use load-controlled experiments with the knee wear simulator to test if the kinematics of the design target can be achieved by the surface-guided TKR design for loading conditions of high flexion activities of lunging and squatting. The current study uses the AMTI ADL knee wear simulator (Advanced Mechanical Technology Inc., Watertown, MA) to measure the relative movements between the femoral and tibial components of the artificial knee joint during load-controlled simulated cycles of knee bending. The internal-external (IE) rotation of the tibia and the anterior-posterior (AP) translation of the medial and lateral femoral condyles were recorded as the criteria showing the kinematic performance for the simulated activities. Another objective was to validate the virtual

simulation of the customized surface-guided TKR by comparing the patterns of motion observed experimentally and virtually under knee bend loads.

Methodology

Virtual simulation of the implants

A model was developed in the virtual prototyping software MSC.ADAMS to simulate the behavior of the implant during weight-bearing activities. In this simulation, the CAD models of the implant were imported into the software and oriented at 0° of flexion based on the reference landmarks and axes extracted from reconstructed model of the patient's joint from MRI. These references include the contact points at zero degrees of flexion, the joint line and the axis of the rotation of the tibia. A three-dimensional contact model, the "Impact" function in MSC.ADAMS, was used to simulate the contact between the femoral and tibial articulating geometries. As described in equation (4-1), the contact force for the articulation of profiles with general shapes was estimated as a function of the combined material properties and the relative curvature of the articulating surfaces.

$$\delta = \left(\frac{9F^2}{16R_e E^{*2}}\right)^{1/3} f_2(r) \qquad (4\text{-}1)$$

where δ is the penetration distance of the solids in contact, F is the contact force, $\mathrm{R_e}$ is the equivalent relative curvature, and $\mathrm{E^*}$ is the equivalent combined material property. In this equation, $\mathrm{f_2}$ is a function of the relative curvature between the two components [44,45]. It results in the simple form of equation (4-2), in which k is the contact stiffness and e is the force exponent.

$$F = k(\delta)^{\mathrm{e}} \tag{4-2}$$

Contact stiffness and the force exponent are the required inputs for the contact function of the MSC.ADAMS (equation (4-3)). In this equation, the contact force (F) is a nonlinear exponential spring-damper that is a function of:

x: distance between the contact markers of the two components

k: stiffness of the intersection between the two surfaces

e: exponent of the force function

C_{max}: maximum damping coefficient

d: penetration distance at which full damping is applied

x_f: free length, and

$\dot{x}$: velocity of penetration

$$F = Max(0, k(x_f - x)^e - STEP(x, x_f - d, C_{max}, x_f, 0) * \dot{x}) \tag{4-3}$$

In this equation, if x gets larger than the free length (x_f) between markers on the contacting surfaces, it means that no penetration has occurred, and the force would be zero. The contact force has a stiffness component that is a function of the penetration of the marker on one of the contacting surfaces through the free length distance from the marker on the other contacting body. Another component of the "Impact" force is the damping that is a step function of the speed of penetration. In this study, k was estimated at 35,000 N/mm based on the dimensions of the contact geometries and material properties of the components, and the exponent was considered to be equal to 1.5 [45]. For the femoral and tibial components, material properties of a CoCr alloy (E= 210GPa, ϑ= 0.3) and UHMWPE (E=680 MPa, ϑ= 0.46)

were used, respectively. In agreement with the previously reported studies [46], a static coefficient of friction of 0.04, and a dynamic coefficient of 0.02 was considered for the friction.

In this model no cruciate ligaments were taken into account; therefore, the constraining factor for the tibial component IE rotation was the contact between the two components. Two scenarios were investigated considering the influence of the remaining ligaments. In the first approach the collateral ligaments were modeled with nonlinear spring force elements paralleled with a damper. In the second approach, the contribution of the remaining ligaments was modeled similar to a knee wear simulator machine by a linear spring (K=9.4 N/mm) in the anterior-posterior (AP) direction, and a torsional spring (K=0.13 N.mm/deg) in the internal-external (IE) direction [47]. The stiffness of the springs was set according to requirements of ISO 14243-1 [47] for the load-controlled experiments.

The influence of the collateral ligaments was investigated by comparing the outcomes of the virtual simulation with no collateral ligaments, and those of the simulation with bundles of the medial collateral ligament (MCL) and the lateral collateral ligament (LCL). Three bundles for each of the medial and lateral collateral ligaments (MCL and LCL) were modeled with nonlinear spring damper functions of force elements in MSC.ADAMS. These functions (equation (4-4)) were adapted from the study by Bloemker et al. [48], in which the force was a function of the reference or original ligament length, the zero load length and the strain. In these equations, "f" is the ligament tension, "ε" is the ligament strain, ε_l is the constant spring parameter (Table 4-2) , "K" is a stiffness parameter (Table 4-2), "C" is damping coefficient of a parallel damper for each bundle (Table 4-2), "L" is the length of the ligament and "l_0" is the zero length of the ligament.

$$f = \begin{cases} \frac{1}{4} K \frac{\varepsilon^2}{\varepsilon_l} + C\dot{L} & 0 < \varepsilon < 2\varepsilon_l \\ K(\varepsilon - \varepsilon_l) + C\dot{L} & \varepsilon > 2\varepsilon_l \\ 0 + C\dot{L} & \varepsilon < 0 \end{cases} \quad (4\text{-}4)$$

The attachment points of the ligaments were extracted from MRI data and verified by comparing the insertion point distance to bone landmarks with the outcomes of previous studies [48-50]. The length of each ligament at zero degrees of flexion, which is the initial point of the simulation in the MSC.ADAMS were considered as the original ligament length (l_r). Using this reference length (l_r) and the strain in the ligament at the reference (zero degree of flexion) position (ε_r) based on data in literature [51], the zero load length (l_0) was calculated by equation (4-5).

$$l_0 = \frac{l_r}{\varepsilon_r + 1} \quad (4\text{-}5)$$

The stiffness and spring parameters for modeling the nonlinear function of the force-displacement and damping coefficient parameter were also adapted from a study by Bloemker et al. [48] and summarized in Table 4-2.

Table 4-2 Ligament bundle properties

Ligament bundle	Stiffness (N)	Spring parameter- ε_l	Damping coefficient (Ns/mm)	Reference strain- ε_r [a]
Anterior Lateral Collateral (ALC)	2000	0.03	0.5	-0.25
Intermediate Lateral Collateral (ILC)	2000	0.03	0.5	-0.05
Posterior Lateral Collateral (PLC)	2000	0.03	0.5	0.08
Anterior Medial Collateral (AMC)	2750	0.03	0.5	0.04
Intermediate Medial Collateral (IMC)	2750	0.03	0.5	0.04
Posterior Medial Collateral (PMC)	2750	0.03	0.5	0.03

a. The reference strain data was extracted from the study by Blankevoort et al. [51]

In the virtual simulation, the tibial component was set free to move in the horizontal plane, while the femur rotated around the FE axis according to the input profile of the flexion angles into the simulation. Consistent with ISO 14243-1 [47], the input load was applied to the center of the tibial insert + 7% of the width of the tibia towards the medial side. (Figure 4-1)

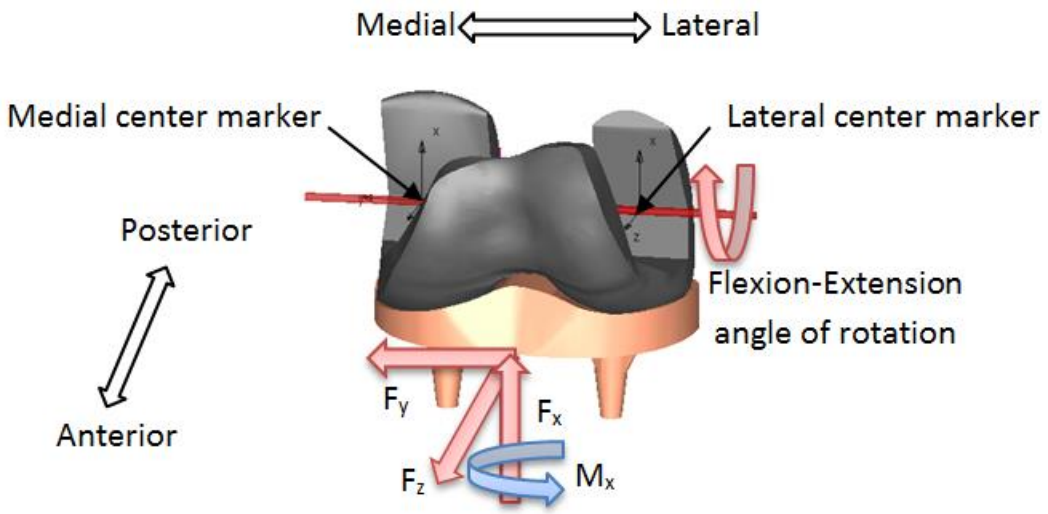

Figure 4-1 Boundary conditions for the simulation. F_x: the axial distal-proximal joint force; F_y: the medial-lateral shear force; F_z: the anterior-posterior shear force; M_x: the internal-external rotational torque applied to the center of the tibial insert.

Simulation load and ligament scenarios

1. Analysis of the primary version of the implant

First, the performance of the initial design of the surface-guided TKR, generated based on the target number 1 for the pattern of motion (Figure 2-5), was investigated for three different activities of daily living, including a cycle of walking, lunging, and squatting with heels down. For this simulation, the influence of the medial and the lateral collateral ligaments was modeled as nonlinear spring damper functions (Table 4-2).

The kinematic behavior of the surface-guided TKR was investigated through a virtual simulation of a gait cycle, considering the input loads and torques, as well as the FE pattern of motion as described by ISO 14243-1 [47]. The standard ISO input load profiles [47] are reported to be different from the actual loads acting on the knee during ADL after total knee replacement [52,53]. Moreover, to perform activities of daily living such as kneeling, a higher range of flexion is required [54,55], than for level walking, as described by ISO profiles for load-controlled testing of a gait cycle [47]. Therefore, the loads (axial proximal-distal load, AP shear force, and IE torque), and the flexion-extension angle data reported by Bergmann et al. [52] for lunging, based on measured data from an instrumented TKR, was used as the input profile for the surface-guided knee simulation.

The behavior of the implant under the joint load of a squat activity was also analyzed by using the load and FE angle data reported by Smith et al. [56] for normal knee subjects. Since only the axial compressive force was available from the published data, merely the axial distal-proximal force was applied to the tibia, while the flexion-extension angle was implemented to the axis of the flexion on the femur. During the analyzed squatting cycle, the compressive force reached 2120 N, and the largest flexion angle was 123 degrees. Next, another simulation was performed using the AP and ML forces for the high flexion knee bend activity from Bergmann et al. [52], while the axial tibial force and flexion angle inputs were kept as what Smith et al. [56] reported for squatting. This study aimed to investigate the effect of shear forces on the outcomes.

In all the virtual simulations of the initial version of the customized surface-guided implant, no cruciate ligament was considered. The influence of collateral ligaments was studied by

comparing the kinematic outcomes of the models with three bundles of MCL and LCL, and those without the collateral ligaments.

2. Analysis of the second version of the implant

In the second version, the surface-guided TKR was created based on the target number 2 for the pattern of motion (Figure 2-5). This TKR was virtually simulated under load and FE angle input profiles for two high flexion activities, lunging and squatting. Similar to the analysis of the initial design, the data from the study by Bergmann et al. [52] for a cycle of lunging, and those from the study by Smith et al. [56] for a cycle of squatting, were used as the inputs of the simulation.

In the case of lunging, the influence of the collateral ligaments was investigated by comparing the outcomes of the virtual simulation with no collateral ligaments, and those of the simulation with three bundles for the MCL and LCL. For squatting, a linear spring (K=9.4 N/mm) in the AP direction, and a torsional spring (K=0.13 N.mm/deg) in the IE direction [47], were considered to simulate the behavior of the ligaments. This approach for modeling the ligaments was similar to the settings of the knee wear simulator during the experimental testing of the lunging and squatting.

The predicted IE rotation of the tibial insert was compared with the expected rotation from the design, which was calculated based on a predefined curve of the pivoting versus the flexion angles. Additionally, the AP translations of the medial and lateral femoral condyles were compared with the target pattern of translation in the AP direction. The normalized root mean

square error (NRMSE) was calculated between the experimentally measured kinematic outcomes and the results of the virtual simulation.

Experimental testing

1- Experiments with the printed plastic TKR prototype

First, the prototypes of the primary design were made from PC-ISO material using a Stratasys Fortus 400mc 3D printer (Orthopaedic Innovation Center, Winnipeg, Canada). The required fixtures were designed and 3D printed to assemble the implant on the test set-up of the AMTI ADL knee wear simulator. Since it was a test without immersing the parts in the synovial fluid substitute, the articulating surface was smoothed as much as possible to minimize the friction. Also, a thick layer of petroleum jelly was applied to the articulating areas. In this experiment, the tibial insert was set free to move in the transverse plane; while, the femur was only free to rotate around the FE axis. Similar to the virtual simulation of the TKR, the squatting activity was simulated by applying input kinematic data (FE rotation of the femoral component) and tibial proximal-distal load from a study by Smith et al. [56]. However, the load was decreased to 40% of the actual data, due to the strength limitation of the plastic prototypes. Also, the influence of the ligaments was set to zero in the knee wear simulator.

The test was performed at 0.7 Hz, and data recording started at the 10th cycle. The IE rotation angle at each increment of motion was compared with the design target. The flexion-extension curve for a cycle of squatting (input profile) was used to calculate the expected pivoting angle (IE rotation of the tibia) based on the predefined target curve for the pivoting versus flexion angle (Figure 2-5).

2- Experiments with the metal prototype femur

The surface-guided TKR design based on the second pattern of motion was used to generate another set of prototypes. A metal prototype of the femoral component was 3D printed using powderized cobalt-chromium-molybdenum (CoCrMo) on an EOS M290 system (Stratasys Direct Manufacturing, CA, USA). The tibial insert was precision-machined out of a solid block of high-density polyethylene (HDPE) utilizing a HAAS machine VF2 with MasterCam software to ran the toolpath (Stratasys Direct Manufacturing, CA, USA). Fixtures were custom designed and manufactured (Fortus 400 MC, Stratasys Inc., Eden Prairie, MN) to assemble the components on an AMTI ADL knee wear simulator (Figure 4-2).

In this simulation, the axial force was applied to the tibia with a medial offset of 40-60% distribution on the lateral and medial sides, respectively. The load was applied through a pivot system placed 10% from the center-line of the tibia, towards the medial side. The input FE angle and load waveforms were applied to the femoral and tibial components in a similar manner as the boundary condition described in ISO 14243-1 [47]. Similar to the virtual simulation, the input waveforms of the axial force, AP shear force and IE torque for a cycle of lunging were extracted from a study by Bergmann et al. [52]. For squatting, only an axial force was applied, from data reported by Smith et al. [56]. During simulation of the lunging activity, the effect of the remaining ligaments was eliminated by setting the stiffness of the virtual ligament of the machine to zero. When squatting was simulated, the stiffness of the constraining springs of the virtual ligament set-up was set based on the requirements of ISO 14243-1 [47].

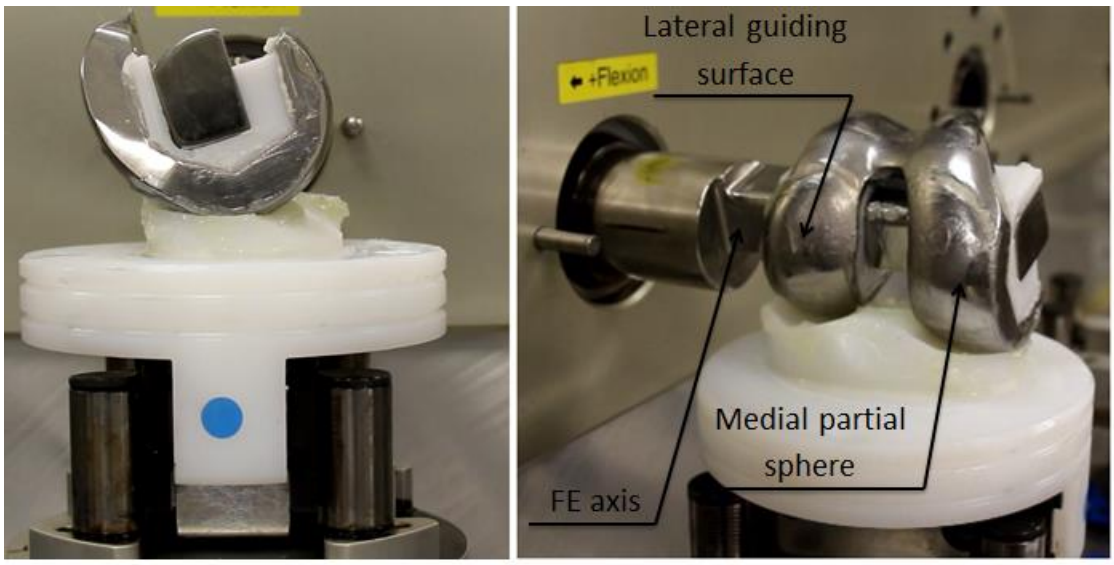

Figure 4-2 The AMTI ADL knee wear simulator test set up (a) sagittal view (b) TKR prototype components

In this test setup, the tibial component was free to move in the medial-lateral direction and rotate internally or externally, while the femur rotated around the FE axis according to the input profile of the flexion angles of the machine. The femur was also free to move in AP direction. A layer of petroleum jelly was applied to the tibiofemoral articulation to reduce friction between the components. This test condition was a less realistic situation than the tests with the synovial-like fluid, because once the lubricant squeezed out there was no backflow. It did; however, make it possible to visually check the motion during the test. Using the non-translucent synovial-like fluid might be more similar to the in vivo condition, but it would have required the TKR to be placed in a bag; therefore, we would not be able to observe the knee.

Testing was performed at 0.33 Hz for 100 cycles as this cycle count was deemed sufficient to evaluate the kinematic behavior. The data recording started after 30 cycles, which was an adequate number of initial cycles before a stationary behavior was reached. The resultant motions, including IE rotation of the tibia and AP translation of the femur, were recorded at 30

cycle intervals throughout the test. At each interval, the data for two cycles were recorded. Therefore the range of the IE rotation was determined based on the results of six recorded consecutive intervals of the cycles from cycle number 30 to 100. Also, the average peak IE rotation and the standard deviation were compared with the design target. The normalized root mean square error (NRMSE) between the measured IE angles of the tibial insert and the expected design target was calculated. The normalized error was computed for the measured data during the last recorded cycle, and was defined relative to the range of the measured IE angles (the maximum value minus the minimum value).

3- Experiments with the prototypes of the optimized TKR

The surface-guided TKR that was designed based on the optimized geometric variables (Chapter 3) were used to generate another set of prototypes. A metal prototype of the femoral component was 3D printed using powderized cobalt-chromium-molybdenum (CoCrMo) on an EOS M290 system (Precision ADM, Winnipeg, Manitoba, CA). Micro-polishing was performed by MMP technology to achieve mirror-finish polish (MicroTek, Cincinnati, Ohio, USA). The polyethylene tibial insert was dry machined on a Fanuc Robodrill 5-Axis CNC vertical milling (PPD Meditech, Waterville, Quebec, CA). The average surface roughness (R_a) was measured using a Zeiss Surfcom 2900-SD2 contact profilometer (OIC Precision Labs, Winnipeg, Manitoba, CA) with a resolution of 0.1nm. Measurements were taken at five points showing 0, 30, 60, 90, and 120 degrees of flexion across the articulating region on each femoral condyle, and the corresponding tibial plateau. The measurements were repeated three times for each point and the average roughness value was measured.

The axial force was applied to the tibia through a pivot system to simulate the medial offset of 40-60% distribution on the lateral and medial sides. The load condition of two activities were tested: lunging based on data reported by Bergmann et al. [52] for the input waveforms of the axial force, AP shear force and IE torque, and deep squatting (up to 140° of flexion) by using only the axial force reported by Smith et al. [56]. During these simulations, the effect of the cruciate knee ligaments was eliminated in the virtual ligament setting of the machine.

In order to be more clinically relevant, the tests on the optimized surface-guided TKR were conducted by putting the components in a bag filled with bovine serum. It is reported that the bovine serum performs as a boundary lubricant and reduce the adhesion similarly to the performance of the synovial joint fluid. However, there is controversy on the stability of the bovine serum as a result of changes in the protein and lipid content [57]. The experiment was performed with bovine serum (Gibco, Life Technologies, NY, USA) with a protein concentration of 20.0 g/L, and diluted from the initial concentration using deionized water. Microbial inhibitor (sodium azide) was 0.2% (weight), and EDTA concentration was 20 mMol.

The test was run at 0.33 Hz for the squatting and lunging activity simulations. Outputs including IE tibial rotation angle and AP translation of the femoral component were recorded for 10 consecutive intervals of the cycles from cycle number 30 to 100. A one-way ANOVA was conducted to compare the results of different recorded cycles based on the absolute deviation between the design target and the kinematic measures for 100 increments of flexion and extension.

Results

Virtual simulation of the implants

1- Analysis of the primary version of the implant

Flexion and extension of the knee during the gait cycle, lunging, and squatting made the lateral condyle move significantly more in the posterior and anterior direction, respectively; in comparison to the medial condyle. Figures 4-3 to 4-5 illustrate the results of the anterior-posterior displacements of the medial and lateral condyles for the simulations of the initial version of the customized surface-guided implant.

When the knee bent from 0 to 58° during a gait cycle under the ISO loading condition, the maximum AP translations of the medial and lateral condyles of the implant were 0.18 and 6.15 mm, respectively, which happened at the 25th and 68th percent of the gait cycle. Based on the design target pattern number 1, it was expected that the medial and lateral center translated 0.00 and 6.4 mm posteriorly at 58° of flexion. When the knee extended during the swing phase, the medial and lateral condyles of the implant translated anteriorly 0.36 and 6.1 mm, respectively.

During a cycle of walking with the new customized surface-guided knee under the loads from the Bergmann et al. study [52], the maximum AP translation in medial and lateral sides were 0.4 and 6.83 mm, respectively, for reaching a flexion angle up to 62 degrees at the swing phase. The average deviation of the IE rotation angle of the tibia from the design target was 0.4±1.17°, while the maximum deviation occurred at the very beginning of the stance phase at around 12 degrees of flexion.

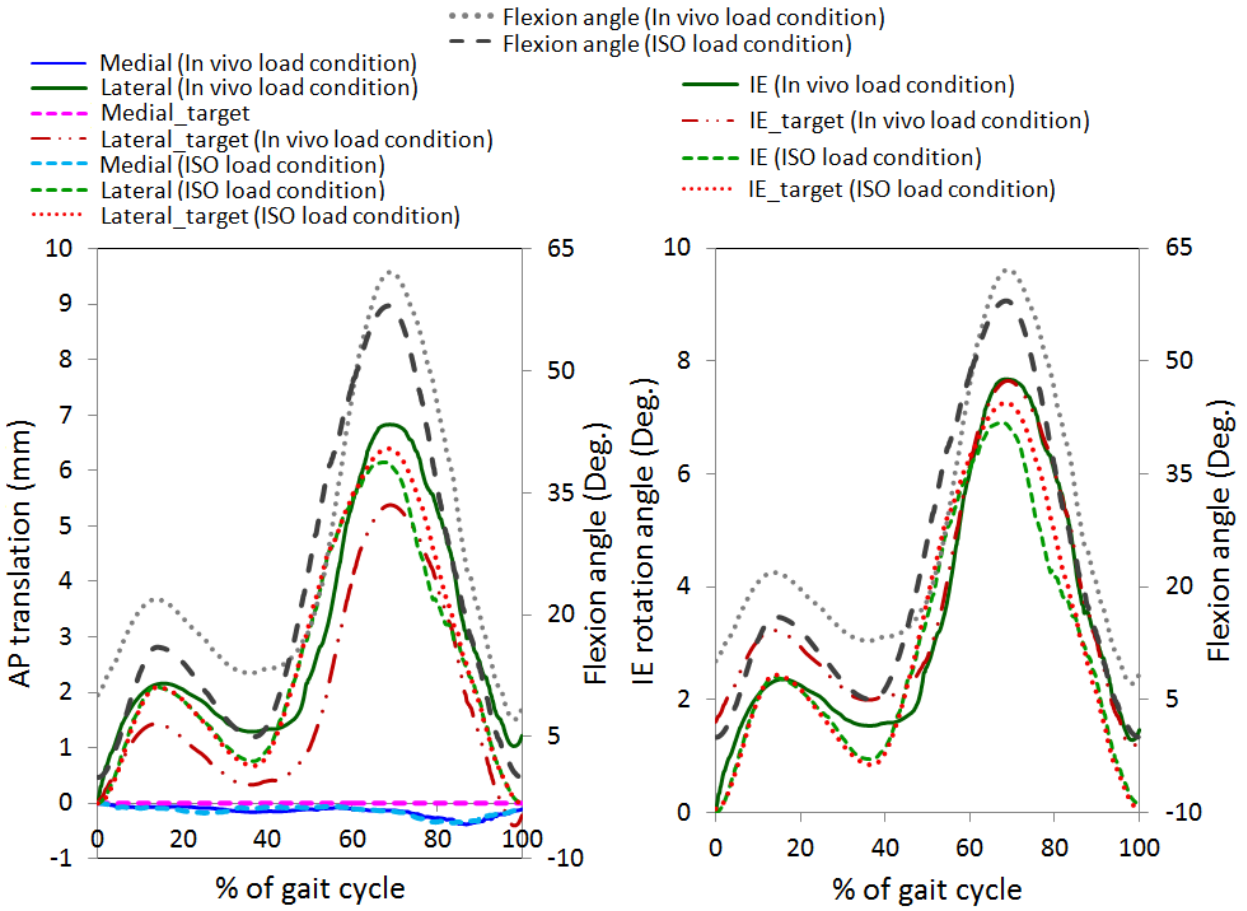

Figure 4-3 Results of the virtual simulation of a gait cycle- positive IE value means internal rotation of the tibia, and positive AP translation of the femoral centers means movement in the posterior direction.

Figure 4-4 compares the outcomes of the virtual simulation of a cycle of lunging for two different loading conditions: one included only the axial proximal-distal force, and the other one experienced the effect of shear forces in the AP and ML directions as well. An average difference of 0.32±0.35° was observed between the IE rotation angles of the tibia with all shear forces, and the one without shear forces. The maximum deviation of 1.4° was recorded at about 15 degrees of flexion. Comparing the results of the simulation with the target pattern of IE rotation angle shows that there was a 3.46% normalized root mean square error considering

the maximum and minimum tibial IE rotation measured by the virtual simulation for the case with the shear forces.

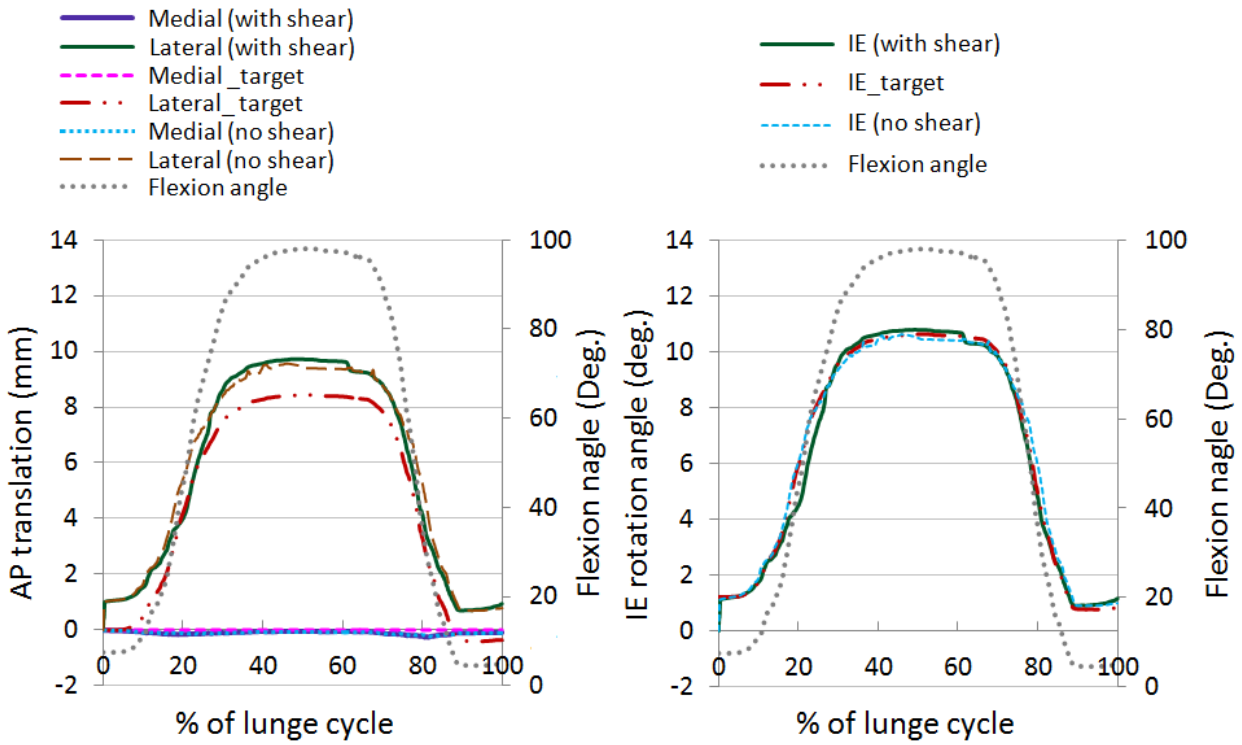

Figure 4-4 Results of the lunging simulation in the virtual simulation environment- Positive IE value means internal rotation of the tibia and positive AP translation of the femoral centers means movement in the posterior direction.

The results of the performance of the TKR under the load and motion conditions of the squat activity for the cases with and without shear forces are shown in Figure 4-5. During simulation of squatting with shear forces included, 0.15 mm medial translation and 11.5 mm lateral posterior translation of the femur led to 12.8° of internal rotation around the center of the medial partial sphere. Based on the design target, 12.65 degrees of pivoting were expected when knee reached 123 degrees of flexion. During the extension phase of the squatting, this knee experienced 0.2 and 11.5 mm of the anterior-posterior translation of the medial and

lateral centers, respectively. In comparison to the target pattern for the tibial IE rotation, there was less than 1% normalized root mean square in one cycle of squatting.

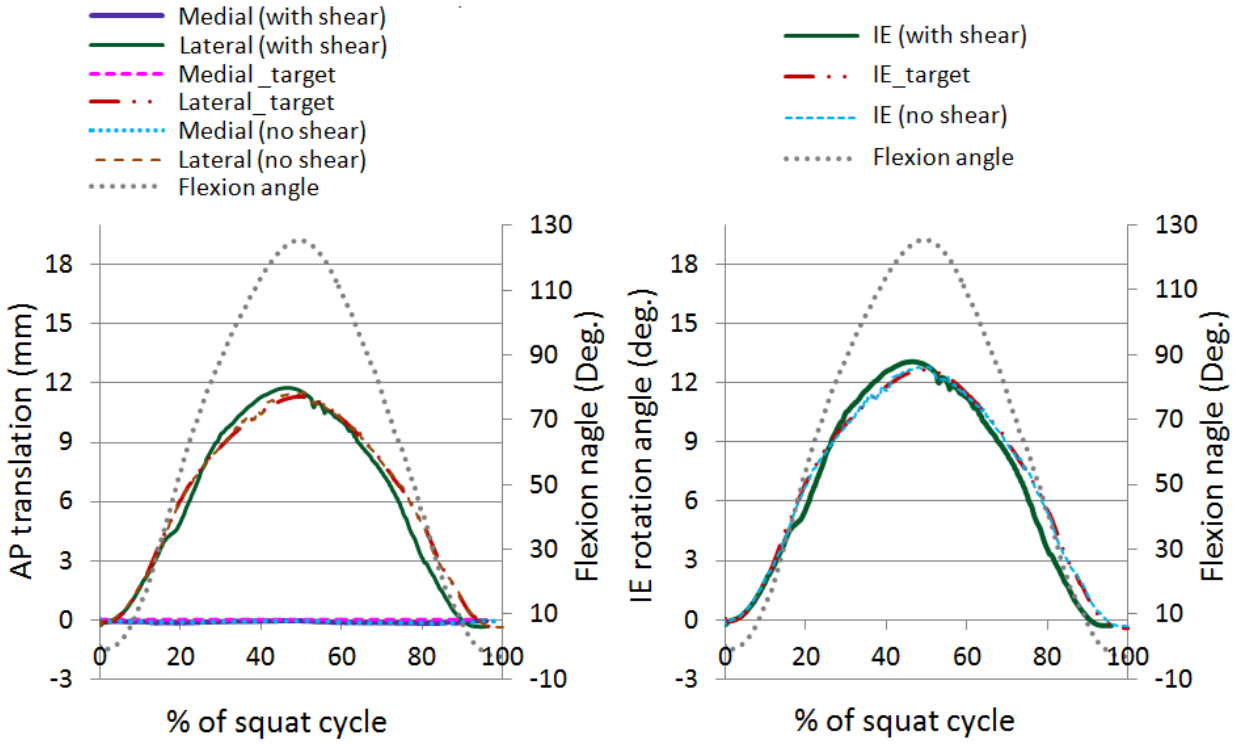

Figure 4-5 Results of the squatting simulation in the virtual simulation environment- Positive IE value means internal rotation of the tibia, and positive AP translation of the femoral centers means movement in the posterior direction.

2- Analysis of the second version of the implant

Results of the virtual simulation of the lunging activity show that during flexion of the joint, the center of the lateral femoral condyle translated 11.7 mm posteriorly on the tibial plateau. On the other hand, the center of the medial condyle moved less than 1 mm in the AP direction throughout the cycles of motion (maximum 0.6 mm anterior translation was observed as the knee extended to zero degrees). A maximum of 13° internal rotation of the tibia was achieved

at a flexion angle of 98 degrees. A peak internal rotation angle of 10.3° is expected for such flexion based on the design target (Figure 4-6).

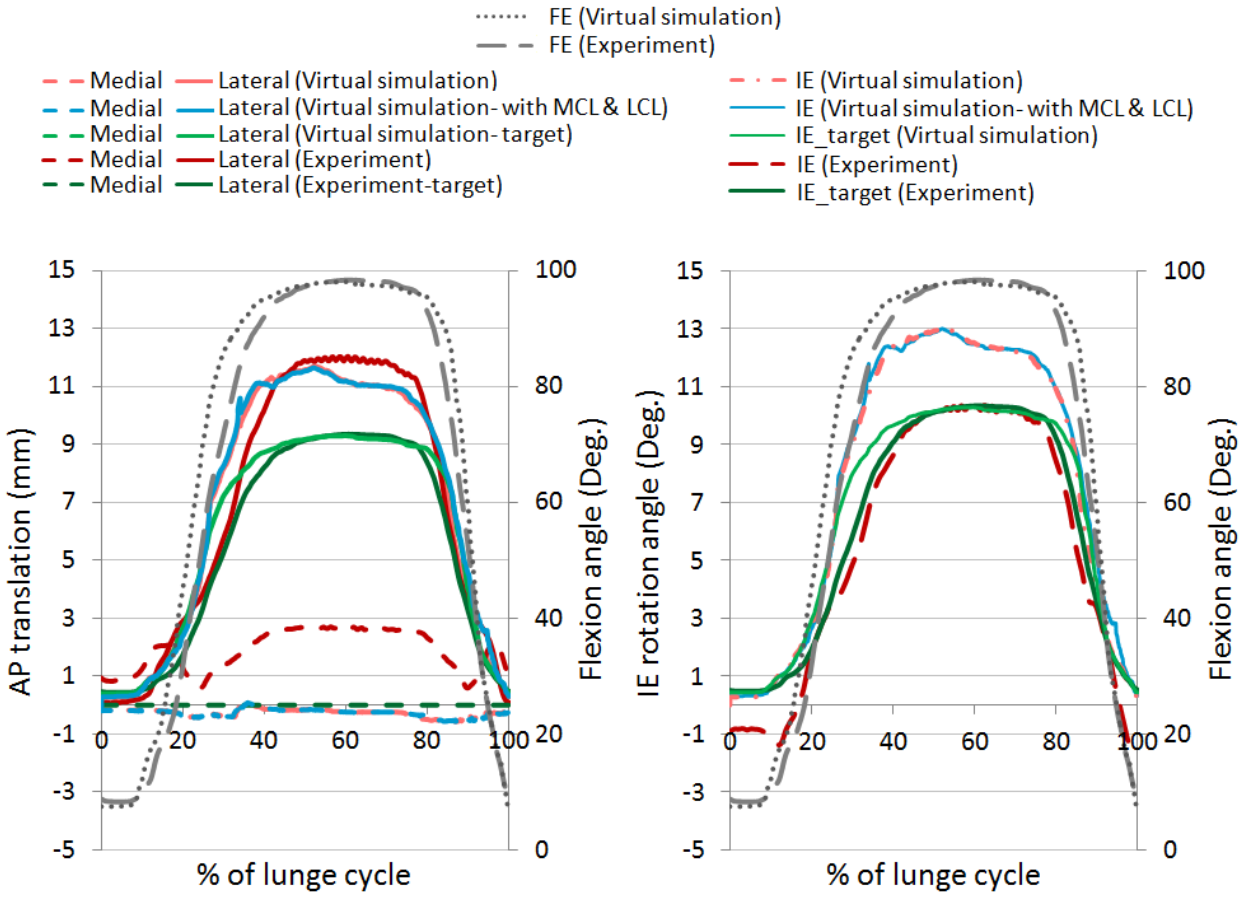

Figure 4-6 The kinematic behavior of the implant as the knee bends during lunging- Positive IE value means internal rotation of the tibia, and positive AP translation of the femoral centers means movement in the posterior direction.

Comparing the outcomes of the virtual simulations that included the collateral ligaments, and those with no collateral ligaments, shows that the forces due to these ligaments would not significantly change the kinematic behavior. During flexion of the knee, there was less than 1.5% average error in the predicted IE rotation of the tibial insert between the two approaches. This deviation increased to 5% during the extension phase of the activity, as the knee went back to the zero degrees of flexion.

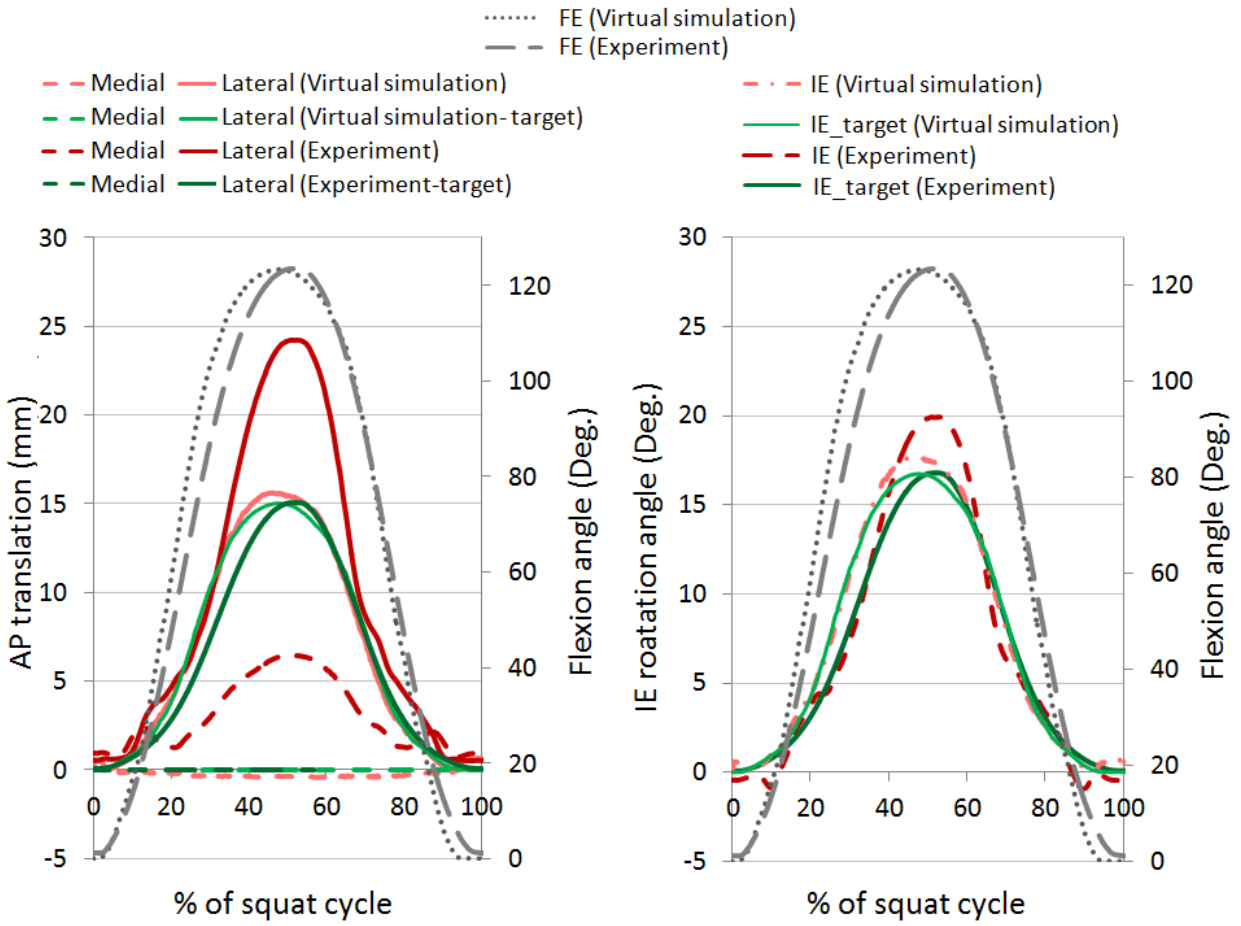

Figure 4-7 Kinematic behavior of the implant as knee bends up to 124 degrees during squatting- Positive IE value means internal rotation of the tibia, and positive AP translation of the femoral centers means movement in the posterior direction

Results of the virtual simulation under the squatting load condition also show that the pattern of rotation of the tibial insert was following the target motion expected from the customized surface-guided TKR (Figure 4-7). As the knee bent from 0 to 123° of flexion, the lateral femoral condyle moved 15.5 mm posteriorly, while the medial condyle moved less than 1 mm in the AP direction. During a cycle of squatting, the virtual simulation predicted 16.7° internal rotation of the tibial insert. The normalized root mean square error between the virtual

simulation outcome for the IE rotation angle and the target pattern of motion was 3.04% in a cycle of squatting, while the maximum difference with the design target was only 1.1 degrees.

Experimental testing

1. Experiments with the plastic prototype femur

Figure 4-8 compares the internal-external rotation of the tibia for a squatting cycle, recorded during an experiment with the results of the virtual simulation and target design for the first version of the surface-guided TKR. The average difference with the expected design target was 0.91° (± 0.88°), while the major deviation occurred in the 40 to 60% and 80 to 100% of the squatting cycle. The maximum rotation of the tibia (15.18°) was achieved as the knee bent to 123°, which was 2.67° larger than the expected design target (12.56°). Except for the first 5% of the cycle of the simulation, no abnormal rotation of the tibia was observed. Therefore, the pattern of the motion was following close to the normal pattern of IE rotation.

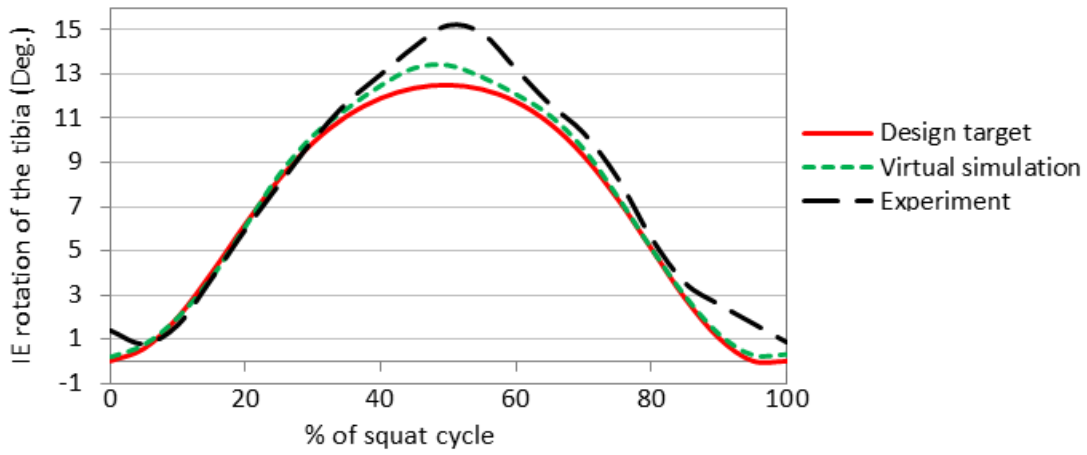

Figure 4-8 Measured IE rotation angle of the tibia from the load-controlled knee simulator experiment, and the virtual simulation of a cycle of squatting

2. Experiments with metal prototype femur

The experimental testing under the lunging load condition resulted in a maximum of 2.5 mm posterior translation of the femoral medial center; while the lateral condyle moved 12 mm in the posterior direction, as the knee reached the highest flexion angle. The predicted range of IE rotation angle by the virtual model for a cycle of lunging of the second version of the surface-guided TKR was 12.7°, and the experimental testing resulted in 11.75° IE rotation for one cycle of lunging (Figure 4-6). As a result, there was an error of 8.2 % between the range of the IE rotation in the virtual simulation and the experimental testing, with most of the deviation occurring at higher flexion angles. The normalized RMSE of the predicted IE rotation angle by the virtual simulation in comparison with the results of the experiment was 14.5% for one cycle of lunging.

The experimental testing shows that during flexion from 0 to 100 degrees under lunging loads, the tibia rotated internally by about 10.6° around its medial center. Figure 4-9 shows the peak IE rotation angle during the simulated lunging at different recorded cycles of the motion. A normal pattern of axial rotation of the tibia was observed throughout the lunging cycles (internal rotation during flexion of the knee, and external rotation as the femur extends). The maximum amount of IE rotation occurred as the femoral flexion increased and reached a mean peak of 98.4°±0.07 (Figures 4-9 and 4-10). The average and maximum standard deviation over the 6 recorded cycles of lunging from cycle number 30 to 100 were 0.12° and 0.31° for the tibial IE rotation, and 0.07 mm and 0.17 mm for the AP translation of the femoral component. These data show that the simulation of the knee bending activity during cycles of load controlled experimental testing was consistent.

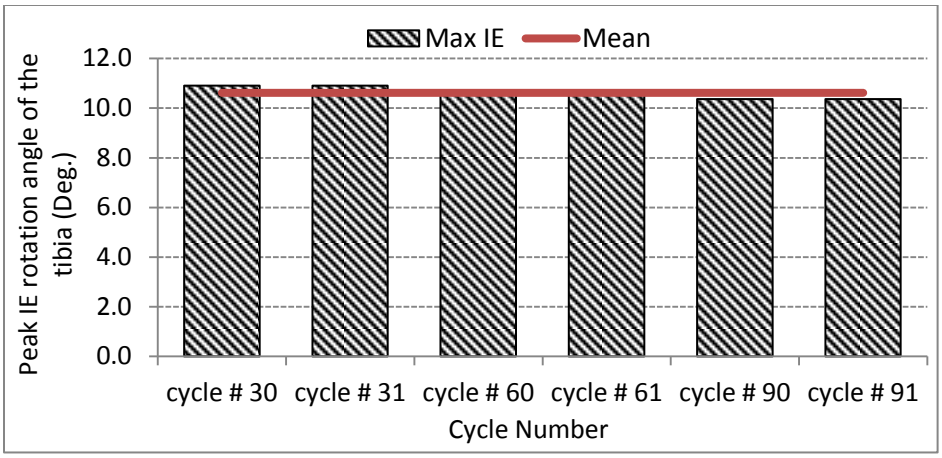

Figure 4-9 Maximum angle of IE rotation at the peak of the flexion angle for recorded cycles of lunging

An average maximum deviation of 2.15±0.01° from the design target was observed for the IE rotation angle, during lunging. This difference was typically encountered when the knee reached around 14 degrees of flexion. There was a mean of 0.78±0.08° difference at peak flexion (average of 98 degrees). (Figure 4-10)

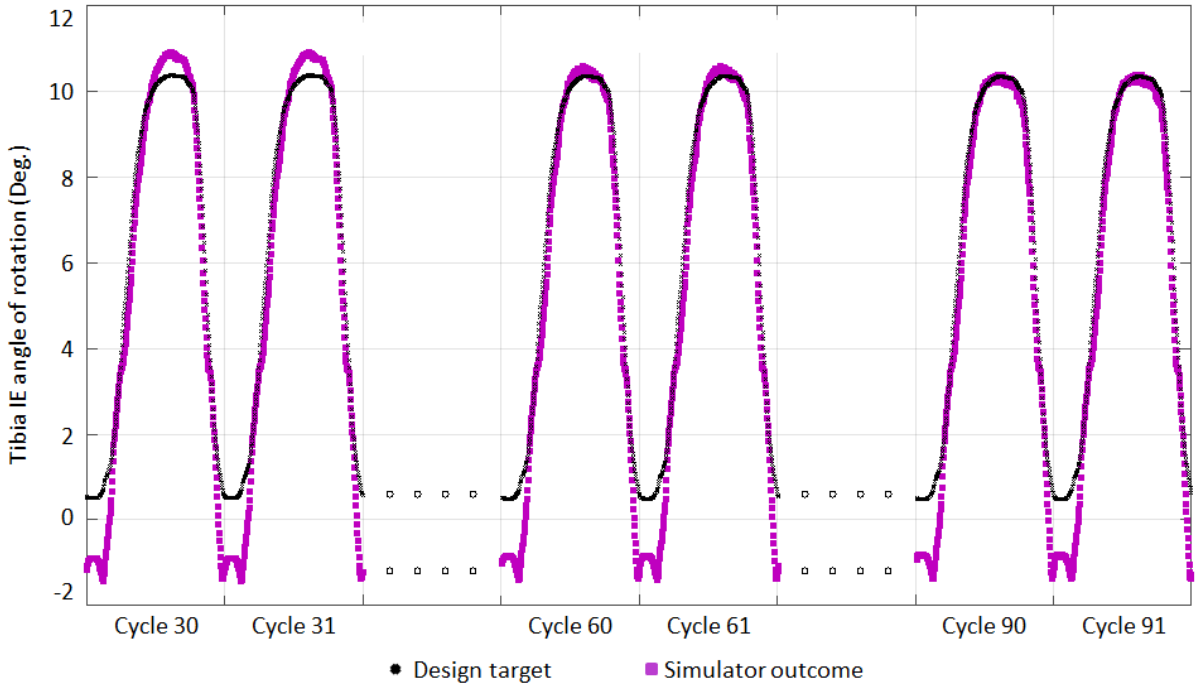

Figure 4-10 IE rotation angle of the tibia during lunging at different cycle numbers

For the first two recorded cycles of lunging, the average difference between the recorded IE rotation and design target was 0.55° at the peak flexion angle. Though, during the last two recorded cycles, this difference was only 0.11 degrees. Based on the last recorded cycle of lunging, the normalized root mean square error was 7.64% from the expected target IE rotation.

Table 4-3 Summary of simulator tibial IE rotation outcomes in comparison to the expected design target

Criteria	Activity	Range of flexion angle (Deg.)	Test outcome	Design target
Peak tibial internal rotation angle (Deg.)[1]	Lunging	0-98	10.6	10.33
	Squatting	0-124	19.94	16.8
Range of IE angle (Deg.)	Lunging	0-98	11.75	9.85
	Squatting	0-124	20.88	16.8
MAE[2]	Lunging	0-98	0.66	N.A
	Squatting	0-124	1.2	
RMSE[3]	Lunging	0-98	0.9	N.A
	Squatting	0-124	1.53	
NRMSE[4]	Lunging	0-98	7.6%	N.A
	Squatting	0-124	7.3%	

1. The average was calculated based on the data of the recorded cycles of simulation.
2. The mean absolute error for the measured data was calculated as $MAE = \frac{\sum_{i=1}^{n} |y_{i\_measured} - y_{i\_target}|}{n}$
3. The RMSE for the measured data was calculated as $RMSE = \sqrt{\frac{\sum_{i=1}^{n} (y_{i\_measured} - y_{i\_target})^2}{n}}$
4. The normalized RMSE for the measured data was calculated as $NRMSE = \frac{RMSE}{y_{max} - y_{min}}$

Results of the experiments under the squatting load condition show, as the knee bent from 0 to 123° of flexion, that the tibial insert rotated 19.9° internally, while the virtual simulation resulted in 16.7° of internal rotation (Figure 4-7). The comparison of the IE rotation angles predicted by virtual simulation for a cycle of squatting and those recorded during experimental testing shows only about one degree of root means square error. It resulted in 5% normalized RMSE, based on the range of the predicted IE rotation angle by the virtual simulation.

The mean absolute error of the IE rotation from the experiment in comparison to the design target was 1.2° for a cycle of squatting. The test outcomes show that there was a 7.3% normalized RMSE between the design target for the IE rotation, and that of the tibial insert in practice. Table 4-3 summarizes the difference between the outcomes of the simulation and the design target.

3. Experiments with the prototypes of the optimized TKR

Results of the measurement of the average roughness (R_a) for the CoCr femoral part and the PE tibial insert before and after simulator testing are summarized in Table 4-4. The roughness of the bearing surface of the femoral component was increased significantly on both medial and lateral condyles after the final test. The lateral tibial plateau roughness showed about 27% of decrease in the average roughness value. The results show that the roughness of the bearing surfaces were less than the limit required for metal and polyethylene surfaces (100 nm and 2000 nm, respectively) according to ASTM F2083-11 [58].

Table 4-4 Summary of simulator tibial IE rotation outcomes in comparison to the expected design target

Component	condition	Medial R_a(nm)	Lateral R_a(nm)
CoCr Femoral part	unworn	7.6	10.5
	worn	26.8	39.7
HDPE tibial insert	unworn	131.6	118.5
	worn	164.9	91.8

Results of the experiments under the deep squatting condition (reaching up to 140° of flexion) showed an average maximum tibial internal rotation of 22.2° (N_{cycle}=10, SD= 0.003). The mean absolute error (MAE) between the result of experimental testing and the design target was calculated based on the difference between the recorded kinematic measure and the design target from 0 to 140° in 0.05° increments (n_{data}=3000) for each recorded cycle. Experimental testing of deep squatting shows an average MAE of 1.6° (N_{cycle}=10, n_{data}=3000, SD= 0.1). During this experiment, the medial femoral condyle translated less than 2 mm in the AP direction (average of 1.6 mm, N_{cycle} =10, SD=0.2), and the lateral femoral condyle translated an average of 20.4 mm (N_{cycle} =10, SD=0.6) posteriorly (Figure 4-11). The analysis of variance showed that there was no significant difference between the cycles of the test, based on the MEA of the tibial IE rotation (P=0.95), and the MEA of the lateral femoral condyle translation (P= 0.82). The MEA of the AP translation of the medial femoral condyle changed significantly with P<0.001; however, the range of AP translation on the medial side was acceptable. The results show that the simulation of the squatting condition was reproducible, with the kinematics outcome of the TKR varying by average standard deviation of 0.12° for the tibial IE rotation and 0.05 mm AP translation of the femoral condyles for the recorded cycles.

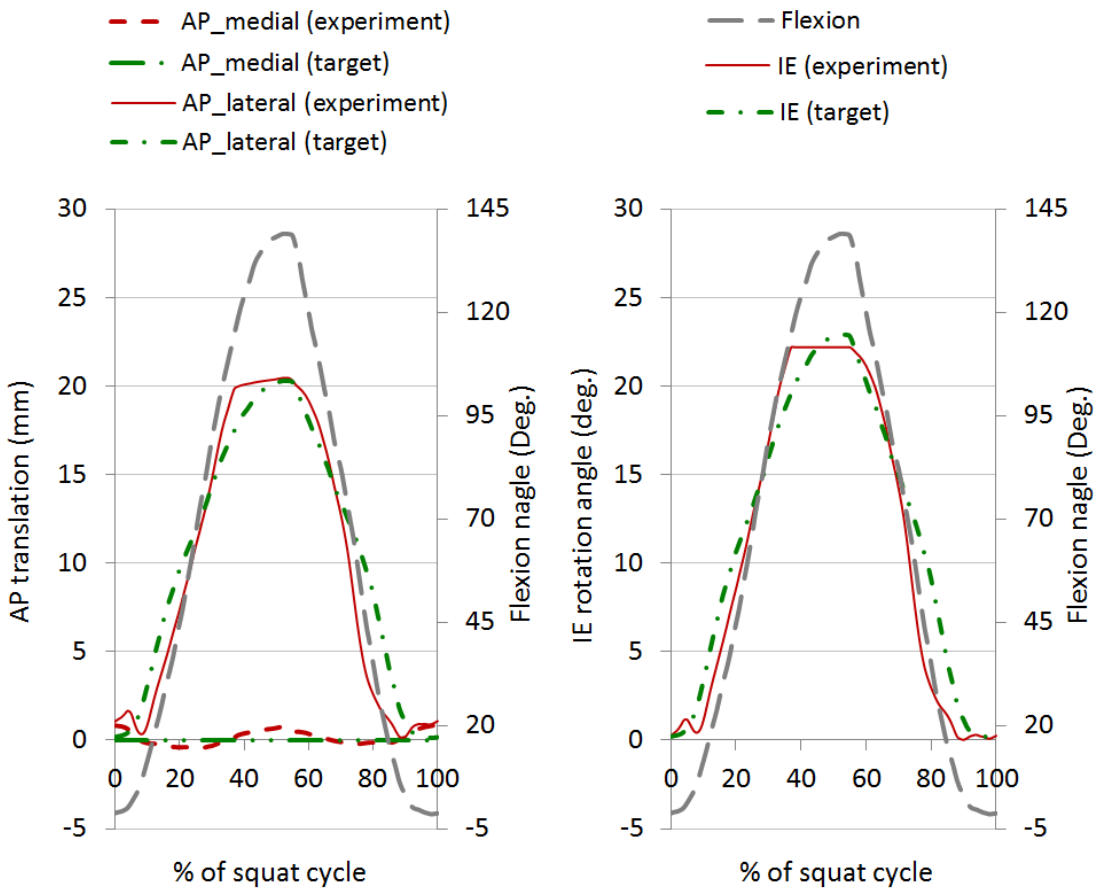

Figure 4-11 Kinematic behavior of the optimized implant as the knee bent up to 139 degrees during deep squatting- Positive IE value means internal rotation of the tibia, and positive AP translation of the femoral condyles means movement in the posterior direction

The results for the cycles of the lunging activity also followed the design target pattern of motion (Figure 4-12) with an average maximum tibial internal rotation of 19.5° (N_{cycle} =10, SD= 0.1). The existence of shear AP force and IE torque did not result into an unexpected translation of the femoral condyle, since the results for the femoral translation show an average of 2.2 mm (N_{cycle} =10, SD= 0.26) and 17.5 mm (N_{cycle} =10, SD=0.78) for the medial and lateral condyles. The analysis of variance for the cycles of the lunging simulation shows that there was no significant difference between the kinematic measures of the recorded cycles of this experiment, P>0.37.

The tibial IE rotation and AP translation of the femoral condyles varied by a standard deviation of 0.39° and 0.19 mm on average between the cycles of lunging.

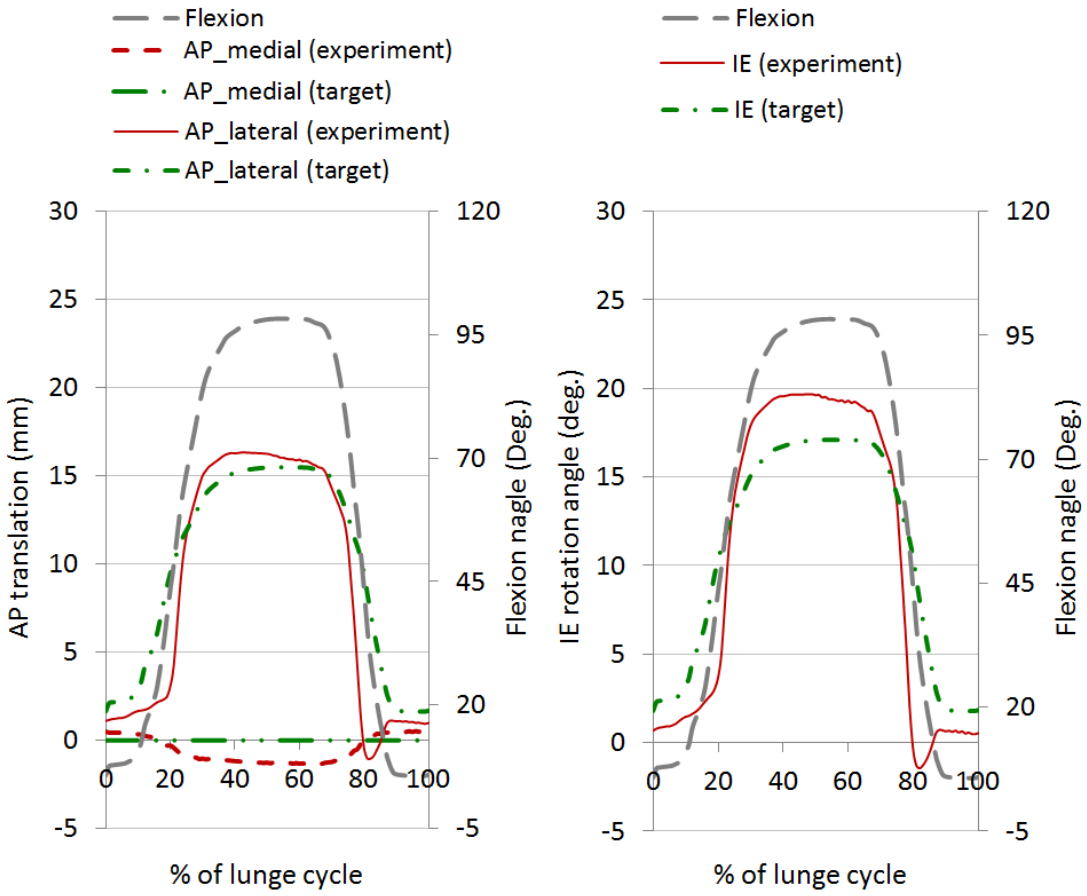

Figure 4-12 Kinematic behavior of the optimized implant as the knee bent up to 98 degrees during lunging- Positive IE value means internal rotation of the tibia, and positive AP translation of the femoral condyles means movement in the posterior direction

Discussion

This study utilized virtual simulation along with experimental testing by a load-controlled knee wear simulator to measure the kinematic behavior of a customized surface-guided TKR during walking and high flexion activities. The new TKR provided a similar pattern of motion as the design target, particularly at high flexion angles. Also, the experimental testing successfully

validated the virtual simulation showing less than 15% error in the average range of the IE rotation of the tibial insert as the knee bent to high flexion angles. The RMSE between the virtual simulation prediction for the IE rotation of the tibial insert during the simulated cycles and those measured by the experimental testing of the metal on PE components was less than two degrees for high flexion activities, such as squatting and lunging.

The results of the study of the femoral metal component and the tibial insert made from HDPE confirm that the customized surface-guided TKR is capable of achieving target keinematics as a result of the tibiofemoral articulation over specially shaped guiding surfaces. During a cycle of lunging with the second revision of the TKR design, at the maximum flexion angle of 98.4±0.07 degrees, the tibia rotated internally 10.6± 0.24 degrees. It is in agreement with the expected target pivot angle (10.3° at 98.4 degrees of flexion). Such rotation of the tibial insert is within the range of IE rotation that has been reported in the literature for similar loading conditions. For a high flexion activity such as squatting, the achieved IE range of motion under the load-controlled test condition was also in agreement with the reported range of rotation of the tibia for the healthy knee joints in the literature (Table 4-5).

Experiments with the plastic prototypes of the proposed design also showed that this TKR can achieve the desired pattern of IE rotation of the tibia as the knee flexes. Such motion was only guided by the geometric shape of the articulating surfaces, while the virtual ligaments were disabled during the experiment. During these experiments, the initial alignment of the plastic components was set manually; therefore, there was a slight deviation (1.39°) in the IE orientation of the tibia at the beginning of each cycle. It led to the inverse rotation during the first 5% of the motion.

Both, the experimental testing and virtual simulation results confirmed a pivot center at the medial condyle, which is a feature of the customized surface-guided TKR design. This is due to almost no posterior translation of the medial center in comparison to the posterior translation laterally. In a normal healthy knee joint, the femoral condyle has a multi-radii circular profile [28,31]; however, a critical assumption of the surface-guided TKR design is achieving minimal medial AP displacement. Therefore, the medial tibiofemoral articulating surface was approximated with a partial ball and socket configuration. Such a pattern of motion is in agreement with reports of the medial pivoting for the tibiofemoral motion in normal knee joints (Table 4-1).

Although there are studies in the literature that contradict the medial pivoting description of the knee during flexion, particularly for deep flexion angles [24,34], the surface-guided TKR design follows the medial pivot concept. The experimental outcomes for squatting show that the current design also provided some laxity on the medial side at high flexion angles (beyond 110 degrees). It is believed that more laxity in the AP direction on the medial side can be provided by using larger radius on the tibia, while the conformity is retained. For the tested cases with metal and PE prototypes, the customized surface-guided TKR has been successful in achieving the objective of the design; that is guided pattern of motion over the predefined lateral trace of contact points along with medial pivoting.

Table 4-5 Comparison of the range of IE angle of rotation in the literature

Study	Activity	Range of flexion angle (Deg.)	Mean range of IE angle (Deg.)	SD	Estimated internal rotation of tibia (Deg.) [1]	
					98° flexion	*124° flexion*
Mu et al. [59]	Squatting	0-120	17.7	±2.3	16	N.A.
Qi et al. [41]	Single-leg lunging	-2.9-145.3	15.2	±9.2	5	7
Moro-oka et al. [54]	Squatting	0-131	30[2]	±2	23	27
Dennis et al. [23]	Deep knee bending	0-120	23.67	±6.09	11	N.A.
Leszko et al. [61]	Deep knee bending	0-150	30.35[3]	±9.2	17	21
Asano et al. [62]	Deep knee bending	0-120	23.8	±4.8	24	N.A.
Johal et al. [37]	Squatting	-5-120	20[4]	N.A.	18.5[4]	N.A.
			14[5]		13[5]	
Current study- Design Target for 2nd version of the implant	-	0-100	10.7[6]	N.A.	10.3[6]	16.8[6]
		0-120	15.7[6]			
		0-150	26.5[6]			
Current study - experimental testing of the 2nd version of the implant	Lunging	0-98	11.75[7]	N.A.	10.6[7]	19.9[7]
	Squatting	0-124	20.88[7]	N.A.		
Optimized TKR					*98° flexion*	*139° flexion*
Current study TKR-Design Target for the optimized implant	-	0-100	17.5[6]	N.A.	17.24[6]	22.72[6]
		0-140	23.1[6]			
Current study TKR-experimental testing of the optimized implant	Lunging	0-98	20.1[7]	N.A.	22.2[7]	19.5[7]
	Deep Squatting	0-139	22.3[7]	N.A.		

1. The estimated amount of internal rotation of the tibia was extracted approximately from the provided data by the studies of this table.
2. The 30° is the outcome based on the "bone-embedded" coordinate systems [54].
3. The pooled mean and standard deviation were calculated based on the results reported for groups of American and Japanese male and female subjects.
4. The results are based on the study under weight-bearing condition [37], and the standard deviation is not reported.
5. The results are based on the study under non-weight bearing condition [37], and the standard deviation is not reported.
6. The design target was defined as described by Amiri et al. [5] for an unloaded knee pattern of motion. For the optimized design a range of 28° of medial rotation was assumed.
7. The average was calculated based on the data of the recorded cycles of simulation.

The virtual simulation predicted the range of IE rotation around the medial center; but the peak rotation of the tibia was overestimated by maximally 3 degrees. It is likely due to the simplifications that were considered for the tibiofemoral contact modeling. For the lunging simulation, the major deviation between the knee wear simulator results and the design target occurred during early flexion angles. This appears to be due to the hysteresis in the knee wear simulator and minimizing the influence of the soft tissues to zero, which are the shortcomings of the current study. The limited control on the friction at the articulating surfaces, and the simplifications considered in the application of the soft tissue forces, affected the results of the experiment on the 2nd verion of the implant, especially at the deep flexion angles. The imperfect control of the friction between the components was also a source of inaccuracies in these experiments, as the friction was expected to be controlled by using petroleum jelly. Chang [57] also reported that use of petroleum-based oils as the lubricant for TKR test would result into high frictional values in comparison to the bovine serum. The results of experiments with the bovine serum and the optimized TKR show that in a more clinically relevant condition, the outcomes of the experiment were less affected.

Several of the activities of daily living result in a similar range of motion as analyzed in this study. Though, there is an increasing need to experience a higher range of flexion of the knee joint to perform activities such as gardening and sitting cross-legged [54,55]. Therefore, investigation of the conditions with deep flexion angles beyond 140 degrees is of great importance. Furthermore, the input load data was limited to the data provided by Bergmann et al.[52] for specific instrumented TKR, and Smith et al.[56] for a group of subjects with normal

knees. The influence of different load conditions either due to the surgical and implantation variables, or the load conditions for other activities, still needs to be investigated.

Moreover, the forces of the collateral ligaments modeled in virtual simulation can be affected by the estimated insertion sites, orientation of the ligament bundles, and the estimated reference length of the bundles for each ligament. Also, the wrapping of the medial collateral ligament was not modeled in this simulation.

Finally, this study did not investigate the influence of the patellofemoral forces and patellar tracking on the kinematics of the joint. It is because the surface-guided TKR design is focused on the guidance of the motion at the tibiofemoral joint. Also, the patellofemoral surface of the femoral component in the current TKR was created by following the geometric shape of the patient's joint, which is assumed to provide close to normal patellofemoral articulation.

This study showed that an implant with a particularly shaped lateral motion guiding surface, a constant tibiofemoral bearing distance, and medial pivot, can provide a close to normal kinematic behavior for high flexion activities such as squatting. The patterns of motion for the simulated walking, lunging and squatting cycles were in agreement with the design target, which in turn is in close agreement with literature data for the normal knee patterns of motions.

References

[1] Bachmeier, Clarissa J. M., L. M. March, M. J. Cross, H. M. Lapsley, K. L. Tribe, B. G. Courtenay, and P. M. Brooks. 2001. "A Comparison of Outcomes in Osteoarthritis Patients Undergoing Total Hip and Knee Replacement Surgery." *Osteoarthritis and Cartilage* 9 (2): 137-146.

[2] Wylde, Vikki, A. W. Blom, S. L. Whitehouse, A. H. Taylor, G. T. Pattison, and G. C. Bannister. 2009. "Patient-Reported Outcomes After Total Hip and Knee Arthroplasty: Comparison of Midterm Results." *The Journal of Arthroplasty* 24 (2): 210-216.

[3] Pejhan, Shabnam, E. Bohm, J. M. Brandt, and U. Wyss. 2016. "Design and Virtual Evaluation of a Customized Surface-Guided Knee Implant." Proc IMechE Part H: J Engineering in Medicine, 230, 10, 949-961.

[4] Wyss, Urs, S. Amiri, and T. D. V. Cooke. 2010. Knee Prosthesis. Patent: US20120179265.

[5] Amiri, Shahram, T. Derek V. Cooke, and Urs P. Wyss. 2011. "Conceptual Design for Condylar Guiding Features of a Total Knee Replacement." *Journal of Medical Devices* 5 (2): 025001-1.

[6] Walker, Peter S. 2014. "Application of a Novel Design Method for Knee Replacements to Achieve Normal Mechanics." *The Knee* 21 (2): 353-358.

[7] Noble, Philip C., M. J. Gordon, J. M. Weiss, R. N. Reddix, M. A. Conditt, and K. B. Mathis. 2005. "Does Total Knee Replacement Restore Normal Knee Function?" *Clinical Orthopaedics and Related Research* 431: 157-165.

[8] *Hip and Knee Replacements in Canada: Canadian Joint Replacement Registry 2016,* Ottawa, ON: Canadian Institute for Health Information (CIHI).

[9] Banks, Scott, J. Bellemans, H. Nozaki, L. A. Whiteside, M. Harman, and W. A. Hodge. 2003. "Knee Motions during Maximum Flexion in Fixed and Mobile-Bearing Arthroplasties." *Clinical Orthopaedics and Related Research* (410): 131-138.

[10] Zavatsky, Amy B. 1997. "A Kinematic-Freedom Analysis of a Flexed-Knee-Stance Testing Rig." *Journal of Biomechanics* 30 (3): 277-280.

[11] Varadarajan, Kartik M., R. E. Harry, T. Johnson, and G. L. 2009. "Can in Vitro Systems Capture the Characteristic Differences between the flexion–extension Kinematics of the Healthy and TKA Knee?" *Medical Engineering & Physics* 31 (8): 899-906.

[12] Arnout, Nele, L. Vanlommel, J. Vanlommel, J. P. Luyckx, L. Labey, B. Innocenti, J. Victor, and J. Bellemans. 2015. "Post-Cam Mechanics and Tibiofemoral Kinematics: A Dynamic in Vitro Analysis of Eight Posterior-Stabilized Total Knee Designs." *Knee Surgery, Sports Traumatology, Arthroscopy* 23 (11): 3343-3353.

[13] D'Lima, Darryl D., M. Trice, A. G. Urquhart, and C. W. Colwell Jr. 2000. "Comparison between the Kinematics of Fixed and Rotating Bearing Knee Prostheses." *Clinical Orthopaedics and Related Research* 380: 151-157.

[14] Guess, Trent M. and L. P. Maletsky. 2005. "Computational Modeling of a Dynamic Knee Simulator for Reproduction of Knee Loading." *Journal of Biomechanical Engineering* 127 (7): 1216-1221.

[15] Patil, Shantanu, C. W. Colwell Jr, K. A. Ezzet, and D. D. D'Lima. 2005. "Can Normal Knee Kinematics be Restored with Unicompartmental Knee Replacement?" *The Journal of Bone and Joint Surgery. American Volume* 87 (2): 332-338.

[16] Halloran, Jason P., C. W. Clary, L. P. Maletsky, M. Taylor, A. J. Petrella, and P. J. Rullkoetter. 2010. "Verification of Predicted Knee Replacement Kinematics during Simulated Gait in the Kansas Knee Simulator." *Journal of Biomechanical Engineering* 132 (8): 081010.

[17] Catani, Fabio, B. Innocenti, C. Belvedere, L. Labey, A. Ensini, and A. Leardini. 2010. "The Mark Coventry Award Articular: Contact Estimation in TKA using in Vivo Kinematics and Finite Element Analysis." *Clinical Orthopaedics and Related Research®* 468 (1): 19-28.

[18] Walker, Peter S. 2015. "The Design and Pre-Clinical Evaluation of Knee Replacements for Osteoarthritis." *Journal of Biomechanics* 48 (5): 742-749.

[19] DesJardins, John D., P. S. Walker, H. Haider, and J. Perry. 2000. "The use of a Force-Controlled Dynamic Knee Simulator to Quantify the Mechanical Performance of Total Knee Replacement Designs during Functional Activity." *Journal of Biomechanics* 33 (10): 1231-1242.

[20] Kurtz, Steven M. 2009. "Ultra High Molecular Weight Polyethylene in Total Joint Replacement and Medical Devices." *UHMWPE Biomaterials Handbook, 2nd Edn.Academic Press, New York*.

[21] Willing, Ryan and I. Y. Kim. 2012. "The Development, Calibration and Validation of a Numerical Total Knee Replacement Kinematics Simulator Considering Laxity and Unconstrained Flexion Motions." *Computer Methods in Biomechanics and Biomedical Engineering* 15 (6): 585-593.

[22] *ADL Knee Simulator Specifications* Advanced Mechanical Technology Inc.

[23] Dennis, Douglas A., M. R. Mahfouz, R. D. Komistek, and W. Hoff. 2005. "In Vivo Determination of Normal and Anterior Cruciate Ligament-Deficient Knee Kinematics." *Journal of Biomechanics* 38 (2): 241-253.

[24] Williams, Andy and M. Logan. 2004. "Understanding Tibio-Femoral Motion." *The Knee* 11 (2): 81-88.

[25] Komistek, Richard D., D. A. Dennis, and M. Mahfouz. 2003. "In Vivo Fluoroscopic Analysis of the Normal Human Knee." *Clinical Orthopaedics and Related Research* (410) (410): 69-81.

[26] Lu, Tung-Wu, T. Tsai, M. Kuo, H. Hsu, and H. Chen. 2008. "In Vivo Three-Dimensional Kinematics of the Normal Knee during Active Extension Under Unloaded and Loaded Conditions using Single-Plane Fluoroscopy." *Medical Engineering & Physics* 30 (8): 1004-1012.

[27] Scarvell, Jennifer M., P. N. Smith, K. M. Refshauge, H. R. Galloway, and K. R. Woods. 2004. "Evaluation of a Method to Map Tibiofemoral Contact Points in the Normal Knee using MRI." *Journal of Orthopaedic Research* 22 (4): 788.

[28] Freeman, Michael A. R. and V. Pinskerova. 2005. "The Movement of the Normal Tibio-Femoral Joint." *Journal of Biomechanics* 38 (2): 197-208.

[29] Pinskerova, Vera, P. Johal, S. Nakagawa, A. Sosna, A. Williams, W. Gedroyc, and M. A. Freeman. 2004. "Does the Femur Roll-Back with Flexion?" *The Journal of Bone and Joint Surgery. British Volume* 86 (6): 925-931.

[30] Frankel, Victor H., A. H. Burstein, and D. B. Brooks. 1971. "Biomechanics of Internal Derangement of the Knee. Pathomechanics as Determined by Analysis of the Instant Centers of Motion." *The Journal of Bone and Joint Surgery. American Volume* 53 (5): 945-962.

[31] Iwaki, H., V. Pinskerova, and MAR Freeman. 2000. "Tibiofemoral Movement 1: The Shapes and Relative Movements of the Femur and Tibia in the Unloaded Cadaver Knee." *Journal of Bone & Joint Surgery, British Volume* 82 (8): 1189-1195.

[32] Martelli, Saulo and V. Pinskerova. 2002. "The Shapes of the Tibial and Femoral Articular Surfaces in Relation to Tibiofemoral Movement." *The Journal of Bone and Joint Surgery. British Volume* 84 (4): 607-613.

[33] Nakagawa, Shinichi, Y. Kadoya, S. Todo, A. Kobayashi, H. Sakamoto, M. A. Freeman, and Y. Yamano. 2000. "Tibiofemoral Movement 3: Full Flexion in the Living Knee Studied by MRI." *The Journal of Bone and Joint Surgery. British Volume* 82 (8): 1199-1200.

[34] Hamai, Satoshi, T. Moro-Oka, N. J. Dunbar, H. Miura, Y. Iwamoto, and S. A. Banks. 2012. "In Vivo Healthy Knee Kinematics during Dynamic Full Flexion." *BioMed Research International* 2013.

[35] DeFrate, Louis E., H. Sun, T. J. Gill, H. E. Rubash, and G. Li. 2004. "In Vivo Tibiofemoral Contact Analysis using 3D MRI-Based Knee Models." *Journal of Biomechanics* 37 (10): 1499-1504.

[36] Hill, Paul F., V. Vedi, A. Williams, H. Iwaki, V. Pinskerova, and M. A. Freeman. 2000. "Tibiofemoral Movement 2: The Loaded and Unloaded Living Knee Studied by MRI." *The Journal of Bone and Joint Surgery. British Volume* 82 (8): 1196-1198.

[37] Johal, Parm, A. Williams, P. Wragg, D. Hunt, and W. Gedroyc. 2005. "Tibio-Femoral Movement in the Living Knee. A Study of Weight Bearing and Non-Weight Bearing Knee Kinematics using 'interventional' MRI." *Journal of Biomechanics* 38 (2): 269-276.

[38] Dennis, Douglas A., R. D. Komistek, M. R. Mahfouz, B. D. Haas, and J. B. Stiehl. 2003. "Multicenter Determination of in Vivo Kinematics after Total Knee Arthroplasty." *Clinical Orthopaedics and Related Research* (416) (416): 37-57.

[39] Dennis, Douglas A., R. D. Komistek, and M. R. Mahfouz. 2003. "In Vivo Fluoroscopic Analysis of Fixed-Bearing Total Knee Replacements." *Clinical Orthopaedics and Related Research* 410 (410): 114-130.

[40] Victor, Jan, S. A. Banks, and J. Bellemans. 2005. "Kinematics of Posterior Cruciate Ligament-Retaining and -Substituting Total Knee Arthroplasty: A Prospective Randomised Outcome Study." *The Journal of Bone and Joint Surgery. British Volume* 87 (5): 646-655.

[41] Horiuchi, Hiroshi, S. Akizuki, T. Tomita, K. Sugamoto, T. Yamazaki, and N. Shimizu. 2012. "In Vivo Kinematic Analysis of Cruciate-Retaining Total Knee Arthroplasty during Weight-Bearing and non–weight-Bearing Deep Knee Bending." *The Journal of Arthroplasty* 27 (6): 1196-1202.

[42] Kuroyanagi, Yuji, S. Mu, S. Hamai, W. J. Robb, and S. A. Banks. 2012. "In Vivo Knee Kinematics during Stair and Deep Flexion Activities in Patients with Bicruciate Substituting Total Knee Arthroplasty." *The Journal of Arthroplasty* 27 (1): 122-128.

[43] Victor, Jan, J. K. P. Mueller, R. D. Komistek, A. Sharma, M. C. Nadaud, and J. Bellemans. 2010. "In Vivo Kinematics after a Cruciate-Substituting TKA." *Clinical Orthopaedics and Related Research®* 468 (3): 807-814.

[44] Johnson, Kenneth Langstreth. 1987. *Contact Mechanics* Cambridge university press.

[45] Guess, Trent M. and L. P. Maletsky. 2005. "Computational Modelling of a Total Knee Prosthetic Loaded in a Dynamic Knee Simulator." *Medical Engineering & Physics* 27 (5): 357-367.

[46] Godest, A. C., M. Beaugonin, E. Haug, M. Taylor, and PJ Gregson. 2002. "Simulation of a Knee Joint Replacement during a Gait Cycle using Explicit Finite Element Analysis." *Journal of Biomechanics* 35 (2): 267-275.

[47] International Standard Organization. 2009. *Implants for Surgery -- Wear of Total Knee-Joint Prostheses -- Part 1: Loading and Displacement Parameters for Wear-Testing Machines with Load Control and Corresponding Environmental Conditions for Test- ISO 14243-1: 2009*. Vol. 1.

[48] Bloemker, Katherine H., T. M. Guess, L. Maletsky, and K. Dodd. 2012. "Computational Knee Ligament Modeling using Experimentally Determined Zero-Load Lengths." *The Open Biomedical Engineering Journal* 6: 33-41.

[49] Guess, Trent M., G. Thiagarajan, M. Kia, and M. Mishra. 2010. "A Subject Specific Multibody Model of the Knee with Menisci." *Medical Engineering & Physics* 32 (5): 505-515.

[50] Guess, Trent M., H. Liu, S. Bhashyam, and G. Thiagarajan. 2013. "A Multibody Knee Model with Discrete Cartilage Prediction of Tibio-Femoral Contact Mechanics." *Computer Methods in Biomechanics and Biomedical Engineering* 16 (3): 256-270.

[51] Blankevoort, Leendert, J. H. Kuiper, R. Huiskes, and H. J. Grootenboer. 1991. "Articular Contact in a Three-Dimensional Model of the Knee." *Journal of Biomechanics* 24 (11): 1019-1031.

[52] Bergmann, Georg, A. Bender, F. Graichen, J. Dymke, A. Rohlmann, A. Trepczynski, M. O. Heller, and I. Kutzner. 2014. "Standardized Loads Acting in Knee Implants." *PloS One* 9 (1): e86035.

[53] D'Lima, Darryl D., S. Patil, N. Steklov, S. Chien, and C. W. Colwell. 2007. "In Vivo Knee Moments and Shear after Total Knee Arthroplasty." *Journal of Biomechanics* 40: S11-S17.

[54] Moro-oka, Taka-aki, S. Hamai, H. Miura, T. Shimoto, H. Higaki, B. J. Fregly, Y. Iwamoto, and S. A. Banks. 2008. "Dynamic Activity Dependence of in Vivo Normal Knee Kinematics." *Journal of Orthopaedic Research* 26 (4): 428-434.

[55] Acker, Stacey M., R. A. Cockburn, J. Krevolin, R. M. Li, S. Tarabichi, and U. P. Wyss. 2011. "Knee Kinematics of High-Flexion Activities of Daily Living Performed by Male Muslims in the Middle East." *The Journal of Arthroplasty* 26 (2): 319-327.

[56] Smith, Stacey M., R. A. Cockburn, A. Hemmerich, R. M. Li, and U. P. Wyss. 2008. "Tibiofemoral Joint Contact Forces and Knee Kinematics during Squatting." *Gait & Posture* 27 (3): 376-386.

[57] Chang, Timothy C. 2005. "Effects of Select Fluid on the Friction of Metal-on-Polyethylene Joint Replacement Surfaces." *MSc dissertation in Mechanical Engineering*, Massachusetts Institute of Technology.

[58] ASTM International. 2011. *ASTM standard: F2083-11: Standard specifications for total knee prosthesis.*

[59] Mu, Shang, T. Moro-Oka, P. Johal, S. Hamai, M. A. R. Freeman, and S. A . Banks. 2011. "Comparison of Static and Dynamic Knee Kinematics during Squatting." *Clinical Biomechanics* 26 (1): 106-108.

[60] Qi, Wei, A. Hosseini, T.Y. Tsai, J.S. Li, H. E. Rubash, and G. Li. 2013. "In vivo Kinematics of the Knee during Weight Bearing High Flexion." *Journal of biomechanics* 46(9): 1576-1582.

[61] Leszko, Filip, K. R. Hovinga, A. L. Lerner, R. D. Komistek, and M. R. Mahfouz. 2011. "In Vivo Normal Knee Kinematics: Is Ethnicity or Gender an Influencing Factor?" *Clinical Orthopaedics and Related Research* 469 (1): 95-106.

[62] Asano, Taiyo, M. Akagi, K. Tanaka, J. Tamura, and T. Nakamura. 2001. "In Vivo Three-Dimensional Knee Kinematics using a Biplanar Image-Matching Technique." *Clinical Orthopaedics and Related Research* 388: 157-166.

Chapter 5

Evaluation of the Tibiofemoral Contact Characteristics of a Customized Surface-Guided Total Knee Replacement

Introduction

A critical factor that influences the performance and longevity of total knee replacements (TKRs) is the wear of the ultra-high molecular weight polyethylene (UHMWPE) bearing due to the tibiofemoral contact interface [1-3]. Research on the wear of the knee implants indicates that the geometric design of the components has a significant influence on the tibiofemoral contact pressure, which in turn contributes to the UHMWPE wear [4-6]. A concern in the design of TKRs is achieving a high range of flexion angle while keeping contact stresses below the material failure limits [5,7]. Different experimental and computational methods have been used to study the tibiofemoral contact characteristics of a TKR, including pressure sensitive films (e.g. Fuji films [8,9], or Tekscan sensors [10,11], and implicit or explicit finite element analysis (FEA) [3,4,9,12-14].

Finite element models have been widely used as an ideal tool to predict the stress and wear in the healthy or injured knees, or in the different implant designs [3,4,9,12-14]. Sathasivam and Walker [12] used static finite element models to evaluate the effect of geometry of the tibiofemoral articulating surfaces on stress distribution and delamination of the tibial insert at various flexion angles. To avoid limitations of statically loading conditions, Halloran et al. [3] and Godest et al. [14] developed explicit finite element models. In their models, the input data for the analysis included the anterior-posterior (AP) load and internal-external (IE) torque applied to the insert, and the flexion–extension (FE) angle with an axial proximal-distal (PD) force applied to the femoral component.

Low cost and simplicity of using the pressure sensitive films have made this approach preferable for testing the TKR designs. Liau et al. [15] reported that the pressure sensitive film is not only efficient and straightforward to use, it also provides satisfactory results. Zdero et al. [8] used pressure sensitive films and ultrasound to measure the contact area of a specific TKR. They reported that these methods determine the lower and upper bounds of the actual region of the tibiofemoral contact. To sum up, the use of pressure sensitive films with low-pressure thresholds is recommended to reduce the risk of the underestimation of the contact area between the components [8,15].

This study investigated the contact at the tibiofemoral interface of a surface-guided total knee replacement [16] by mechanical experiments using pressure sensitive films. The customized surface-guided TKR of this study was designed to achieve a high range of flexion, while following the target pattern of motion. High flexion activities; however, result in greater risk of increased contact loads or decreased contact area, both of which affect the contact

stress distribution on the tibial insert and the longevity of the implant. Therefore, it is necessary to analyze the contact characteristics of the designed TKR for different activities, such as lunging and squatting, to assure the sound performance of the implant at various loading and flexion conditions. The primary purpose of this study was to examine tibiofemoral contact stress of the customized surface-guided TKR using pressure-sensitive film between the prototypes of the TKR components mounted in a knee wear simulator. In this study, different combinations of the load and flexion angle during lunging and squat activities were investigated. The results were compared with the outcomes of computational analysis using a finite element model [17]. Furthermore, a standard test condition, reported by Shiramizu et al. [10], was studied to compare the test results with other common implants.

Methodology

A 3D-printed prototype of the femoral component (Co-Cr alloy) and the corresponding tibial insert (HDPE) were manufactured for the experiment. The components were oriented and positioned at specific flexion angles on an AMTI knee wear simulator (Advanced Mechanical Technology Inc., Watertown, MA) as shown in Figure 5-1. The kinematic input waveforms were applied under displacement-controlled conditions of the knee wear simulator and were defined such that the expected orientation of the TKR components and the load on the tibial insert was achieved. The loading and flexion for three cases were tested; lunging, squatting, and constant load applied at 30, 45, 60, 90, 100, and 120 degrees (Figure 5-1 and Table 5-1).

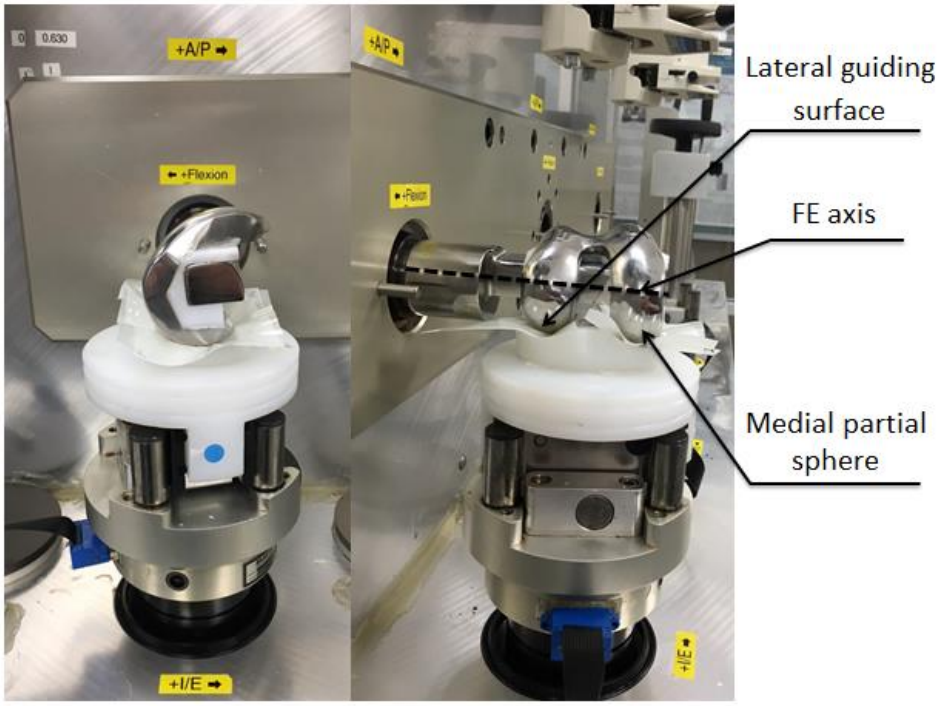

Figure 5-1 Knee wear simulator and prototypes of the TKR test set up, (a) sagittal view, (b) TKR components as the knee bends

The contact area of the tibiofemoral articulating surfaces at different flexion angles was then measured by Fuji pressure sensitive film (Fuji film Holdings, Japan). In this study, the super-low grade film (LLW: 0.5 to 2.5 MPa pressure range) was used at an average room temperature of 20-35°C. For each test, a double-sheet layer of the LLW Fuji film was cut and put between the two articulating components. Axial force was applied and remained for one minute in a steady condition, and each test was repeated three times using a new film each time. Films were scanned at a resolution of 1400 dpi and analyzed using ImageJ software (National Institutes of Health, USA), and the area of the marked patch on the film at the interface of the metal on PE was measured to compute the contact area and the average contact pressure. The maximum detectable pressure by a LLW Fuji pressure sensitive film is 2.5

MPa, which is lower than the contact pressure at most regions of the articulating surfaces. So, an almost evenly dark area marked on the film showed the tibiofemoral contact area.

The contact areas of the medial and lateral sides were measured conservatively by measuring the dark areas of contact region marked on the films. The total weight bearing area was computed as the sum of the medial and lateral contact areas. An average was taken between the three repeats of the test for each flexion angle. The total contact area was then used to compute the corresponding average contact pressure at the tibiofemoral interface. Finally, 60-40% load splitting (i.e. 60% and 40% of the load was transferred through the medial and lateral condyles, respectively) was examined and the corresponding average medial and lateral contact stresses for different flexion angles were calculated.

Table 5-1 Input loads and flexion angle for measuring contact area with pressure sensitive films

Activity	**Flexion Angle (Deg.)**	**Axial Force (N)**	**IE (Deg.)[1]**	**AP (mm)[1]**
Knee bend[2]	30	1497.61	1.79	0.85
	45	1853.92	2.99	1.42
	60	2305.62	4.39	2.09
	90	3038.42	8.68	4.13
	100	2950.29	10.68	5.1
Squat[3]	30	704.76	1.79	1.63
	45	847.59	2.99	2.66
	60	1035.30	4.39	3.98
	90	1488.79	8.68	7.93
	100	1620.89	10.68	9.75
	120	2038.24	15.75	7.45
High constant Load[4]	0	3600	0	0
	30	3600	1.79	1.63
	60	3600	4.39	3.98
	90	3600	8.68	7.93
	110	3600	13.03	6.19
	130	3600	18.88	8.95

1. The amount of IE rotation angle and AP translation was set based on the design target [16].
2. The axial force was based on the study by Bergmann et al. [18]
3. The axial force was based on the study by Smith et al. [19]
4. The axial force was based on the study by Shiramizu et al. [10]

Results

According to results of the experiment, for squatting and the lunging conditions, the area of the contact reached its maximum at 60 and 90 degrees of flexion, respectively. The contact area then decreased with increasing flexion angle (Figure 5-2). High flexion (100 degrees) resulted in an average contact area of 270.5 mm^2 for the lunging; whereas, the squat load condition resulted in an area of 244.9 mm^2 at the tibiofemoral contact. When the load was held constant, the contact area decreased as the knee bent from full extension to the deep flexion, resulting in an increase in contact pressure. Figure 5-2 compares the tibiofemoral contact area and pressure versus the flexion angle for different load scenarios. Also, the experiment results were compared with the contact areas predicted by a previous FEA study [17].

For the lunging load condition, the mean overall contact pressure calculated based on the sum of the mechanically measured medial and lateral contact areas changed from 4.8 MPa at 30° of flexion to 10.9 MPa at 100° of knee flexion (Figure 5-2). The squatting resulted in smaller average contact pressure with a maximum of 8.1 MPa at 120 degrees of flexion. With a constant load applied, the mean contact pressure increased with increasing knee flexion, as was expected due to the decrease in the contact area.

In general, the FEA analysis [17] predicted larger contact areas and a smaller amount of average contact pressure, for the different load conditions. There is a mean error of 19.5 %, 19.7%, and 22.6% between the predicted contact area by the FEA [17] and the experimentally measured areas for the lunging, squatting and constant load condition, respectively.

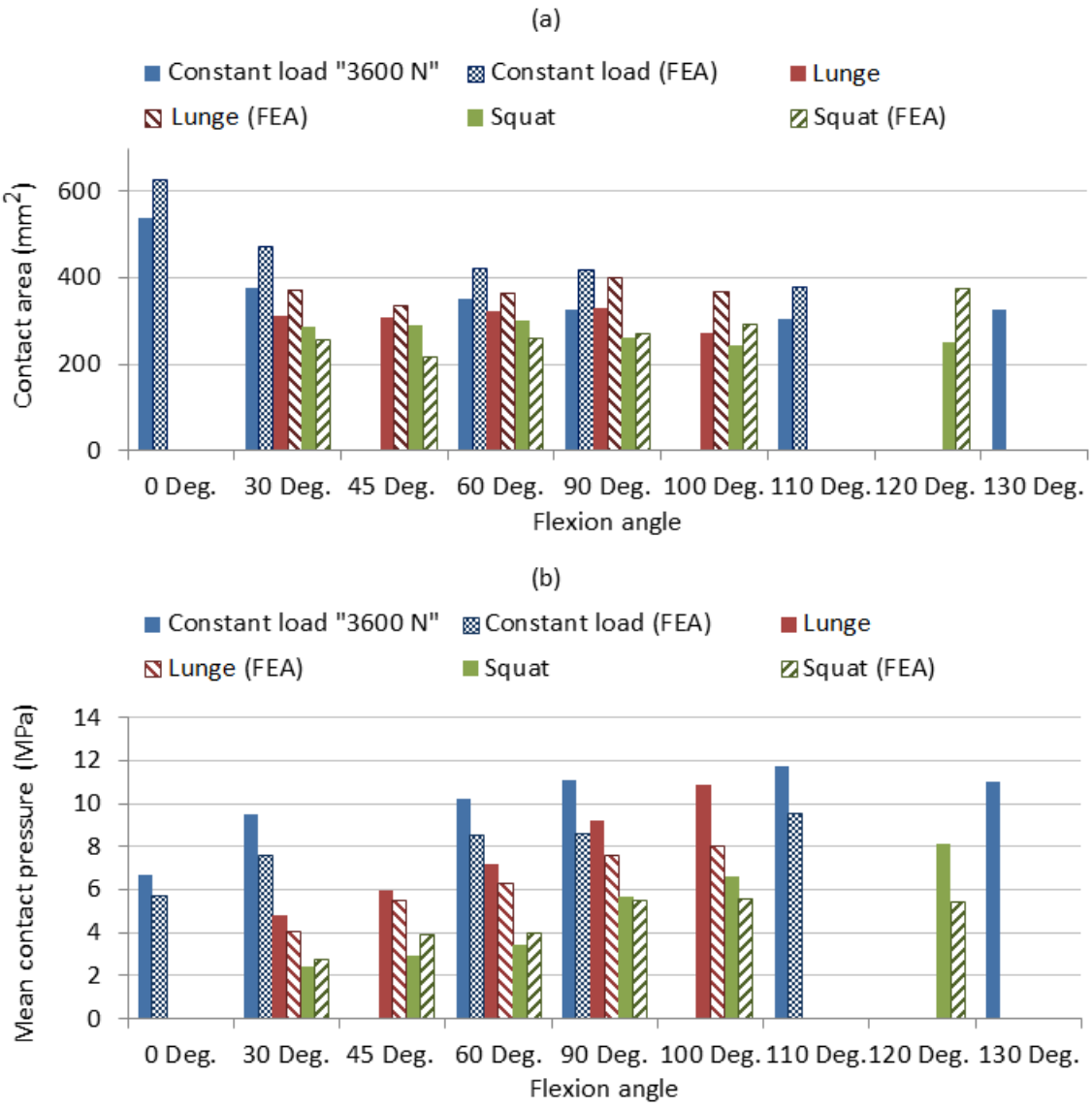

Figure 5-2 Mean overall (a) contact area, (b) contact pressure at specific flexion angles

As Figure 5-3 illustrates, the contact area on both the medial and lateral sides decreased as the knee bends from zero to 100 degrees. When the knee reached higher flexion angles (beyond 110°), the total contact area increased slightly. The contact area rose 6.7% between 110° and 130° flexion angles with a constant load of 3600 N. Though, such an increase was

mostly happening on the medial side, while the contact area detected on the lateral side did not change significantly (Figure 5-3).

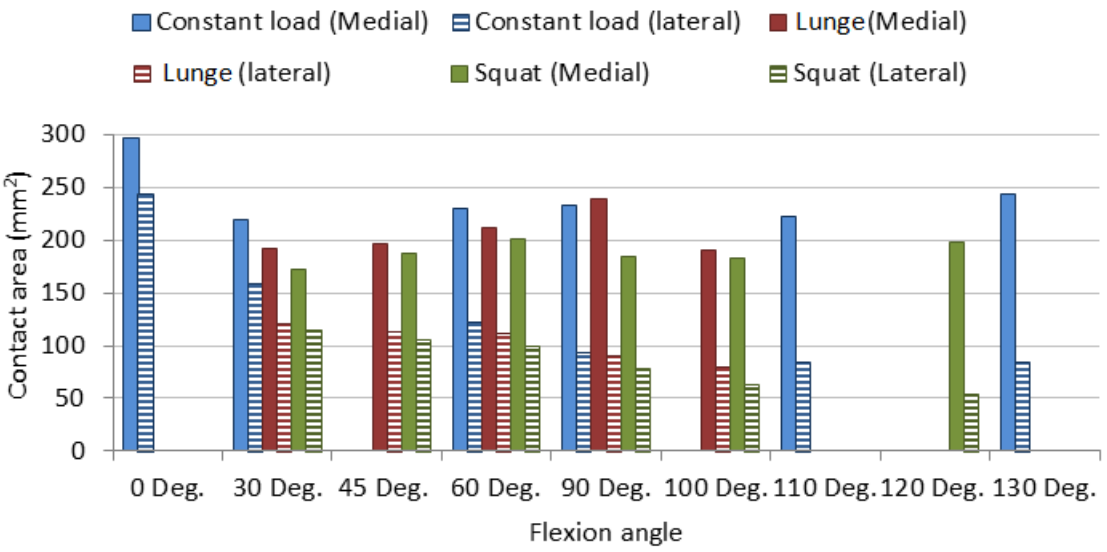

Figure 5-3 Mean contact area on the medial and lateral sides at specific flexion angles

Discussion

The total contact area was found to decrease as the knee reached high flexion angles (100°). However, total average contact pressure on the tibial insert remained below 20 MPa. In addition, the contact area increased slightly at deep flexion of the knee (above 100°). Both the previously performed FEA [17] and the current experimental data show that at each specific flexion angle, the higher load on the insert results in the larger contact area at the tibiofemoral interface. Still, the average contact pressure would be larger due to the greater amount of load on the joint (Figure 5-4).

The tibiofemoral contact surface on the lateral side translated to the posterior section of the tibial insert with increasing flexion angles. The size of the contact area on the lateral plateau

of the tibial insert decreased, as the knee bent to higher flexion angles. However, the reduction in the contact area on the lateral side was not significant. Therefore, even at high flexion angles, the mean contact pressure on the lateral side did not exceed 20 MPa. On the medial side, the lower level of mean contact pressure was due to the increase of the contact area at deep flexion angles.

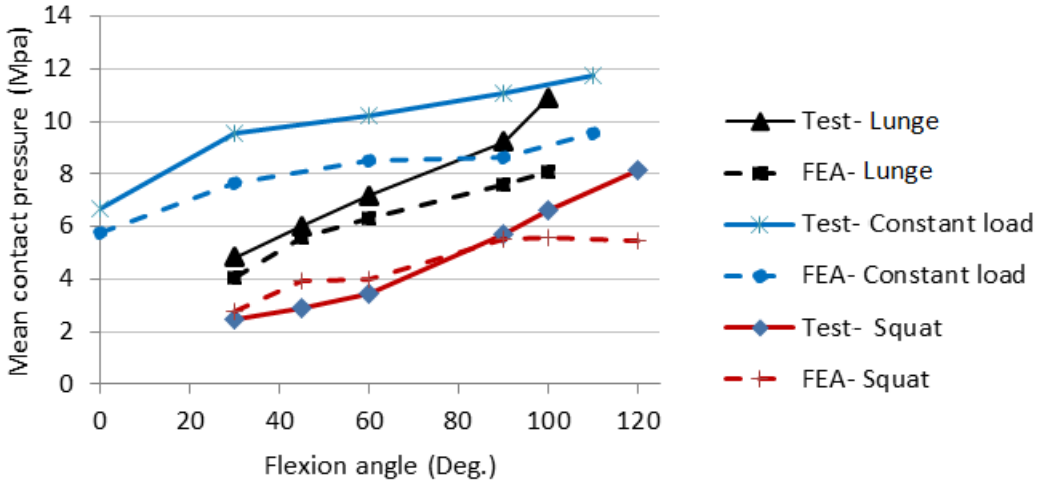

Figure 5-4 Diagram of the trend of the mean contact pressure for different combinations of load and flexion angle

The tibiofemoral contact characteristics of the surface-guided TKR was compared with six different TKR designs studied by Shiramizu et al. [10] under a constant load of 3600 N and at 0, 30, 60, 90, 110, and 130 degrees of flexion. As Figure 5-5 illustrates, the contact area of the surface-guided TKR was higher than all the investigated TKR designs by Shiramizu et al. [10], except the Vanguard RP HI-Flex knee. At the mid flexion angles (30 to 90°), the contact area of the proposed surface guided TKR was even larger than the Vanguard RP HI-Flex knee, which has full tibiofemoral conformity. Shiramizu et al. [10] also reported that such a full compliance between the tibial insert and femoral component resulted in the larger contact areas of the

Vanguard RP HI-Flex knee. At deep flexion angles (beyond 110°), the surface-guided TKR had significantly greater total contact area.

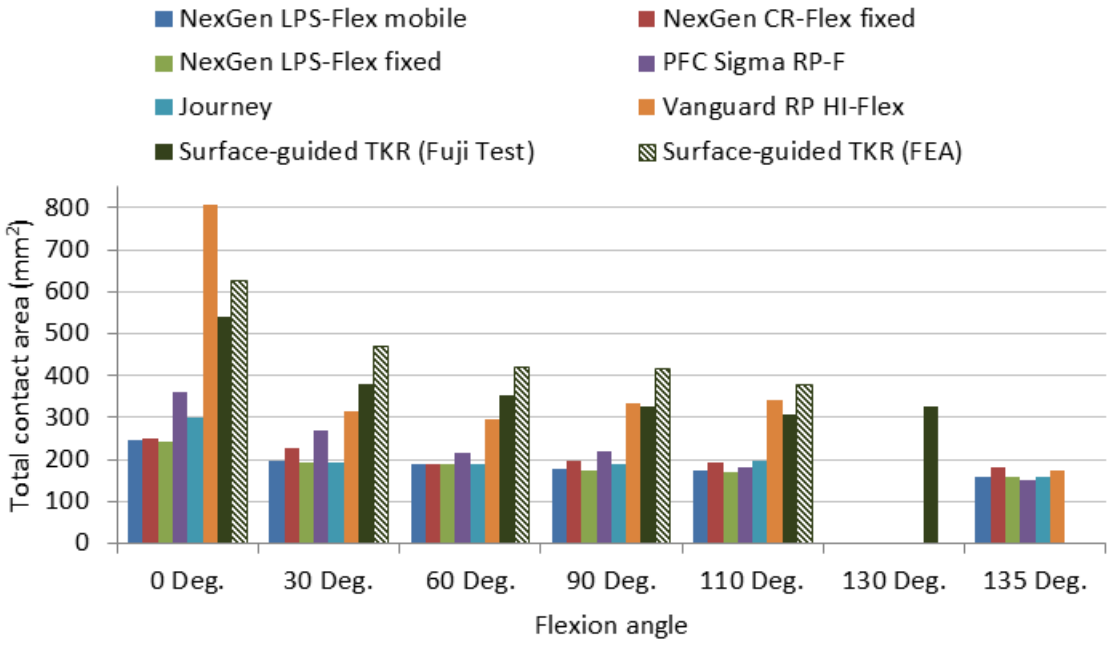

Figure 5-5 Comparison of the measured contact area of the surface-guided TKR and six different TKR from literature- The FEA study included 0, 30, 60, 90 and 110 degrees of flexion, and the test with the pressure sensitive film included 130° of flexion too.

FEA predicted larger contact areas in almost all cases, except for 30, 45, and 60° of squatting [17]. An average difference of 64.5 mm^2 exists between the FEA prediction of the contact area and the experimental data. The range of detectable contact pressure with the LLW grade film is limited. Such limitation of the pressure sensitive films in the detection of the amount of the contact area contributes to the difference between the FEA [17] and the current experimental outcomes.

In addition, the pressure sensitive film measurements define the lower bounds of the contact area. It is, therefore, a potential factor resulting in the difference between the contact

area measured by using the Fuji films on the designed TKR and the outcomes of the study of Shiramizu et al. [10], where the I-scan system was used to measure contact area. Moreover, some modifications had been performed on the TKR designs in the study of Shiramizu et al. [10], to make them capable of going through deep flexion angles. Such modifications could also result in a larger area of contact and consequently lower tibiofemoral contact stresses.

This study showed that the customized surface-guided implant can perform high flexion activities of daily living, while the tibiofemoral contact pressure does not exceed the UHMWPE limits of failure. The contact area decreases at high flexion angles; however, it is such that the average contact pressure did not increase significantly. In addition, the contact area on the lateral side translated posteriorly on the tibial insert similar to a healthy knee joint pattern of motion.

References

[1] Chapman-Sheath, Phillip J. , W. J. M. Bruce, W. K. Chung, P. Morberg, R. M. Gillies, and W. R. Walsh. "In Vitro Assessment of Proximal Polyethylene Contact Surface Areas and Stresses in Mobile Bearing Knees." *Medical Engineering & Physics* 25 (6): 437-443.

[2] Rawlinson, Jeremy J. and D. L. Bartel. 2002. "Flat medial–lateral Conformity in Total Knee Replacements does Not Minimize Contact Stresses." *Journal of Biomechanics* 35 (1): 27-34.

[3] Halloran, Jason P., S. K. Easley, A. J. Petrella, and P. J. Rullkoetter. 2005. "Comparison of Deformable and Elastic Foundation Finite Element Simulations for Predicting Knee Replacement Mechanics." *Journal of Biomechanical Engineering* 127 (5): 813-818.

[4] Bartel, Donald L., J. J. Rawlinson, A. H. Burstein, C. S. Ranawat, and W. F. Flynn Jr. 1995. "Stresses in Polyethylene Components of Contemporary Total Knee Replacements." *Clinical Orthopaedics and Related Research* 317: 76-82.

[5] Barink, Marco, M. De Waal Malefijt, P. Celada, P. Vena, A. Van Kampen, and N. Verdonschot. 2008. "A Mechanical Comparison of High-Flexion and Conventional Total Knee

Arthroplasty." *Proceedings of the Institution of Mechanical Engineers. Part H, Journal of Engineering in Medicine* 222 (3): 297-307.

[6] Simpson, David J, H. Gray, D. D'Lima, D. W Murray, and H. S. Gill. 2008. "The Effect of Bearing Congruency, Thickness and Alignment on the Stresses in Unicompartmental Knee Replacements." *Clinical Biomechanics* 23 (9): 1148-1157.

[7] Willing, Ryan and I. Y. Kim. 2009. "Three Dimensional Shape Optimization of Total Knee Replacements for Reduced Wear." *Structural and Multidisciplinary Optimization* 38 (4): 405-414.

[8] Zdero, Radovan, P. V. Fenton, J. Rudan, and J. T. Bryant. 2001. "Fuji Film and Ultrasound Measurement of Total Knee Arthroplasty Contact Areas." *The Journal of Arthroplasty* 16 (3): 367-375.

[9] D'Lima, Darryl D., P. C. Chen, and C. W. Colwell Jr. 2001. "Polyethylene Contact Stresses, Articular Congruity, and Knee Alignment." *Clinical Orthopaedics and Related Research* 392: 232-238.

[10] Shiramizu, Kei, F. Vizesi, W. Bruce, S. Herrmann, and W. R. Walsh. 2009. "Tibiofemoral Contact Areas and Pressures in Six High Flexion Knees." *International Orthopaedics* 33 (2): 403-406.

[11] Walker, Peter S. 2015. "The Design and Pre-Clinical Evaluation of Knee Replacements for Osteoarthritis." *Journal of Biomechanics* 48 (5): 742-749.

[12] Sathasivam, Shivani and P. S. Walker. 1998. "Computer Model to Predict Subsurface Damage in Tibial Inserts of Total Knees." *Journal of Orthopaedic Research* 16 (5): 564-571.

[13] Fregly, Benjamin J., W. G. Sawyer, M. K. Harman, and S. A. Banks. 2005. "Computational Wear Prediction of a Total Knee Replacement from in Vivo Kinematics." *Journal of Biomechanics* 38 (2): 305-314.

[14] Godest, A. C., M. Beaugonin, E. Haug, M. Taylor, and PJ Gregson. 2002. "Simulation of a Knee Joint Replacement during a Gait Cycle using Explicit Finite Element Analysis." *Journal of Biomechanics* 35 (2): 267-275.

[15] Liau, Jiann-Jong, C. Hu, C. Cheng, C. Huang, and W. Lo. 2001. "The Influence of Inserting a Fuji Pressure Sensitive Film between the Tibiofemoral Joint of Knee Prosthesis on Actual Contact Characteristics." *Clinical Biomechanics* 16 (2): 160-166.

[16] Pejhan, Shabnam, E. Bohm, J. M. Brandt, and U. Wyss. 2016. "Design and Virtual Evaluation of a Customized Surface-Guided Knee Implant." Proc IMechE Part H: J Engineering in Medicine, 230, 10, 949-961.

[17] Khosravipour, Ida, Y. Luo, S. Pejhan, and U. Wyss. 2015. "Contact Stress Analysis of Surface Guided Knee Implant." London, Ontario, Canada, May 31-June 4, 2015.

[18] Bergmann, Georg, A. Bender, F. Graichen, J. Dymke, A. Rohlmann, A. Trepczynski, M. O. Heller, and I. Kutzner. 2014. "Standardized Loads Acting in Knee Implants." *PloS One* 9 (1): e86035.

[19] Smith, Stacey M., R. A. Cockburn, A. Hemmerich, R. M. Li, and U. P. Wyss. 2008. "Tibiofemoral Joint Contact Forces and Knee Kinematics during Squatting." *Gait & Posture* 27 (3): 376-386.

Chapter 6

Discussion

General overview

Meeting patients' expectations, including relief of pain and restoring normal function, is reported as a critical contributing factor in the satisfaction after knee arthroplasty [1]. Research on the performance of the TKRs shows that although knee arthroplasty is a successful surgery for pain reduction, it has limited functionality for the activities of daily living with a high range of flexion [2,3]. Different factors affect the range of flexion and pattern of motion after TKR, some of which are the design of the implant, alignment and sizing of the components, and the ligament balance [4-7]. As a result, a great variety of high flexion knee implants have been developed, including cruciate-retaining designs, one or both cruciate stabilized TKRs, motion guiding designs, and patient-specific implants [8-12]. However, it has remained controversial whether the high-flexion knee designs can improve the range of flexion as well as the pattern of motion of the joint [4,13-18].

In this study, the design requirements of a customized surface-guided knee implant were investigated. This design was based on the assumption that closer to normal physiological

kinematics results in the enhancement of the functionally of the TKR, which is in agreement with previous studies on the design of motion guiding TKRs [8,12,19]. The lateral tibiofemoral articulating surfaces were designed, such that the femoral AP translation and tibial Internal-External (IE) rotation is achieved through the contact between the novel geometries of the tibiofemoral compartments. Also, a partial ball and socket joint was considered on the medial side, which means there is a restriction for the Anterior-Posterior (AP) translation of the medial femoral condyle. The medial pivot knee types are reported to be successful in relieving pain and improving functionality after TKR [20-22].

Furthermore, this study evaluated the effectiveness of such specially shaped tibiofemoral articulating surfaces in replicating close to normal kinematics as defined by the target pattern of motion. Therefore, the kinematic performance of the new customized surface-guided TKR was evaluated through virtual simulations, and experimental testing under different load conditions. The load-controlled experimental testing by utilizing a knee wear simulator evaluates the customized surface-guided TKR ability to achieve the design target pattern of motion. Such a method is assumed to be capable of isolating the influence of the TKR design on the kinematic behavior. In addition, such experiments validate the virtual simulation models used for the prediction of the kinematic behavior of the implant.

This study utilized pressure sensitive films to measure the contact characteristics of the tibiofemoral joint of the surface-guided TKR design. The outcomes revealed that at different flexion angle and load conditions of squatting and lunging, the mean contact pressure remained below the material limits of the tibial polyethylene insert.

Surface-guided TKR design

The initial geometric design parameters and required axes of motion were determined from the extracted models of the patient's knee joint by using MRI. The design algorithm aimed to implement the surface-guided design concept based on the customized geometric parameters and a predefined target pattern of motion (pivoting around the medial center). The estimated trace of contact points based on such a target pattern of motion was in agreement with the movement pattern reported in the literature for normal healthy knee joints (Figure 2-9). In this design, the flexion-extension (FE) axis was defined as the line connecting the centers of the best-fitted spheres on the posterior femoral condyles. A region between the posterior ends of the medial and lateral condyles and the intercondylar notch was used to fit the spheres. Studies on the location and orientation of the knee rotation axes reported that the FE axis passes through the posterior part of the femoral condyles, whereas the condyles have a circular shape in the sagittal plane [23-26].

The asymmetric configuration of the tibiofemoral articulation surface of this TKR included a fully congruent partial ball and socket joint on the medial posterior segment and a lateral multi-radii guiding surface with two tangent articulating arcs at each increment of motion. The concept of the medial pivot has been used for over 20 years in the design of the TKRs. The "Medial Rotation Knee (MRK)" by Finsbury Orthopaedics (Surrey, UK) and the "Medial Pivot" by Wright Medical Company (Memphis, TN) are the early medial pivoting designs with asymmetric tibiofemoral articulating surfaces. These TKRs have a congruent medial condyle with identical frontal and sagittal curvature, while the lateral condyle is formed as a cylindrical or conical

configuration [27-29]. Previous research on kinematics also indicated that in a normal knee, a medial centered pivoting occurs due to slight posterior translation of the medial femoral condyle and larger movement of the lateral condyle during flexion [30-32]. It has been reported that the medial pivot knee designs are successful in providing stability throughout the range of motion [27,33-35]. Similar to the normal knee, a pivot pattern motion is reported for such knee designs during both small ranges of motion and deep flexion activities. However, the extent of IE rotation after TKR with medial pivot knees is reported to be smaller, than had been observed in normal healthy knee joints [21,27,30,34,35].

In the surface-guided TKR of this study, the medial pivot concept is combined with particularly shaped articulating surfaces on the lateral side to guide the motion with no need for an extra intercondylar feature to provide sufficient lateral rollback of the femur. The bicruciate stabilized TKRs such as the Journey® knee (Smith & Nephew, Memphis, TN, USA) replace both ACL and PCL with intercondylar features to provide closer to normal rollback and guidance of motion during flexion [12,36]. Durren et al. [37] studied the performance of 10 patients with bicruciate stabilized (BCS) implants during the lunge and step-up activities, and they reported that the anterior cam engaged during extension at early flexion angles (13°) and the posterior cam got engaged during mid-flexion at 45°. Although BCS knees are almost unconstrained between these two angles, the cam-post mechanism provides closer to normal condylar contact movement than conventional TKRs [37,38]. However, a large variation is reported in the rotational behavior with abnormal rotation pattern at extension [37]. One of the limitations of the BCS design is that the femoral component is positioned far posterior relative to the tibia [37]. Also, the study by Ruiz et al. [36] about the clinical outcome of the

bicruciate TKR shows low pain scores, and no difference in the level of satisfaction of the patients.

Another design approach is the bicruciate retaining (BCR) TKR, that preserves both ACL and PCL. However, the guidance of the motion depends on the functionality of the remaining ligaments after TKR. Zumbrunn and colleagues [11] introduced a novel TKR design with both cruciate retained (BCR), while the articular surfaces were generated by the average anatomy of knee joint. The tibial insert was machined by mounting the femoral part over the tibia and moving it through average in vivo kinematics collected from 40 healthy subjects [11]. The results of virtual simulations in their study showed that the implant is capable of providing more normal kinematics than conventional ACL retaining implants, or those with a post-cam mechanism [11]. However, this study only investigated the average knee model with inactive ACL; therefore, patient specific variations in ligament properties and balancing of the ligaments were not considered. Moreover, Zumbrunn et al. [11] also indicated that validation of the virtual analysis under force-controlled conditions was a critical limitation of their study.

Therefore, in this study, the guiding features considered for the medial and lateral articulating surfaces of the surface-guided TKR aimed to reach high flexion angles, while following a close to normal pattern of motion. In this design, the distance between the medial and the lateral contact points remains constant throughout flexion or extension of the joint. So, the incremental changes of the radii on the lateral guiding arcs provide the required guidance of the movement. The anterior segments of the medial and lateral condyles were generated matching the anatomic shape of the patient's joint to maximize the stability of the joint and provide close to normal patellofemoral articulation. In the initial versions of this TKR, no

clearance was implemented between the femoral and tibial components. However, creating the tibial articulating surface with larger radii than the corresponding femoral part can provide some laxity. The parametric study of the influence of the geometric design variables on the kinematic performance of this surface-guided TKR resulted in little clearance between the tibiofemoral guiding arcs to achieve the kinematic behavior with the minimum overall error (Table 3-1).

Moreover, since there is no intercondylar feature in this design, the cruciate ligaments could be preserved in this TKR, and their function can improve the performance of the joint. Keeping the cruciate ligaments would develop stability at hyper-extension or deep flexion angels of the joint. Also, the accurately balanced cruciate ligaments provide the chance of decreasing the constraint on the tibial insert, which will, in turn, reduce the stress at the implant and enhance the longevity of the TKR components [39]. There have been numerous studies on the influence of balancing the ligament tensions and their impact on the functionality of the joint [39-41]. An unbalanced knee is reported as a cause of the ACL rupture, or the tibial eminence fracture (fracture of the bony attachment of the ACL on the tibia) during the operation [40]. Jacofsky [39] pointed out that restoring the anatomic joint line is a crucial issue during TKR surgeries with both cruciate remaining to avoid any extra tension or abnormal restraining behavior.

The principal component analysis (PCA) was used to study the influence of different input variables on kinematic performance. As a result, the AP location of the lateral femoral center was determined as the most influential parameter. Variations of this variable could lead to a limited range of the tibial IE rotation, due to the significant correlation between the posterior translation of the medial side during early flexion and the initial location of the lateral femoral

condyle. Also, a combination of the sagittal slope of the medial tibial plateau, the radius of the partial medial sphere, and AP location of the lateral femoral center, contribute to the anterior translation of the femoral condyles during deep flexion angles. Several studies investigated the influence of different design variables on the kinematic or the wear performance of conventional total knee replacements [5,42-46]. Similar to the outcomes of the PCA on the customized surface-guided TKR, Fitzpatrick et al. [43] reported a strong correlation between the radius of the posterior section of the femoral condyle, and the slope of the tibial insert with the tibiofemoral IE rotation and AP displacement during high flexion activities. The sensitivity analysis by Ardestani et al. [46] showed that the range of IE rotation of the tibial insert, correlated first to the femoral posterior radius and second to the tibial posterior and anterior radii.

Evaluation of kinematic performance

The pattern of motion of the knee joint alters after TKR, which is due to changes in the particular asymmetric shape of the tibiofemoral articulating surfaces, and resection or malfunction of the cruciate ligaments [47-49]. Weiss et al. [50] reported that more than 75% of patients with TKRs experienced difficulties and limitations in performing high flexion activities including squatting, kneeling, and gardening, which were in fact amongst the activities that they called as essential activities of daily living (ADL). According to Mulholland and Wyss [51], 111° to 165° of knee flexion would be required for activities such as deep squatting and kneeling. Therefore, one of the goals of the advancements in artificial knee designs is to restore close to normal kinematics, and to achieve a higher range of flexion. The results of the virtual and

mechanical simulation of the surface-guided TKR of this study confirm that a combination of the constraint on a medial partial ball and socket configuration, and guiding features on the lateral articulation surface is successful in restoring normal kinematics. Such close to the normal pattern of motion is achieved not only during walking, but also for high flexion activities with different load conditions including squatting and lunging.

The anatomic geometric design variables created an asymmetric tibiofemoral articulation surface with a multi-radii lateral bearing surface, and a pivot center at the medial condyle, which is approximated with a constant radius on the posterior facet. Kinematic analysis of the surface-guided TKR design, as described in Chapter 4, demonstrated that there is a pivot center at the medial condyle around which the internal rotation of the tibial insert occurs. This was due to the larger posterior translation of the lateral condyle in comparison to the medial throughout the flexion of the knee. In the conventional TKRs, the resection of ACL results in abnormal posterior translation of the femoral component during extension. Furthermore, paradoxical motion (anterior femoral movement) during flexion is reported due to lack of PCL, insufficient control of stability by the remaining soft tissues, and the simplified shapes of the articulating surfaces [47-49,52]. Although the TKRs with both cruciate retained are capable of avoiding the paradoxical motion, they are still limited in restoring the medial pivot motion and normal IE rotation [53,54]. The surface-guided TKR showed a small amount of AP movement on the medial side, while the lateral femoral condyle rolled backward through joint flexion. It resulted in a close to the normal pattern of IE pivot around a medial center for the simulated cases of walking, squatting with heels up or down, and lunging.

Both virtual simulations and experimental testing with the load-controlled knee wear simulator confirm that the customized surface-guided TKR achieved close to the target pattern and range of motion. For a high flexion activity such as squatting, the achieved IE range of rotation (22°) under the load-controlled test condition was within the reported range of rotation in the literature for similar amount of flexion of the joint. For a normal healthy knee joint, an average IE rotation from 15 to 30 degrees has been reported for comparable weight-bearing activities [24,30,53,55,56]. It is believed that such development in the design of knee implants with the aim of achieving a higher range of flexion angles improves the quality of life of the patients with TKR, particularly for those who have an active lifestyle.

Limitations

The current study has certain limitations. First, the design input variables of the surface-guided TKR were extracted from 3D models of the knee joint reconstructed from MRI of the patient. Improvement in the quality and specifications of the MRI or CT data enhance the accuracy of the geometric model of the joint, and helps to be more accurate in determining input parameters.

In addition, the design target pattern of pivoting versus the flexion angle was set based on the passive characteristics of a normal knee. Amiri et al. [57,58] described the passive or neutral motion as the articulation of the knee compartments in virtually unloaded condition. The passive motion is regarded as external rotation of the tibia during extension and posterior translation of the femur during flexion of the joint [57,59,60]. Wilson et al. [60] specified a path of passive motion, in which the internal rotation of the tibia is coupled to the flexion of the

joint; however, external loads affect the exact pattern of motion within an envelope of laxity. Johal et al. [30] reported that the internal tibial rotation occurs with or without weight-bearing knee flexion, but they found a greater amount of rotation under the loaded condition. In this design, the passive motion was considered as the design criteria for the target pattern of motion. The findings from experimental testing with the knee wear simulator confirm that in the case of weight-bearing conditions such as lunging and squatting, the joint would function similarly.

In the principal component analysis and the parametric study aiming to determine the optimized design variable combinations, the number of design candidates was limited. Due to the cost of the design process and computation, the confidence coefficient for the sampling method was set to 0.9 to determine 30 randomized combinations of design variables. Furthermore, Fitzpatrick et al. [43] described the Latin Hypercube sampling method as a successful method for generating a uniform arrangement of variables using a small sample size. Finally, a globally optimized design could be achieved by combining this sampling method, current kinematic virtual simulation, and an optimization algorithm with more iteration.

In the virtual and experimental simulations, it was assumed that the TKR components were ideally oriented, while the variations in alignment and placement of the components could change the kinematic performance. Another limitation of the kinematic simulations is that only three weight-bearing conditions (walking, lunging, and squatting) were tested and analyzed. However, the chosen cases are among the crucial weight-bearing activities [50]. Also, the input load data was limited to the data provided for a specific instrumented TKR [61], as well as those reported for a group of normal subjects [62]. The influence of different load conditions due to

the surgical and implantation variables were not investigated. In addition, the simplifications considered in modeling the contact between the components, the approximated stiffness at the articulation surfaces affect the outcome of the virtual simulations. There were also limitations in modeling the force-displacement of the ligaments, including the estimation of the insertion sites and the alignment and reference length of the ligament bundles, as well as the assumption of no wrapping of the bundles.

Although further in vitro and in vivo studies are required to investigate the functionality of the new surface-guided TKR, the experimental testing by the load-controlled knee wear simulator validated the virtual simulations and provided valuable information about the kinematic behavior of this TKR. The hysteresis from the knee wear simulator, and the simplifications in the virtual ligament and soft tissue settings are the major shortcomings in the test methodology. Furthermore, during experimental testing of the initial revisions of the TKR, the friction was not controlled and applying a layer of petroleum jelly possibly oversimplified the tribology situation between the prototype components. However, this method provided the opportunity to visually check the pattern of motion, as it was not necessary to put the implant components in not-translucent synovial-like fluid filled bags.

References

[1] Dunbar, Michael J., G. Richardson, and O. Robertsson. 2013. "I can't Get no Satisfaction after My Total Knee Replacement: Rhymes and Reasons." *The Bone & Joint Journal* 95-B (11 Suppl A): 148-152.

[2] Noble, Philip C., M. J. Gordon, J. M. Weiss, R. N. Reddix, M. A. Conditt, and K. B. Mathis. 2005. "Does Total Knee Replacement Restore Normal Knee Function?" *Clinical Orthopaedics and Related Research* 431: 157-165.

[3] Wylde, Vikki, P. Dieppe, S. Hewlett, and I. D. Learmonth. 2007. "Total Knee Replacement: Is it really an Effective Procedure for all?" *The Knee* 14 (6): 417-423.

[4] Goldstein, Wayne M., D. J. Raab, T. F. Gleason, J. J. Branson, and K. Berland. 2006. "Why Posterior Cruciate-Retaining and Substituting Total Knee Replacements have Similar Ranges of Motion. the Importance of Posterior Condylar Offset and Cleanout of Posterior Condylar Space." *The Journal of Bone and Joint Surgery. American Volume* 88 Suppl 4: 182-188.

[5] Fitzpatrick, Clare K., C. W. Clary, and P. J. Rullkoetter. 2012. "The Role of Patient, Surgical, and Implant Design Variation in Total Knee Replacement Performance." *Journal of Biomechanics* 45 (12): 2092-2102.

[6] Lozano-Calderón, Santiago A., J. Shen, D. F. Doumato, D. A. Greene, and S. B. Zelicof. 2013. "Cruciate-Retaining Vs Posterior-Substituting Inserts in Total Knee Arthroplasty: Functional Outcome Comparison." *The Journal of Arthroplasty* 28 (2): 234-242. e1.

[7] Tanzer, Michael, K. Smith, and S. Burnett. 2002. "Posterior-Stabilized Versus Cruciate-Retaining Total Knee Arthroplasty: Balancing the Gap." *The Journal of Arthroplasty* 17 (7): 813-819.

[8] Walker, Peter S. 2015. "The Design and Pre-Clinical Evaluation of Knee Replacements for Osteoarthritis." *Journal of Biomechanics* 48 (5): 742-749.

[9] Steklov, Nick, J. Slamin, S. Srivastav, and D. D'Lima. 2010. "Unicompartmental Knee Resurfacing: Enlarged Tibio-Femoral Contact Area and Reduced Contact Stress using Novel Patient-Derived Geometries." *The Open Biomedical Engineering Journal* 4: 85-92.

[10] McCalden, Richard W., S. J. MacDonald, K. D. J. Charron, R. B. Bourne, and D. D. Naudie. 2010. "The Role of Polyethylene Design on Postoperative TKA Flexion: An Analysis of 1534 Cases." *Clinical Orthopaedics and Related Research®* 468 (1): 108-114.

[11] Zumbrunn, Thomas, K. Mangudi Varadarajan, H. E. Rubash, H. Malchau, G. Li, and O. K. Muratoglu. 2015. "Regaining Native Knee Kinematics Following Joint Arthroplasty: A Novel Biomimetic Design with ACL and PCL Preservation." *The Journal of Arthroplasty* 30 (12): 2143-2148.

[12] Victor, Jan and J. Bellemans. 2006. "Physiologic Kinematics as a Concept for Better Flexion in TKA." *Clinical Orthopaedics and Related Research* 452: 53-58.

[13] Nutton, Richard W., M. L. van der Linden, P. J. Rowe, P. Gaston, and F. A. Wade. 2008. "A Prospective Randomised Double-Blind Study of Functional Outcome and Range of Flexion Following Total Knee Replacement with the NexGen Standard and High Flexion Components." *The Journal of Bone and Joint Surgery. British Volume* 90 (1): 37-42.

[14] Endres, Stefan. and A. Wilke. 2011. "High Flexion Total Knee Arthroplasty - Mid-Term Follow Up of 5 Years." *The Open Orthopaedics Journal* 5: 138-142.

[15] Yoshiya, Shinichi, N. Matsui, R. D. Komistek, D. A. Dennis, M. Mahfouz, and M. Kurosaka. 2005. "In Vivo Kinematic Comparison of Posterior Cruciate-Retaining and Posterior Stabilized Total Knee Arthroplasties under Passive and Weight-Bearing Conditions." *The Journal of Arthroplasty* 20 (6): 777-783.

[16] Kim, Young-Hoo, Y. Choi, and J. S. Kim. 2009. "Range of Motion of Standard and High-Flexion Posterior Cruciate-Retaining Total Knee Prostheses a Prospective Randomized Study." *The Journal of Bone and Joint Surgery. American Volume* 91 (8): 1874-1881.

[17] Yagishita, Kazuyoshi, T. Muneta, Y. Ju, T. Morito, J. Yamazaki, and I. Sekiya. 2012. "High-Flex Posterior Cruciate-Retaining Vs Posterior Cruciate-Substituting Designs in Simultaneous Bilateral Total Knee Arthroplasty: A Prospective, Randomized Study." *The Journal of Arthroplasty* 27 (3): 368-374.

[18] Cho, Sung-Do, Y. Youm, and K. Park. 2011. "Three-to Six-Year Follow-Up Results After High-Flexion Total Knee Arthroplasty: Can we Allow Passive Deep Knee Bending?" *Knee Surgery, Sports Traumatology, Arthroscopy* 19 (6): 899-903.

[19] Amiri, Shahram, T. Derek V. Cooke, and Urs P. Wyss. 2011. "Conceptual Design for Condylar Guiding Features of a Total Knee Replacement." *Journal of Medical Devices* 5 (2): 025001-1.

[20] Bae, Dae Kyung, S. J. Song, and S. D. Cho. 2011. "Clinical Outcome of Total Knee Arthroplasty with Medial Pivot Prosthesis: A Comparative Study between the Cruciate Retaining and Sacrificing." *The Journal of Arthroplasty* 26 (5): 693-698.

[21] Omori, Go, N. Onda, M. Shimura, T. Hayashi, T. Sato, and Y. Koga. 2009. "The Effect of Geometry of the Tibial Polyethylene Insert on the Tibiofemoral Contact Kinematics in Advance Medial Pivot Total Knee Arthroplasty." *Journal of Orthopaedic Science* 14 (6): 754-760.

[22] Brinkman, Justus-Martijn, P. Singh Bubra, P. Walker, W. R. Walsh, and W. J. M. Bruce. 2014. "Midterm Results using a Medial Pivot Total Knee Replacement Compared with the Australian National Joint Replacement Registry Data." *ANZ Journal of Surgery* 84 (3): 172-176.

[23] Victor, Jan, D. Van Doninck, L. Labey, F. Van Glabbeek, P. Parizel, and J. Bellemans. 2009. "A Common Reference Frame for Describing Rotation of the Distal Femur: A Ct-Based Kinematic Study using Cadavers." *The Journal of Bone and Joint Surgery. British Volume* 91 (5): 683-690.

[24] Iwaki, H., V. Pinskerova, and MAR Freeman. 2000. "Tibiofemoral Movement 1: The Shapes and Relative Movements of the Femur and Tibia in the Unloaded Cadaver Knee." *Journal of Bone & Joint Surgery, British Volume* 82 (8): 1189-1195.

[25] Kozanek, Michal, A. Hosseini, F. Liu, S. K. Van de Velde, T. J. Gill, H. E. Rubash, and G. Li. 2009. "Tibiofemoral Kinematics and Condylar Motion during the Stance Phase of Gait." *Journal of Biomechanics* 42 (12): 1877-1884.

[26] Eckhoff, Donald G., J. M. Bach, V. M. Spitzer, K. D. Reinig, M. M. Bagur, T. H. Baldini, and N. M. Flannery. 2005. "Three-Dimensional Mechanics, Kinematics, and Morphology of the Knee Viewed in Virtual Reality." *The Journal of Bone and Joint Surgery. American Volume* 87 Suppl 2: 71-80.

[27] Moonot, Pradeep, M. Shang, G. T. Railton, R. E. Field, and S. A. Banks. 2010. "In Vivo Weight-Bearing Kinematics with Medial Rotation Knee Arthroplasty." *The Knee* 17 (1): 33-37.

[28] Causero, Araldo, P. Di Benedetto, A. Beltrame, R. Gisonni, V. Cainero, and M. Pagano. 2014. "Design Evolution in Total Knee Replacement: Which is the Future?" *Acta Bio Medica Atenei Parmensis* 85 (2): 5-19.

[29] Walker, Peter S. 2001. "A New Concept in Guided Motion Total Knee Arthroplasty." *The Journal of Arthroplasty* 16 (8): 157-163.

[30] Johal, Parm, A. Williams, P. Wragg, D. Hunt, and W. Gedroyc. 2005. "Tibio-Femoral Movement in the Living Knee. A Study of Weight Bearing and Non-Weight Bearing Knee Kinematics using 'interventional'MRI." *Journal of Biomechanics* 38 (2): 269-276.

[31] Asano, Taiyo, M. Akagi, K. Tanaka, J. Tamura, and T. Nakamura. 2001. "In Vivo Three-Dimensional Knee Kinematics using a Biplanar Image-Matching Technique." *Clinical Orthopaedics and Related Research* 388: 157-166.

[32] Dennis, Douglas A., M. R. Mahfouz, R. D. Komistek, and W. Hoff. 2005. "In Vivo Determination of Normal and Anterior Cruciate Ligament-Deficient Knee Kinematics." *Journal of Biomechanics* 38 (2): 241-253.

[33] Saari, Tuuli, J. Uvehammer, L. V. Carlsson, P. Herberts, L. Regner, and J. Karrholm. 2003. "Kinematics of Three Variations of the Freeman-Samuelson Total Knee Prosthesis." *Clinical Orthopaedics and Related Research* 410: 235-247.

[34] Schmidt, Robert, R. D. Komistek, J. D. Blaha, B. L. Penenberg, and W. J. Maloney. 2003. "Fluoroscopic Analyses of Cruciate-Retaining and Medial Pivot Knee Implants." *Clinical Orthopaedics and Related Research* (410) (410): 139-147.

[35] Moonot, Pradeep, S. Mu, G. T. Railton, R. E. Field, and S. A. Banks. 2009. "Tibiofemoral Kinematic Analysis of Knee Flexion for a Medial Pivot Knee." *Knee Surgery, Sports Traumatology, Arthroscopy* 17 (8): 927-934.

[36] Sanz-Ruiz, Pablo, E. Carbo-Laso, B. Alonso-Polo, J. Antonio Matas-Diez, and J. Vaquero-Martín. 2016. "Does a New Implant Design with More Physiological Kinematics Provide Better Results After Knee Arthroplasty?" *The Knee* 23(3): 399-405.

[37] Van Duren, Bernard H., H. Pandit, M. Price, S. Tilley, H. S. Gill, D. W. Murray, and N. P. Thomas. 2012. "Bicruciate Substituting Total Knee Replacement: How Effective are the Added Kinematic Constraints in Vivo?" *Knee Surgery, Sports Traumatology, Arthroscopy* 20 (10): 2002-2010.

[38] Catani, Fabio, A. Ensini, C. Belvedere, A. Feliciangeli, M. Grazia Benedetti, A. Leardini, and S. Giannini. 2009. "In Vivo Kinematics and Kinetics of a bi-cruciate Substituting Total Knee Arthroplasty: A Combined Fluoroscopic and Gait Analysis Study." *Journal of Orthopaedic Research* 27 (12): 1569-1575.

[39] Jacofsky, David. 2005. "Bicruciate-Retaining Total Knee Arthroplasty." In *Total Knee Arthroplasty*, 291-294: Springer.

[40] Pritchett, James W. 2015. "Bicruciate-Retaining Total Knee Replacement Provides Satisfactory Function and Implant Survivorship at 23 Years." *Clinical Orthopaedics and Related Research®* 473 (7): 2327-2333.

[41] Amiri, Shahram and D. R. Wilson. 2012. "A Computational Modeling Approach for Investigating Soft Tissue Balancing in Bicruciate Retaining Knee Arthroplasty." *Computational and Mathematical Methods in Medicine* 2012.

[42] Willing, Ryan and I. Y. Kim. 2011. "Design Optimization of a Total Knee Replacement for Improved Constraint and Flexion Kinematics." *Journal of Biomechanics* 44 (6): 1014-1020.

[43] Fitzpatrick, Clare K., C. W. Clary, P. J. Laz, and P. J. Rullkoetter. 2012. "Relative Contributions of Design, Alignment, and Loading Variability in Knee Replacement Mechanics." *Journal of Orthopaedic Research* 30 (12): 2015-2024.

[44] Sathasivam, Shivani and P. S. Walker. 1999. "The Conflicting Requirements of Laxity and Conformity in Total Knee Replacement." *Journal of Biomechanics* 32 (3): 239-247.

[45] Willing, Ryan and I. Y. Kim. 2009. "Three Dimensional Shape Optimization of Total Knee Replacements for Reduced Wear." *Structural and Multidisciplinary Optimization* 38 (4): 405-414.

[46] Ardestani, Marzieh M., M. Moazen, and Z. Jin. 2015. "Contribution of Geometric Design Parameters to Knee Implant Performance: Conflicting Impact of Conformity on Kinematics and Contact Mechanics." *The Knee* 22 (3): 217-224.

[47] Dennis, Douglas A., R. D. Komistek, M. R. Mahfouz, B. D. Haas, and J. B. Stiehl. 2003. "Multicenter Determination of in Vivo Kinematics after Total Knee Arthroplasty." *Clinical Orthopaedics and Related Research* (416) (416): 37-57.

[48] Dennis, Douglas A., R. D. Komistek, and M. R. Mahfouz. 2003. "In Vivo Fluoroscopic Analysis of Fixed-Bearing Total Knee Replacements." *Clinical Orthopaedics and Related Research* 410 (410): 114-130.

[49] Victor, Jan, J. K. P. Mueller, R. D. Komistek, A. Sharma, M. C. Nadaud, and J. Bellemans. 2010. "In Vivo Kinematics after a Cruciate-Substituting TKA." *Clinical Orthopaedics and Related Research®* 468 (3): 807-814.

[50] Weiss, Jennifer M., P. C. Noble, M. A. Conditt, H. W. Kohl, S. Roberts, K. F. Cook, M. J. Gordon, and K. B. Mathis. 2002. "What Functional Activities are Important to Patients with Knee Replacements?" *Clinical Orthopaedics and Related Research* 404: 172-188.

[51] Mulholland, Susan J. and U. P. Wyss. 2001. "Activities of Daily Living in Non-Western Cultures: Range of Motion Requirements for Hip and Knee Joint Implants." *International Journal of Rehabilitation Research* 24 (3): 191-198.

[52] Siston, Robert A., N. J. Giori, S. B. Goodman, and S. L. Delp. 2006. "Intraoperative Passive Kinematics of Osteoarthritic Knees before and After Total Knee Arthroplasty." *Journal of Orthopaedic Research* 24 (8): 1607-1614.

[53] Moro-oka, Taka-aki, M. Muenchinger, J. Canciani, and S. A. Banks. 2007. "Comparing in Vivo Kinematics of Anterior Cruciate-Retaining and Posterior Cruciate-Retaining Total Knee Arthroplasty." *Knee Surgery, Sports Traumatology, Arthroscopy* 15 (1): 93-99.

[54] Stiehl, James B., R. D. Komistek, J. Cloutier, and D. A. Dennis. 2000. "The Cruciate Ligaments in Total Knee Arthroplasty: A Kinematic Analysis of 2 Total Knee Arthroplasties." *The Journal of Arthroplasty* 15 (5): 545-550.

[55] Hamai, Satoshi, T. Moro-Oka, N. J. Dunbar, H. Miura, Y. Iwamoto, and S. A. Banks. 2012. "In Vivo Healthy Knee Kinematics during Dynamic Full Flexion." *BioMed Research International* 2013.

[56] Leszko, Filip, K. R. Hovinga, A. L. Lerner, R. D. Komistek, and M. R. Mahfouz. 2011. "In Vivo Normal Knee Kinematics: Is Ethnicity or Gender an Influencing Factor?" *Clinical Orthopaedics and Related Research®* 469 (1): 95-106.

[57] Amiri, Shahram, D. Cooke, I. Y. Kim, and U. Wyss. 2006. "Mechanics of the Passive Knee Joint. Part 1: The Role of the Tibial Articular Surfaces in Guiding the Passive Motion." *Proceedings of the Institution of Mechanical Engineers. Part H, Journal of Engineering in Medicine* 220 (8): 813-822.

[58] Amiri, Shahram, D. Cooke, I. Y. Kim, and U. Wyss. 2007. "Mechanics of the Passive Knee Joint. Part 2: Interaction between the Ligaments and the Articular Surfaces in Guiding the Joint Motion." *Proceedings of the Institution of Mechanical Engineers. Part H, Journal of Engineering in Medicine* 221 (8): 821-832.

[59] Hill, Paul F., V. Vedi, A. Williams, H. Iwaki, V. Pinskerova, and M. A. Freeman. 2000. "Tibiofemoral Movement 2: The Loaded and Unloaded Living Knee Studied by MRI." *The Journal of Bone and Joint Surgery. British Volume* 82 (8): 1196-1198.

[60] Wilson, Davis R, J. D. Feikes, A. B. Zavatsky, and J. J. O'connor. 2000. "The Components of Passive Knee Movement are Coupled to Flexion Angle." *Journal of Biomechanics* 33 (4): 465-473.

[61] Bergmann, Georg, A. Bender, F. Graichen, J. Dymke, A. Rohlmann, A. Trepczynski, M. O. Heller, and I. Kutzner. 2014. "Standardized Loads Acting in Knee Implants." *PloS One* 9 (1): e86035.

[62] Smith, Stacey M., R. A. Cockburn, A. Hemmerich, R. M. Li, and U. P. Wyss. 2008. "Tibiofemoral Joint Contact Forces and Knee Kinematics during Squatting." *Gait & Posture* 27 (3): 376-386.

Chapter 7

Conclusions and Recommendations for Future Work

Summary

The goal of this study was to introduce and improve the design features of a customized surface-guided total knee replacement (TKR) aiming to fulfill a normal pattern of motion. Deviation from normal kinematics is usually reported after knee replacements with conventional TKRs. The proposed design promises the development of an artificial knee joint, which enables the patients to reach high flexion angles, and perform activities of daily living such as kneeling, squatting, and cross-legged sitting. The study on the design of a novel surface-guided TKR reconstructed the asymmetric shapes of the articular surfaces with guiding bearing arcs on the lateral compartment, and a medial partial ball and socket configuration. This design does not require any intercondylar space feature like cam and post. In the proposed design, particular geometric design features guide the motion of the joint to produce close to normal patterns of motion, with little dependence on the function of the cruciate ligaments. These features include the incremental variation of the radii of the lateral guiding arcs, a constant distance between the medial and the lateral tibiofemoral contact points, and the location and

orientation of the flexion-extension (FE) and internal-external (IE) axes. Also, the design process of this study creates a platform for generating customized tibiofemoral articulating surfaces based on essential geometric parameters, which are extracted from the 3D model of the patient's knee joint MRI. The parametric analysis describes an approach to determine the combination of geometric design variables with the best kinematic performance. This analysis is based on an objective function of the overall error between the measured kinematic results and the design target kinematics.

In the design concept of the new surface-guided TKR, a predefined desired passive pattern of motion and contact points was assumed. Also, it was hypothesized that specially shaped asymmetric tibiofemoral bearing surfaces would result in a TKR with normal kinematics during weight-bearing activities of daily living. The virtual simulation of the kinematic behavior of the new surface-guided knee implant provides a tool to evaluate and measure the kinematic performance of the proposed design of the TKR, as the knee bends and extends during different activities. Furthermore, such simulations can investigate the influence of various combinations of joint forces exerted from remaining soft tissue such as the cruciate and collateral ligaments. A load-controlled knee wear simulator was used for the experimental testing of the customized surface-guided TKR. This test set-up can evaluate the effectiveness of the particular design of the implant in providing close to normal kinematics. It is because the surgery-related variables such as the placement and alignment of the implanted components or the balance of the ligament forces after implantation do not impact the results of the test. Furthermore, the forces that can be expected in vivo were applied. The load-controlled tests for the squatting and lunging activities validated the models of the virtual simulation. Therefore, the simulation

can be used to study the kinematic performance of the TKR under other load and motion conditions. The final experiments on the optimized TKR were performed by bovine serum in order to provide boundary lubrication and recreate frictional situation closer to the body joint fluid situation.

The evaluation of the contact characteristics of the implant was critical, as the tibiofemoral contact stress influences the short-term and long-term performance of the implants. The tests with the pressure sensitive films examined the tibiofemoral contact area and mean contact pressure at various flexion angles under squat and lunge loads. Findings of these experiments show that the contact area on the lateral side translated posteriorly on the tibial insert as the knee bent, which was similar to design target and a healthy knee joint pattern of motion. The contact area decreased at high flexion angles; however, it was such that the average contact pressure did not increase significantly.

Contributions

The primary goal of this research was to develop design features of a customized surface-guided TKR that can provide a target normal pattern of motion even at high flexion angles. Therefore, a combination of the anatomic geometry of the tibiofemoral articulating surfaces of the knee joint, and design features of the surface-guided TKR was utilized to guide the motion and provide stability. The major contributions of this study are:

- Determining the patient-specific geometric features of the tibiofemoral articulating surfaces based on the surface-guided design concept.

- Investigating and quantifying the influence of the design variables on the kinematic performance of the surface-guided TKR through parametric analysis.
- Modification of the design features with the goal of achieving high range of flexion and close to target normal pattern of motion.
- Evaluation of the proposed design of the implant by conducting load-controlled tests on the knee wear simulator under weight-bearing conditions of the activities of daily living including lunging and squatting.

Conclusions

The number of younger and more active patients who need total knee replacements is increasing. Therefore, there is a rise in demand for improving the design of the artificial knee joints to not only relieve pain, but also to restore function and close to normal patterns of motion. The work in this dissertation resulted in the development of a customized surface-guided TKR with a combination of geometric design variables that provide the least deviation from the desired target kinematics, during various activities from walking to squatting. The major findings of this dissertation are:

- The asymmetric tibiofemoral articulating surfaces of the surface-guided TKR with multi-radii guiding arcs on the lateral compartment, and a pivot axis passing the center of the congruent medial were developed from patient-specific models of the joint.
- The experimental testing with a load-controlled knee wear simulator successfully evaluated the behavior of the new customized surface-guided TKR, with loads from in vivo measurements of high flexion activities, including squatting and lunging.

- The patterns of motion, as well as the range of tibial internal-external rotation, for the simulated walking, lunging and squatting cycles were in close agreement with the design target, which in turn is consistent with the findings of previous studies for the normal knee kinematic behavior.
- The location and orientation of the flexion-extension axis, the sagittal slope of the tibial insert and the radius of the partial medial sphere are the first three main geometric parameters affecting the kinematic performance.
- The AP location of the lateral center of the femoral condyle is correlated with the posterior translation of the medial condyle during early flexion of the knee. This could limit the range of the IE rotation of the tibial insert as the knee bends.
- A combination of the sagittal slope of the tibial insert, the radius of the partial medial sphere, and the AP location of the center of the lateral femoral condyle has an influence on the anterior translation of the femoral condyles during high flexion angles.
- The surface-guided knee replacement with the optimum kinematic performance allows deep knee bending activities requiring around 140 degrees of flexion. The simulations and experimental testing of flexion of the TKR to 140° showed less than 2 mm AP translation of the medial femoral condyle on the tibial component and around 21 mm posterior translation of the lateral condyle. These translations resulted in about 23° of internal rotation of the tibial insert.
- There was less than 15% error in the average range of the virtually predicted and experimentally measured IE rotation of the tibial insert during squatting. Thus, the

experimental testing successfully validated the virtual simulations prediction for the kinematic performance of the surface-guided implant.

Recommendations for future work

The findings of this study show that the primary objective of improving the design features of a customized surface-guided total knee replacement, with the goal of closer to normal kinematics has been achieved. Considering certain limitations in this research (Chapter 5) and the potential for further development of the new surface-guided TKR, the following future work is recommended:

1. Include the contribution of the variables other than the tibiofemoral geometric design parameters in the principal component analysis of the kinematic performance. Such variables include the alignment of the components on the bone, balancing of the remaining ligaments, or the patellofemoral articulation kinematics.
2. Perform a multi-objective optimization process to include other functional criteria such as the patellofemoral kinematics, or the tibiofemoral contact pressure analysis.
3. Conduct cadaveric experiments to investigate the influence of the post-implant parameters impacting the motion of the TKR, such as placement and orientation of the implant components, as well as the surgery techniques for the ligament balancing.
4. Compare the kinematic outputs and wear of the new surface-guided TKR against experimental testing results of different conventional implants.

5. Investigate and implement the methods to estimate the deformations from the healthy tibiofemoral cartilage geometry based on the measurements performed on patient's MRI.

All advancements in the total knee replacement are ultimately aimed to enhance the functional performance of the artificial joints and improve the quality of life the patients. This study has taken major steps toward a novel design of a surface-guided knee implant, which guides the motion of the compartments through specially shaped tibiofemoral bearing surfaces. The findings of this study and the recommended future work can lead to a more normal feeling knee that will reach the crucial goal of increasing the level of satisfaction of the patients after total knee arthroplasty.

Bibliography

This is the list of all references used for this dissertation:

"American Academy of Orthopaedic Surgeons.", http://orthoinfo.aaos.org/topic.cfm?topic=A00591

"American Academy of Orthopaedic Surgeons." http://orthoinfo.aaos.org/icm/PrintModule.cfm?screen=icm005_s08_p1&module=icm005

Abdi, Hervé and L. J. Williams. 2010. "Principal Component Analysis." Wiley Interdisciplinary Reviews: Computational Statistics 2 (4): 433-459.

Acker, Stacey M., R. A. Cockburn, J. Krevolin, R. M. Li, S. Tarabichi, and U. P. Wyss. 2011. "Knee Kinematics of High-Flexion Activities of Daily Living Performed by Male Muslims in the Middle East." The Journal of Arthroplasty 26 (2): 319-327.

ADL Knee Simulator Specifications Advanced Mechanical Technology Inc.

Amiri, Shahram, D. Cooke, I. Y. Kim, and U. Wyss. 2006. "Mechanics of the Passive Knee Joint. Part 1: The Role of the Tibial Articular Surfaces in Guiding the Passive Motion." Proceedings of the Institution of Mechanical Engineers. Part H, Journal of Engineering in Medicine 220 (8): 813-822.

Amiri, Shahram, D. Cooke, I. Y. Kim, and U. Wyss. 2007. "Mechanics of the Passive Knee Joint. Part 2: Interaction between the Ligaments and the Articular Surfaces in Guiding the Joint Motion." Proceedings of the Institution of Mechanical Engineers. Part H, Journal of Engineering in Medicine 221 (8): 821-832.

Amiri, Shahram and D. R. Wilson. 2012. "A Computational Modeling Approach for Investigating Soft Tissue Balancing in Bicruciate Retaining Knee Arthroplasty." Computational and Mathematical Methods in Medicine 2012.

Amiri, Shahram, T. D. V. Cooke, and U. P. Wyss. 2011. "Conceptual Design for Condylar Guiding Features of a Total Knee Replacement." Journal of Medical Devices 5 (2): 025001.

Ardestani, Marzieh M., M. Moazen, and Z. Jin. 2015. "Contribution of Geometric Design Parameters to Knee Implant Performance: Conflicting Impact of Conformity on Kinematics and Contact Mechanics." The Knee 22 (3): 217-224.

Arnout, Nele, L. Vanlommel, J. Vanlommel, J. P. Luyckx, L. Labey, B. Innocenti, J. Victor, and J. Bellemans. 2015. "Post-Cam Mechanics and Tibiofemoral Kinematics: A Dynamic in Vitro Analysis of Eight Posterior-Stabilized Total Knee Designs." Knee Surgery, Sports Traumatology, Arthroscopy 23 (11): 3343-3353.

Asano, Taiyo, M. Akagi, K. Tanaka, J. Tamura, and T. Nakamura. 2001. "In Vivo Three-Dimensional Knee Kinematics using a Biplanar Image-Matching Technique." Clinical Orthopaedics and Related Research 388: 157-166.

ASTM International. 2011. ASTM standard: F2083-11: Standard specifications for total knee prosthesis.

Bachmeier, Clarissa J. M., L. M. March, M. J. Cross, H. M. Lapsley, K. L. Tribe, B. G. Courtenay, and P. M. Brooks. 2001. "A Comparison of Outcomes in Osteoarthritis Patients Undergoing Total Hip and Knee Replacement Surgery." Osteoarthritis and Cartilage 9 (2): 137-146.

Bae, Dae Kyung, S. J. Song, and S. D. Cho. 2011. "Clinical Outcome of Total Knee Arthroplasty with Medial Pivot Prosthesis: A Comparative Study between the Cruciate Retaining and Sacrificing." The Journal of Arthroplasty 26 (5): 693-698.

Baker, Paul N., J. H. van der Meulen, J. Lewsey, P. J. Gregg, and National Joint Registry for England and Wales. 2007. "The Role of Pain and Function in Determining Patient Satisfaction after Total Knee Replacement. Data from the National Joint Registry for England and Wales." The Journal of Bone and Joint Surgery. British Volume 89 (7): 893-900.

Banks, Scott, J. Bellemans, H. Nozaki, L. A. Whiteside, M. Harman, and W. A. Hodge. 2003. "Knee Motions during Maximum Flexion in Fixed and Mobile-Bearing Arthroplasties." Clinical Orthopaedics and Related Research (410): 131-138.

Barink, Marco, M. De Waal Malefijt, P. Celada, P. Vena, A. Van Kampen, and N. Verdonschot. 2008. "A Mechanical Comparison of High-Flexion and Conventional Total Knee Arthroplasty." Proceedings of the Institution of Mechanical Engineers. Part H, Journal of Engineering in Medicine 222 (3): 297-307.

Barnett, Petra I., J. Fisher, D. D. Auger, M. H. Stone, and E. Ingham. 2001. "Comparison of Wear in a Total Knee Replacement under Different Kinematic Conditions." Journal of Materials Science: Materials in Medicine 12 (10-12): 1039-1042.

Bartel, Donald L., J. J. Rawlinson, A. H. Burstein, C. S. Ranawat, and W. F. Flynn Jr. 1995. "Stresses in Polyethylene Components of Contemporary Total Knee Replacements." Clinical Orthopaedics and Related Research 317: 76-82.

Benjamin, James, J. Szivek, G. Dersam, S. Persselin, and R. Johnson. 2001. "Linear and Volumetric Wear of Tibial Inserts in Posterior Cruciate-Retaining Knee Arthroplasties." Clinical Orthopaedics and Related Research 392: 131-138.

Bergmann, Georg, A. Bender, F. Graichen, J. Dymke, A. Rohlmann, A. Trepczynski, M. O. Heller, and I. Kutzner. 2014. "Standardized Loads Acting in Knee Implants." PloS One 9 (1): e86035.

Blankevoort, Leendert, R. Huiskes, and A. De Lange. 1991. "Recruitment of Knee Joint Ligaments." Journal of Biomechanical Engineering 113 (1): 94-103.

Blankevoort, Leendert, J. H. Kuiper, R. Huiskes, and H. J. Grootenboer. 1991. "Articular Contact in a Three-Dimensional Model of the Knee." Journal of Biomechanics 24 (11): 1019-1031.

Bloemker, Katherine H., T. M. Guess, L. Maletsky, and K. Dodd. 2012. "Computational Knee Ligament Modeling using Experimentally Determined Zero-Load Lengths." The Open Biomedical Engineering Journal 6: 33-41.

Blunn, Gordon W., A. B. Joshi, R. J. Minns, L. Lidgren, P. Lilley, L. Ryd, E. Engelbrecht, and P. S. Walker. 1997. "Wear in Retrieved Condylar Knee Arthroplasties: A Comparison of Wear in Different Designs of 280 Retrieved Condylar Knee Prostheses." The Journal of Arthroplasty 12 (3): 281-290.

Bombardier, Claire, G. Hawker, and D. Mosher. 2011. The Impact of Arthritis in Canada: Today and Over the Next 30 Years. Toronto, CA: Arthritis Alliance of Canada.

Bourne, Robert B., B. M. Chesworth, A. M. Davis, N. N. Mahomed, and K. D. J. Charron. 2010. "Patient Satisfaction After Total Knee Arthroplasty: Who is Satisfied and Who is Not?" Clinical Orthopaedics and Related Research® 468 (1): 57-63.

Brinkman, Justus-Martijn, P. Singh Bubra, P. Walker, W. R. Walsh, and W. J. M. Bruce. 2014. "Midterm Results using a Medial Pivot Total Knee Replacement Compared with the Australian National Joint Replacement Registry Data." ANZ Journal of Surgery 84 (3): 172-176.

Carr, Brandi C. and T. Goswami. 2009. "Knee implants–Review of Models and Biomechanics." Materials & Design 30 (2): 398-413.

Catani, Fabio, A. Ensini, C. Belvedere, A. Feliciangeli, M. Grazia Benedetti, A. Leardini, and S. Giannini. 2009. "In Vivo Kinematics and Kinetics of a bi-cruciate Substituting Total Knee Arthroplasty: A Combined Fluoroscopic and Gait Analysis Study." Journal of Orthopaedic Research 27 (12): 1569-1575.

Catani, Fabio, B. Innocenti, C. Belvedere, L. Labey, A. Ensini, and A. Leardini. 2010. "The Mark Coventry Award Articular: Contact Estimation in TKA using in Vivo Kinematics and Finite Element Analysis." Clinical Orthopaedics and Related Research® 468 (1): 19-28.

Causero, Araldo, P. Di Benedetto, A. Beltrame, R. Gisonni, V. Cainero, and M. Pagano. 2014. "Design Evolution in Total Knee Replacement: Which is the Future?" Acta Bio Medica Atenei Parmensis 85 (2): 5-19.

Chang, Timothy C. 2005. "Effects of Select Fluid on the Friction of Metal-on-Polyethylene Joint Replacement Surfaces." MSc dissertation in Mechanical Engineering, Massachusetts Institute of Technology.

Chapman-Sheath, Phillip J. , W. J. M. Bruce, W. K. Chung, P. Morberg, R. M. Gillies, and W. R. Walsh. 2003. "In Vitro Assessment of Proximal Polyethylene Contact Surface Areas and Stresses in Mobile Bearing Knees." Medical Engineering & Physics 25 (6): 437-443.

Cho, Sung-Do, Y. Youm, and K. Park. 2011. "Three-to Six-Year Follow-Up Results after High-Flexion Total Knee Arthroplasty: Can we Allow Passive Deep Knee Bending?" Knee Surgery, Sports Traumatology, Arthroscopy 19 (6): 899-903.

Cinotti, Gianluca, P. Sessa, F. R. Ripani, R. Postacchini, R. Masciangelo, and G. Giannicola. 2012. "Correlation between Posterior Offset of Femoral Condyles and Sagittal Slope of the Tibial Plateau." Journal of Anatomy 221 (5): 452-458.

Clark, Charles R., C. H. Rorabeck, S. MacDonald, D. MacDonald, J. Swafford, and D. Cleland. 2001. "Posterior-Stabilized and Cruciate-Retaining Total Knee Replacement: A Randomized Study." Clinical Orthopaedics and Related Research 392: 208-212.

Conditt, Michael A., M. T. Thompson, M. M. Usrey, S. K. Ismaily, and P. C. Noble. 2005. "Backside Wear of Polyethylene Tibial Inserts: Mechanism and Magnitude of Material Loss." The Journal of Bone and Joint Surgery. American Volume 87 (2): 326-331.

Conover, William Jay and W. J. Conover. 1980. "Practical Nonparametric Statistics."

Cooke, Derek, A. Scudamore, J. Li, U. Wyss, T. Bryant, and P. Costigan. 1997. "Axial Lower-Limb Alignment: Comparison of Knee Geometry in Normal Volunteers and Osteoarthritis Patients." Osteoarthritis and Cartilage 5 (1): 39-47.

Cornwall, Bryan G., J. T. Bryant, and C. M. Hansson. 2001. "The Effect of Kinematic Conditions on the Wear of Ultrahigh Molecular Weight Polyethylene (UHMWPE) in Orthopaedic Bearing Applications." Proc IMechE Part H: J Engineering in Medicine 215 (1): 95-106.

D'Lima, Darryl D., S. Patil, N. Steklov, S. Chien, and C. W. Colwell. 2007. "In Vivo Knee Moments and Shear after Total Knee Arthroplasty." Journal of Biomechanics 40: S11-S17.

D'Lima, Darryl D., M. Trice, A. G. Urquhart, and C. W. Colwell Jr. 2000. "Comparison between the Kinematics of Fixed and Rotating Bearing Knee Prostheses." Clinical Orthopaedics and Related Research 380: 151-157.

D'Lima, Darryl D., P. C. Chen, and C. W. Colwell Jr. 2001. "Polyethylene Contact Stresses, Articular Congruity, and Knee Alignment." Clinical Orthopaedics and Related Research 392: 232-238.

DeFrate, Louis E., H. Sun, T. J. Gill, H. E. Rubash, and G. Li. 2004. "In Vivo Tibiofemoral Contact Analysis using 3D MRI-Based Knee Models." Journal of Biomechanics 37 (10): 1499-1504.

Dennis, Douglas A., R. D. Komistek, and M. R. Mahfouz. 2003. "In Vivo Fluoroscopic Analysis of Fixed-Bearing Total Knee Replacements." Clinical Orthopaedics and Related Research 410 (410): 114-130.

Dennis, Douglas A., R. D. Komistek, M. R. Mahfouz, B. D. Haas, and J. B. Stiehl. 2003. "Multicenter Determination of in Vivo Kinematics after Total Knee Arthroplasty." Clinical Orthopaedics and Related Research (416) (416): 37-57.

Dennis, Douglas A., R. D. Komistek, S. A. Walker, E. J. Cheal, and J. B. Stiehl. 2001. "Femoral Condylar Lift-Off in Vivo in Total Knee Arthroplasty." The Journal of Bone and Joint Surgery. British Volume 83 (1): 33-39.

Dennis, Douglas A., M. R. Mahfouz, R. D. Komistek, and W. Hoff. 2005. "In Vivo Determination of Normal and Anterior Cruciate Ligament-Deficient Knee Kinematics." Journal of Biomechanics 38 (2): 241-253.

Dennis, Douglas A., R. D. Komistek, J. B. Stiehl, S. A. Walker, and K. N. Dennis. 1998. "Range of Motion after Total Knee Arthroplasty the Effect of Implant Design and Weight-Bearing Conditions." The Journal of Arthroplasty 13 (7): 748-752.

DesJardins, John D., P. S. Walker, H. Haider, and J. Perry. 2000. "The use of a Force-Controlled Dynamic Knee Simulator to Quantify the Mechanical Performance of Total Knee Replacement Designs during Functional Activity." Journal of Biomechanics 33 (10): 1231-1242.

Drake, Richard, A. Wayne Vogl, and A. W. M. Mitchell. 2014. Gray's Anatomy for Students Elsevier Health Sciences.

Dunbar, Michael J., G. Richardson, and O. Robertsson. 2013. "I can't Get no Satisfaction After My Total Knee Replacement: Rhymes and Reasons." The Bone & Joint Journal 95-B (11 Suppl A): 148-152.

Eckhoff, Donald G., J. M. Bach, V. M. Spitzer, K. D. Reinig, M. M. Bagur, T. H. Baldini, and N. M. Flannery. 2005. "Three-Dimensional Mechanics, Kinematics, and Morphology of the Knee Viewed in Virtual Reality." The Journal of Bone and Joint Surgery. American Volume 87 Suppl 2: 71-80.

Endres, Stefan. and A. Wilke. 2011. "High Flexion Total Knee Arthroplasty - Mid-Term Follow Up of 5 Years." The Open Orthopaedics Journal 5: 138-142.

Fitzpatrick, Clare K., C. W. Clary, and P. J. Rullkoetter. 2012. "The Role of Patient, Surgical, and Implant Design Variation in Total Knee Replacement Performance." Journal of Biomechanics 45 (12): 2092-2102.

Fitzpatrick, Clare K., C. W. Clary, P. J. Laz, and P. J. Rullkoetter. 2012. "Relative Contributions of Design, Alignment, and Loading Variability in Knee Replacement Mechanics." Journal of Orthopaedic Research 30 (12): 2015-2024.

Fitzpatrick, Clare K., M. A. B., P. J. Rullkoetter, and P. J. Laz. 2011. "Combined Probabilistic and Principal Component Analysis Approach for Multivariate Sensitivity Evaluation and Application to Implanted Patellofemoral Mechanics." Journal of Biomechanics 44 (1): 13-21.

Frankel, Victor H., A. H. Burstein, and D. B. Brooks. 1971. "Biomechanics of Internal Derangement of the Knee. Pathomechanics as Determined by Analysis of the Instant Centers of Motion." The Journal of Bone and Joint Surgery. American Volume 53 (5): 945-962.

Freeman, Michael A. R. and V. Pinskerova. 2005. "The Movement of the Normal Tibio-Femoral Joint." Journal of Biomechanics 38 (2): 197-208.

Fregly, Benjamin J., W. G. Sawyer, M. K. Harman, and S. A. Banks. 2005. "Computational Wear Prediction of a Total Knee Replacement from in Vivo Kinematics." Journal of Biomechanics 38 (2): 305-314.

Godest, A. C., M. Beaugonin, E. Haug, M. Taylor, and P. J. Gregson. 2002. "Simulation of a Knee Joint Replacement during a Gait Cycle using Explicit Finite Element Analysis." Journal of Biomechanics 35 (2): 267-275.

Goldstein, Wayne M., D. J. Raab, T. F. Gleason, J. J. Branson, and K. Berland. 2006. "Why Posterior Cruciate-Retaining and Substituting Total Knee Replacements have Similar Ranges of Motion. the Importance of Posterior Condylar Offset and Cleanout of Posterior Condylar Space." The Journal of Bone and Joint Surgery. American Volume 88 Suppl 4: 182-188.

Guess, Trent M. and L. P. Maletsky. 2005. "Computational Modeling of a Dynamic Knee Simulator for Reproduction of Knee Loading." Journal of Biomechanical Engineering 127 (7): 1216-1221.

Guess, Trent M. and L. P. Maletsky. 2005. "Computational Modelling of a Total Knee Prosthetic Loaded in a Dynamic Knee Simulator." Medical Engineering & Physics 27 (5): 357-367.

Guess, Trent M., G. Thiagarajan, M. Kia, and M. Mishra. 2010. "A Subject Specific Multibody Model of the Knee with Menisci." Medical Engineering & Physics 32 (5): 505-515.

Guess, Trent M., H. Liu, S. Bhashyam, and G. Thiagarajan. 2013. "A Multibody Knee Model with Discrete Cartilage Prediction of Tibio-Femoral Contact Mechanics." Computer Methods in Biomechanics and Biomedical Engineering 16 (3): 256-270.

Halloran, Jason P., C. W. Clary, L. P. Maletsky, M. Taylor, A. J. Petrella, and P. J. Rullkoetter. 2010. "Verification of Predicted Knee Replacement Kinematics during Simulated Gait in the Kansas Knee Simulator." Journal of Biomechanical Engineering 132 (8): 081010.

Halloran, Jason P., S. K. Easley, A. J. Petrella, and P. J. Rullkoetter. 2005. "Comparison of Deformable and Elastic Foundation Finite Element Simulations for Predicting Knee Replacement Mechanics." Journal of Biomechanical Engineering 127 (5): 813-818.

Hamai, Satoshi, T. Moro-Oka, N. J. Dunbar, H. Miura, Y. Iwamoto, and S. A. Banks. 2012. "In Vivo Healthy Knee Kinematics during Dynamic Full Flexion." BioMed Research International 2013.

Harato, Kengo, R. B. Bourne, J. Victor, M. Snyder, J. Hart, and M. D. Ries. 2008. "Midterm Comparison of Posterior Cruciate-Retaining Versus-Substituting Total Knee Arthroplasty using the Genesis II Prosthesis: A Multicenter Prospective Randomized Clinical Trial." The Knee 15 (3): 217-221.

Harrysson, Ola L., Y. A. Hosni, and J. F. Nayfeh. 2007. "Custom-Designed Orthopedic Implants Evaluated using Finite Element Analysis of Patient-Specific Computed Tomography Data: Femoral-Component Case Study." BMC Musculoskeletal Disorders 8: 91.

Hashemi, Javad, N. Chandrashekar, B. Gill, B. D. Beynnon, J. R. Slauterbeck, R. C. Schutt Jr, H. Mansouri, and E. Dabezies. 2008. "The Geometry of the Tibial Plateau and its Influence on the Biomechanics of the Tibiofemoral Joint." The Journal of Bone and Joint Surgery. American Volume 90 (12): 2724-2734.

Hernigou, P., A. Poignard, P. Filippini, and S. Zilber. 2008. "Retrieved Unicompartmental Implants with Full PE Tibial Components: The Effects of Knee Alignment and Polyethylene Thickness on Creep and Wear." The Open Orthopaedics Journal 2: 51-56.

Hill, Paul F., V. Vedi, A. Williams, H. Iwaki, V. Pinskerova, and M. A. Freeman. 2000. "Tibiofemoral Movement 2: The Loaded and Unloaded Living Knee Studied by MRI." The Journal of Bone and Joint Surgery. British Volume 82 (8): 1196-1198.

Hip and Knee Replacements in Canada: Canadian Joint Replacement Registry 2016. Ottawa, ON: Canadian Institute for Health Information (CIHI).

Horiuchi, Hiroshi, S. Akizuki, T. Tomita, K. Sugamoto, T. Yamazaki, and N. Shimizu. 2012. "In Vivo Kinematic Analysis of Cruciate-Retaining Total Knee Arthroplasty during Weight-Bearing and non–weight-Bearing Deep Knee Bending." The Journal of Arthroplasty 27 (6): 1196-1202.

Hudek, Robert, S. Schmutz, F. Regenfelder, B. Fuchs, and P. P. Koch. 2009. "Novel Measurement Technique of the Tibial Slope on Conventional MRI." Clinical Orthopaedics and Related Research® 467 (8): 2066-2072.

International Standard Organization. 2002. Implants for Surgery -- Wear of Total Knee-Joint Prostheses -- Part 1: Loading and Displacement Parameters for Wear-Testing Machines with Load Control and Corresponding Environmental Conditions for Test.

International Standard Organization. 2009. Implants for Surgery -- Wear of Total Knee-Joint Prostheses -- Part 1: Loading and Displacement Parameters for Wear-Testing Machines with Load Control and Corresponding Environmental Conditions for Test- ISO 14243-1: 2009. Vol. 1.

Iwaki, H., V. Pinskerova, and M. A. R. Freeman. 2000. "Tibiofemoral Movement 1: The Shapes and Relative Movements of the Femur and Tibia in the Unloaded Cadaver Knee." Journal of Bone & Joint Surgery, British Volume 82 (8): 1189-1195.

Jacofsky, David. 2005. "Bicruciate-Retaining Total Knee Arthroplasty." In Total Knee Arthroplasty, 291-294: Springer.

Johal, Parm, A. Williams, P. Wragg, D. Hunt, and W. Gedroyc. 2005. "Tibio-Femoral Movement in the Living Knee. A Study of Weight Bearing and Non-Weight Bearing Knee Kinematics using 'interventional' MRI." Journal of Biomechanics 38 (2): 269-276.

Johnson, Kenneth Langstreth. 1987. Contact Mechanics Cambridge university press.

Jun, Yongtae. 2011. "Morphological Analysis of the Human Knee Joint for Creating Custom-made Implant Models." The International Journal of Advanced Manufacturing Technology 52 (9-12): 841-853.

Kawanabe, Keiichi, I. C. Clarke, J. Tamura, M. Akagi, V. D. Good, P. A. Williams, and K. Yamamoto. 2001. "Effects of A–P Translation and Rotation on the Wear of UHMWPE in a Total Knee Joint Simulator." Journal of Biomedical Materials Research 54 (3): 400-406.

Khosravipour, Ida, Y. Luo, S. Pejhan, and U. Wyss. 2015. "Contact Stress Analysis of Surface Guided Knee Implant." London, Ontario, Canada, May 31-June 4, 2015.

Kim, Young-Hoo, Y. Choi, and J. S. Kim. 2009. "Range of Motion of Standard and High-Flexion Posterior Cruciate-Retaining Total Knee Prostheses a Prospective Randomized Study." The Journal of Bone and Joint Surgery. American Volume 91 (8): 1874-1881.

Komistek, Richard D., D. A. Dennis, and M. Mahfouz. 2003. "In Vivo Fluoroscopic Analysis of the Normal Human Knee." Clinical Orthopaedics and Related Research (410) (410): 69-81.

Kozanek, Michal, A. Hosseini, F. Liu, S. K. Van de Velde, T. J. Gill, H. E. Rubash, and G. Li. 2009. "Tibiofemoral Kinematics and Condylar Motion during the Stance Phase of Gait." Journal of Biomechanics 42 (12): 1877-1884.

Kretzer, Philippe J., E. Jakubowitz, R. Sonntag, K. Hofmann, C. Heisel, and M. Thomsen. 2010. "Effect of Joint Laxity on Polyethylene Wear in Total Knee Replacement." Journal of Biomechanics 43 (6): 1092-1096.

Kuroyanagi, Yuji, S. Mu, S. Hamai, W. J. Robb, and S. A. Banks. 2012. "In Vivo Knee Kinematics during Stair and Deep Flexion Activities in Patients with Bicruciate Substituting Total Knee Arthroplasty." The Journal of Arthroplasty 27 (1): 122-128.

Kurtz, Steven M., K. Ong, E. Lau, F. Mowat, and M. Halpern. 2007. "Projections of Primary and Revision Hip and Knee Arthroplasty in the United States from 2005 to 2030." The Journal of Bone and Joint Surgery. American Volume 89 (4): 780-785.

Kurtz, Steven M. 2009. "Ultra High Molecular Weight Polyethylene in Total Joint Replacement and Medical Devices." UHMWPE Biomaterials Handbook, 2nd Edn.Academic Press, New York.

Kurtz, Steven M., E. Lau, K. Ong, K. Zhao, M. Kelly, and K. J. Bozic. 2009. "Future Young Patient Demand for Primary and Revision Joint Replacement: National Projections from 2010 to 2030." Clinical Orthopaedics and Related Research® 467 (10): 2606-2612.

Laz, Peter J., S. Pal, A. Fields, A. J. Petrella, and P. J. Rullkoetter. 2006. "Effects of Knee Simulator Loading and Alignment Variability on Predicted Implant Mechanics: A Probabilistic Study." Journal of Orthopaedic Research 24 (12): 2212-2221.

Laz, Peter J. and M. Browne. 2010. "A Review of Probabilistic Analysis in Orthopaedic Biomechanics." Proceedings of the Institution of Mechanical Engineers. Part H, Journal of Engineering in Medicine 224 (8): 927-943.

Leszko, Filip, K. R. Hovinga, A. L. Lerner, R. D. Komistek, and M. R. Mahfouz. 2011. "In Vivo Normal Knee Kinematics: Is Ethnicity Or Gender an Influencing Factor?" Clinical Orthopaedics and Related Research® 469 (1): 95-106.

Liau, Jiann-Jong, C. Hu, C. Cheng, C. Huang, and W. Lo. 2001. "The Influence of Inserting a Fuji Pressure Sensitive Film between the Tibiofemoral Joint of Knee Prosthesis on Actual Contact Characteristics." Clinical Biomechanics 16 (2): 160-166.

Public Health Agency of Canada. 2010. Life with Arthritis in Canada: A Personal and Public Health Challenge.

Liu, Yu-Liang, K. Lin, C. Huang, W. Chen, C. Chen, T. Chang, Y. Lai, and C. Cheng. 2011. "Anatomic-Like Polyethylene Insert could Improve Knee Kinematics after Total Knee arthroplasty—a Computational Assessment." Clinical Biomechanics 26 (6): 612-619.

Lozano-Calderón, Santiago A., J. Shen, D. F. Doumato, D. A. Greene, and S. B. Zelicof. 2013. "Cruciate-Retaining Vs Posterior-Substituting Inserts in Total Knee Arthroplasty: Functional Outcome Comparison." The Journal of Arthroplasty 28 (2): 234-242. e1.

Lu, Tung-Wu, T. Tsai, M. Kuo, H. Hsu, and H. Chen. 2008. "In Vivo Three-Dimensional Kinematics of the Normal Knee during Active Extension Under Unloaded and Loaded Conditions using Single-Plane Fluoroscopy." Medical Engineering & Physics 30 (8): 1004-1012.

Martelli, Saulo and V. Pinskerova. 2002. "The Shapes of the Tibial and Femoral Articular Surfaces in Relation to Tibiofemoral Movement." The Journal of Bone and Joint Surgery. British Volume 84 (4): 607-613.

Maruyama, Shigeki, S. Yoshiya, N. Matsui, R. Kuroda, and M. Kurosaka. 2004. "Functional Comparison of Posterior Cruciate-Retaining Versus Posterior Stabilized Total Knee Arthroplasty." The Journal of Arthroplasty 19 (3): 349-353.

Masouros, Spyros D., A. M. J. Bull, and A. A. Amis. 2010. "(i) Biomechanics of the Knee Joint." Orthopaedics and Trauma 24 (2): 84-91.

Matsuda, Shuichi, H. Miura, R. Nagamine, K. Urabe, T. Ikenoue, K. Okazaki, and Y. Iwamoto. 1999. "Posterior Tibial Slope in the Normal and Varus Knee." The American Journal of Knee Surgery 12 (3): 165-168.

McCalden, Richard W., S. J. MacDonald, K. D. J. Charron, R. B. Bourne, and D. D. Naudie. 2010. "The Role of Polyethylene Design on Postoperative TKA Flexion: An Analysis of 1534 Cases." Clinical Orthopaedics and Related Research® 468 (1): 108-114.

McEwen, HMJ, PI Barnett, CJ Bell, R. Farrar, DD Auger, MH Stone, and J. Fisher. 2005. "The Influence of Design, Materials and Kinematics on the in Vitro Wear of Total Knee Replacements." Journal of Biomechanics 38 (2): 357-365.

Moonot, Pradeep, M. Shang, G. T. Railton, R. E. Field, and S. A. Banks. 2010. "In Vivo Weight-Bearing Kinematics with Medial Rotation Knee Arthroplasty." The Knee 17 (1): 33-37.

Moonot, Pradeep, S. Mu, G. T. Railton, R. E. Field, and S. A. Banks. 2009. "Tibiofemoral Kinematic Analysis of Knee Flexion for a Medial Pivot Knee." Knee Surgery, Sports Traumatology, Arthroscopy 17 (8): 927-934.

Mootanah, Rajshree, C. Imhauser, F. Reisse, D. Carpanen, R. W. Walker, M. Koff, M. Lenhoff, R. Rozbruch, A. Fragomen, and Y. Kirane. 2014. "Development and Verification of a Computational Model of the Knee Joint for the Evaluation of Surgical Treatments for Osteoarthritis." Computer Methods in Biomechanics and Biomedical Engineering 17: 1502-1517.

Moro-oka, Taka-aki, M. Muenchinger, J. Canciani, and S. A. Banks. 2007. "Comparing in Vivo Kinematics of Anterior Cruciate-Retaining and Posterior Cruciate-Retaining Total Knee Arthroplasty." Knee Surgery, Sports Traumatology, Arthroscopy 15 (1): 93-99.

Moro-oka, Taka-aki, S. Hamai, H. Miura, T. Shimoto, H. Higaki, B. J. Fregly, Y. Iwamoto, and S. A. Banks. 2008. "Dynamic Activity Dependence of in Vivo Normal Knee Kinematics." Journal of Orthopaedic Research 26 (4): 428-434.

MSC Software Corporation. 2013. MSC. ADAMS User Manual MSC.

Mu, Shang, T. Moro-Oka, P. Johal, S. Hamai, M. A. R. Freeman, and S. A. Banks. 2011. "Comparison of Static and Dynamic Knee Kinematics during Squatting." Clinical Biomechanics 26 (1): 106-108.

Mulholland, Susan J. and U. P. Wyss. 2001. "Activities of Daily Living in Non-Western Cultures: Range of Motion Requirements for Hip and Knee Joint Implants." International Journal of Rehabilitation Research 24 (3): 191-198.

Muratoglu, Orhun K., A. Mark, D. A. Vittetoe, W. H. Harris, and H. E. Rubash. 2003. "Polyethylene Damage in Total Knees and use of Highly Crosslinked Polyethylene." The Journal of Bone and Joint Surgery. American Volume 85-A Suppl 1: S7-S13.

Murphy, Louise B., S. Moss, B. T. Do, C. G. Helmick, T. A. Schwartz, K. E. Barbour, J. Renner, W. Kalsbeek, and J. M. Jordan. 2016. "Annual Incidence of Knee Symptoms and Four Knee Osteoarthritis Outcomes in the Johnston County Osteoarthritis Project." Arthritis Care & Research 68 (1): 55-65.

Murphy, Louise, T. A. Schwartz, C. G. Helmick, J. B. Renner, G. Tudor, G. Koch, A. Dragomir, W. D. Kalsbeek, G. Luta, and J. M. Jordan. 2008. "Lifetime Risk of Symptomatic Knee Osteoarthritis." Arthritis Care & Research 59 (9): 1207-1213.

Nakagawa, Shinichi, Y. Kadoya, S. Todo, A. Kobayashi, H. Sakamoto, M. A. Freeman, and Y. Yamano. 2000. "Tibiofemoral Movement 3: Full Flexion in the Living Knee Studied by MRI." The Journal of Bone and Joint Surgery. British Volume 82 (8): 1199-1200.

Naudie, Douglas D. R., D. J. Ammeen, G. A. Engh, and C. H. Rorabeck. 2007. "Wear and Osteolysis Around Total Knee Arthroplasty." Journal of the American Academy of Orthopaedic Surgeons 15 (1): 53-64.

Noble, Philip C., M. J. Gordon, J. M. Weiss, R. N. Reddix, M. A. Conditt, and K. B. Mathis. 2005. "Does Total Knee Replacement Restore Normal Knee Function?" Clinical Orthopaedics and Related Research 431: 157-165.

Nutton, Richard W., M. L. van der Linden, P. J. Rowe, P. Gaston, and F. A. Wade. 2008. "A Prospective Randomized Double-Blind Study of Functional Outcome and Range of Flexion Following Total Knee Replacement with the NexGen Standard and High Flexion Components." The Journal of Bone and Joint Surgery. British Volume 90 (1): 37-42.

O'Brien, Sean, Y. Luo, C. Wu, M. Petrak, E. Bohm, and J. M. Brandt. 2013. "Computational Development of a Polyethylene Wear Model for the Articular and Backside Surfaces in Modular Total Knee Replacements." Tribology International 59: 284-291.

Omori, Go, N. Onda, M. Shimura, T. Hayashi, T. Sato, and Y. Koga. 2009. "The Effect of Geometry of the Tibial Polyethylene Insert on the Tibiofemoral Contact Kinematics in Advance Medial Pivot Total Knee Arthroplasty." Journal of Orthopaedic Science 14 (6): 754-760.

Patil, Shantanu, C. W. Colwell Jr, K. A. Ezzet, and D. D. D'Lima. 2005. "Can Normal Knee Kinematics be Restored with Unicompartmental Knee Replacement?" The Journal of Bone and Joint Surgery. American Volume 87 (2): 332-338.

Patten, Eli W., D. Van Citters, M. D. Ries, and L. A. Pruitt. 2013. "Wear of UHMWPE from Sliding, Rolling, and Rotation in a Multidirectional Tribo-System." Wear 304 (1): 60-66.

Pejhan, Shabnam, E. Bohm, J. M. Brandt, and U. Wyss. 2016. "Design and Virtual Evaluation of a Customized Surface-Guided Knee Implant." Proc IMechE Part H: J Engineering in Medicine 230 (10): 949-961.

Pinskerova, Vera, P. Johal, S. Nakagawa, A. Sosna, A. Williams, W. Gedroyc, and M. A. Freeman. 2004. "Does the Femur Roll-Back with Flexion?" The Journal of Bone and Joint Surgery. British Volume 86 (6): 925-931.

Pritchett, James W. 2004. "Patient Preferences in Knee Prostheses." The Journal of Bone and Joint Surgery. British Volume 86 (7): 979-982.

Pritchett, James W. 2015. "Bicruciate-Retaining Total Knee Replacement Provides Satisfactory Function and Implant Survivorship at 23 Years." Clinical Orthopaedics and Related Research® 473 (7): 2327-2333.

Qi, Wei, A. Hosseini, T.Y. Tsai, J.S. Li, H. E. Rubash, and G. Li. 2013. "In vivo kinematics of the knee during weight bearing high flexion." Journal of biomechanics 46(9): 1576-1582.

Rand, James A., R. T. Trousdale, D. M. Ilstrup, and W. S. Harmsen. 2003. "Factors Affecting the Durability of Primary Total Knee Prostheses." The Journal of Bone and Joint Surgery. American Volume 85-A (2): 259-265.

Rawlinson, Jeremy J. and D. L. Bartel. 2002. "Flat medial–lateral Conformity in Total Knee Replacements does Not Minimize Contact Stresses." Journal of Biomechanics 35 (1): 27-34.

Riley Jr, lee H. 1976. "The Evolution of Total Knee Arthroplasty." Clinical Orthopaedics and Related Research 120: 7-10.

Robertsson, Otto, M. Dunbar, T. Pehrsson, K. Knutson, and L. Lidgren. 2000. "Patient Satisfaction after Knee Arthroplasty: A Report on 27,372 Knees Operated on between 1981 and 1995 in Sweden." Acta Orthopaedica Scandinavica 71 (3): 262-267.

Robinson, Raymond P. 2005. "The Early Innovators of Today's Resurfacing Condylar Knees." The Journal of Arthroplasty 20: 2-26.

Saari, Tuuli, J. Uvehammer, L. V. Carlsson, P. Herberts, L. Regner, and J. Karrholm. 2003. "Kinematics of Three Variations of the Freeman-Samuelson Total Knee Prosthesis." Clinical Orthopaedics and Related Research 410: 235-247.

Sanz-Ruiz, Pablo, E. Carbo-Laso, B. Alonso-Polo, J. Antonio Matas-Diez, and J. Vaquero-Martín. 2016. "Does a New Implant Design with More Physiological Kinematics Provide Better Results After Knee Arthroplasty?" The Knee 23 (3): 399-405.

Sathasivam, Shivani, and P. S. Walker. 1999. "The Conflicting Requirements of Laxity and Conformity in Total Knee Replacement." Journal of Biomechanics 32 (3): 239-247.

Sathasivam, Shivani, and P. S. Walker. 1998. "Computer Model to Predict Subsurface Damage in Tibial Inserts of Total Knees." Journal of Orthopaedic Research 16 (5): 564-571.

Scarvell, Jennifer M., P. N. Smith, K. M. Refshauge, H. R. Galloway, and K. R. Woods. 2004. "Evaluation of a Method to Map Tibiofemoral Contact Points in the Normal Knee using MRI." Journal of Orthopaedic Research 22 (4): 788.

Schmidt, Robert, R. D. Komistek, J. D. Blaha, B. L. Penenberg, and W. J. Maloney. 2003. "Fluoroscopic Analyses of Cruciate-Retaining and Medial Pivot Knee Implants." Clinical Orthopaedics and Related Research (410) (410): 139-147.

Shiramizu, Kei, F. Vizesi, W. Bruce, S. Herrmann, and W. R. Walsh. 2009. "Tibiofemoral Contact Areas and Pressures in Six High Flexion Knees." International Orthopaedics 33 (2): 403-406.

Simpson, David J., H. Gray, D. D'Lima, D. W. Murray, and H. S. Gill. 2008. "The Effect of Bearing Congruency, Thickness and Alignment on the Stresses in Unicompartmental Knee Replacements." Clinical Biomechanics 23 (9): 1148-1157.

Siston, Robert A., N. J. Giori, S. B. Goodman, and S. L. Delp. 2006. "Intraoperative Passive Kinematics of Osteoarthritic Knees before and After Total Knee Arthroplasty." Journal of Orthopaedic Research 24 (8): 1607-1614.

Smith, Stacey M., R. A. Cockburn, A. Hemmerich, R. M. Li, and U. P. Wyss. 2008. "Tibiofemoral Joint Contact Forces and Knee Kinematics during Squatting." Gait & Posture 27 (3): 376-386.

Steklov, Nick, J. Slamin, S. Srivastav, and D. D'Lima. 2010. "Unicompartmental Knee Resurfacing: Enlarged Tibio-Femoral Contact Area and Reduced Contact Stress using Novel Patient-Derived Geometries." The Open Biomedical Engineering Journal 4: 85-92.

Stiehl, James B., R. D. Komistek, J. Cloutier, and D. A. Dennis. 2000. "The Cruciate Ligaments in Total Knee Arthroplasty: A Kinematic Analysis of 2 Total Knee Arthroplasties." The Journal of Arthroplasty 15 (5): 545-550.

Tanner, Michael G., L. A. Whiteside, and S. E. White. 1995. "Effect of Polyethylene Quality on Wear in Total Knee Arthroplasty." Clinical Orthopaedics and Related Research 317: 83-88.

Tanzer, Michael, K. Smith, and S. Burnett. 2002. "Posterior-Stabilized Versus Cruciate-Retaining Total Knee Arthroplasty: Balancing the Gap." The Journal of Arthroplasty 17 (7): 813-819.

The Arthritis Society. 2013. Arthritis in Canada: Arthritis Community Research and Evaluation Unit (ACREU).

United States Bone and Joint Initiative. 2014. The Burden of Musculoskeletal Diseases in the United States (BMUS).

Van den Heever, D. Jacobus. 2011. "Development of Patient-Specific Knee Joint Prostheses for Unicompartmental Knee Replacement (UKR)." PhD dissertation, Stellenbosch University

Van den Heever, Dawie J, C. Scheffer, P. Erasmus, and E. Dillon. 2011. "Contact Stresses in a Patient-Specific Unicompartmental Knee Replacement." Clinical Biomechanics 26 (2): 159-166.

Van Duren, Bernard H., H. Pandit, M. Price, S. Tilley, H. S. Gill, D. W. Murray, and N. P. Thomas. 2012. "Bicruciate Substituting Total Knee Replacement: How Effective are the Added Kinematic Constraints in Vivo?" Knee Surgery, Sports Traumatology, Arthroscopy 20 (10): 2002-2010.

Varadarajan, Kartik M., R. E. Harry, T. Johnson, and G. Li. 2009. "Can in Vitro Systems Capture the Characteristic Differences between the flexion–extension Kinematics of the Healthy and TKA Knee?" Medical Engineering & Physics 31 (8): 899-906.

Victor, Jan and J. Bellemans. 2006. "Physiologic Kinematics as a Concept for Better Flexion in TKA." Clinical Orthopaedics and Related Research 452: 53-58.

Victor, Jan, D. Van Doninck, L. Labey, F. Van Glabbeek, P. Parizel, and J. Bellemans. 2009. "A Common Reference Frame for Describing Rotation of the Distal Femur: A Ct-Based Kinematic Study using Cadavers." The Journal of Bone and Joint Surgery. British Volume 91 (5): 683-690.

Victor, Jan, S. A. Banks, and J. Bellemans. 2005. "Kinematics of Posterior Cruciate Ligament-Retaining and -Substituting Total Knee Arthroplasty: A Prospective Randomised Outcome Study." The Journal of Bone and Joint Surgery. British Volume 87 (5): 646-655.

Victor, Jan, J. K. P. Mueller, R. D. Komistek, A. Sharma, M. C. Nadaud, and J. Bellemans. 2010. "In Vivo Kinematics After a Cruciate-Substituting TKA." Clinical Orthopaedics and Related Research® 468 (3): 807-814.

Victor, Jan. 2009. "A Comparative Study on the Biomechanics of the Native Human Knee Joint and Total Knee Arthroplasty." Doctoral thesis in Medical Sciences, Universiteit Leuven.

Walker, Peter. S., G. Yildirim, S. Arno, and Y. Heller. 2010. "Future Directions in Knee Replacement." Proceedings of the Institution of Mechanical Engineers. Part H, Journal of Engineering in Medicine 224 (3): 393-414.

Walker, Peter S. 2014. "Application of a Novel Design Method for Knee Replacements to Achieve Normal Mechanics." The Knee 21 (2): 353-358.

Walker, Peter S. 2001. "A New Concept in Guided Motion Total Knee Arthroplasty." The Journal of Arthroplasty 16 (8): 157-163.

Walker, Peter S. 2014. "Application of a Novel Design Method for Knee Replacements to Achieve Normal Mechanics." The Knee 21 (2): 353-358.

Walker, Peter S. 2015. "The Design and Pre-Clinical Evaluation of Knee Replacements for Osteoarthritis." Journal of Biomechanics 48 (5): 742-749.

Weiss, Jennifer M., P. C. Noble, M. A. Conditt, H. W. Kohl, S. Roberts, K. F. Cook, M. J. Gordon, and K. B. Mathis. 2002. "What Functional Activities are Important to Patients with Knee Replacements?" Clinical Orthopaedics and Related Research 404: 172-188.

Williams, Andy and M. Logan. 2004. "Understanding Tibio-Femoral Motion." The Knee 11 (2): 81-88.

Willing, Ryan and I. Y. Kim. 2009. "Three Dimensional Shape Optimization of Total Knee Replacements for Reduced Wear." Structural and Multidisciplinary Optimization 38 (4): 405-414.

Willing, Ryan and I. Y. Kim. 2011. "Design Optimization of a Total Knee Replacement for Improved Constraint and Flexion Kinematics." Journal of Biomechanics 44 (6): 1014-1020.

Willing, Ryan and I. Y. Kim. 2012. "Quantifying the Competing Relationship between Durability and Kinematics of Total Knee Replacements using Multiobjective Design Optimization and Validated Computational Models." Journal of Biomechanics 45 (1): 141-147.

Willing, Ryan and I. Y. Kim. 2012. "The Development, Calibration and Validation of a Numerical Total Knee Replacement Kinematics Simulator Considering Laxity and Unconstrained Flexion Motions." Computer Methods in Biomechanics and Biomedical Engineering 15 (6): 585-593.

Wilson, David R., J. D. Feikes, A. B. Zavatsky, and J. J. O'connor. 2000. "The Components of Passive Knee Movement are Coupled to Flexion Angle." Journal of Biomechanics 33 (4): 465-473.

Wimmer, Markus A. and T. P. Andriacchi. 1997. "Tractive Forces during Rolling Motion of the Knee: Implications for Wear in Total Knee Replacement." Journal of Biomechanics 30 (2): 131-137.

Wylde, Vikki, P. Dieppe, S. Hewlett, and I. D. Learmonth. 2007. "Total Knee Replacement: Is it really an Effective Procedure for all?" The Knee 14 (6): 417-423.

Wylde, Vikki, A. W. Blom, S. L. Whitehouse, A. H. Taylor, G. T. Pattison, and G. C. Bannister. 2009. "Patient-Reported Outcomes After Total Hip and Knee Arthroplasty: Comparison of Midterm Results." The Journal of Arthroplasty 24 (2): 210-216.

Wyss, Urs, S. Amiri, and T. D. V. Cooke. 2010. Knee Prosthesis. Patent: US20120179265

Yagishita, Kazuyoshi, T. Muneta, Y. Ju, T. Morito, J. Yamazaki, and I. Sekiya. 2012. "High-Flex Posterior Cruciate-Retaining Vs Posterior Cruciate-Substituting Designs in Simultaneous Bilateral Total Knee Arthroplasty: A Prospective, Randomized Study." The Journal of Arthroplasty 27 (3): 368-374.

Yoshioka, Yuki, D. Siu, and T. D. Cooke. 1987. "The Anatomy and Functional Axes of the Femur." The Journal of Bone and Joint Surgery. American Volume 69 (6): 873-880.

Yoshioka, Yuki, D. W. Siu, R. A. Scudamore, and T. D. V. Cooke. 1989. "Tibial Anatomy and Functional Axes." Journal of Orthopaedic Research 7 (1): 132-137.

Yoshiya, Shinichi, N. Matsui, R. D. Komistek, D. A. Dennis, M. Mahfouz, and M. Kurosaka. 2005. "In Vivo Kinematic Comparison of Posterior Cruciate-Retaining and Posterior Stabilized Total Knee Arthroplasties Under Passive and Weight-Bearing Conditions." The Journal of Arthroplasty 20 (6): 777-783.

Zavatsky, Amy B. 1997. "A Kinematic-Freedom Analysis of a Flexed-Knee-Stance Testing Rig." Journal of Biomechanics 30 (3): 277-280.

Zdero, Radovan, P. V. Fenton, J. Rudan, and J. T. Bryant. 2001. "Fuji Film and Ultrasound Measurement of Total Knee Arthroplasty Contact Areas." The Journal of Arthroplasty 16 (3): 367-375.

Zumbrunn, Thomas, K. Mangudi Varadarajan, H. E. Rubash, H. Malchau, G. Li, and O. K. Muratoglu. 2015. "Regaining Native Knee Kinematics Following Joint Arthroplasty: A Novel Biomimetic Design with ACL and PCL Preservation." The Journal of Arthroplasty 30 (12): 2143-2148.

Publications

Refereed published journal publications:

- Shabnam Pejhan, Eric Bohm, Jan-Mels Brandt, and Urs Wyss. "Design and Virtual Evaluation of a Customized Surface-Guided Knee Implant." 2016, Proc IMechE Part H: J Engineering in Medicine 230 (10): 949-961.

Refereed journal papers under publication:

- Shabnam Pejhan, Eric Bohm, Jan-Mels Brandt, and Urs Wyss., "The Influence of Geometric Design Variables on Kinematic Performance of a Surface-guided TKR", 2017, Journal of Orthopaedic Surgery.
- Shabnam Pejhan, Eric Bohm, Jan-Mels Brandt, Trevor Gascoyne, and Urs Wyss. "Kinematic Behavior of a Customized Surface-Guided Knee Implant during Simulated Knee-bending", 2017, Journal of Medical Engineering & Physics.
- Shabnam Pejhan, Ida Khosravipour, Trevor Gascoyne, Eric Bohm, Jan-Mels Brandt, Yunhua Luo, and Urs Wyss "Evaluation of the Tibiofemoral Contact Characteristics of a Customized Surface-Guided Knee Implant". 2017, Journal of Clinical Biomechanics.

Refereed proceedings and symposia articles:

- Shabnam Pejhan, Eric Bohm, Jan-Mels Brandt, and Urs Wyss “Geometric Design Variables Influence on the Kinematic Behavior of a Customized Surface-guided TKR”. Paper No.861, Orthopedic Research Society Annual Meeting, San Diego, California, USA, 2017
- Shabnam Pejhan, Ida Khosravipour, Eric Bohm, Jan-Mels Brandt, and Urs Wyss. “Preliminary Evaluation of a Customized Surface-Guided Knee Implant”, Paper No. 1872, Orthopedic Research Society Annual Meeting, Orlando, Florida, USA, 2016.
- Shabnam Pejhan, Eric Bohm, Jan-Mels Brandt, and Urs Wyss “Design Features and Kinematic Behavior of a Customized Surface-Guided Knee Implant”. Paper No.861, Orthopedic Research Society Annual Meeting, Las Vegas, Nevada, USA, 2015.
- Ida Khosravipour, Yunhua Luo, Shabnam Pejhan, and Urs Wyss, “ Contact Stress Analysis of Surface-guided Knee Implant using Finite Element Modeling”, Proceedings of the 25th CANCAM, London, Ontario, Canada, 2014.